Development of analytical techniques for biomedical applications toward point-of-care testing devices

Manmana Yanawut

2022

Contents

Chapter I

General introduction

1. Background

1.1 Biomedical analysis

Health-related issues are usually one of the global challenges. Every year, many people get infected with infectious diseases, especially in developing countries. On the other hand, non-communicable diseases, such as diabetes, cancer, and heart disease, are the main health problems in developed countries.[1] In order to prevent and treat these diseases, quick detection of the diseases is the crucial step. A biomarker refers to any substances, structures, or processes that are measured and evaluated as an indicator of normal biological processes, pathogenic processes, or pharmacologic responses to a therapeutic intervention.[2] A variety of biomolecules have been discovered as high potential biomarkers, including metabolites, lipids, proteins, and nucleic acid.[3] Biomarkers play a vital role in disease detection and treatment follow-up. Detecting the biomarkers in body fluids such as blood and urine is a powerful medical tool for the early diagnosis and treatment of diseases.[4] The recent global pandemic occurred in 2019 shows the critical and urgent needs for the development of biomedical analysis.[3]

From the viewpoint of analytical chemistry, the evaluation of biomarkers involves applications of analytical techniques for separation, identification, and quantitative determination.[4] Many analytical techniques, such as spectrophotometry, chromatography, electrochemistry, and electrophoresis, have been used in biomedical analysis. Capillary electrophoresis (CE) is one of the conventional techniques used in biomedical and pharmaceutical applications. Saving analysis time, sample, and solvent consumption, and high separation resolution,[4] are the advantages of CE. CE can be applied in aqueous and non-aqueous media and can be coupled with several detectors. Generally, CE can separate analytes based on a mass to charge ratio. Besides, many separation modes have been developed, such as micellar electrokinetic

chromatography (MEKC), microemulsion electrokinetic chromatography (MEEKC), capillary isoelectric focusing (CIEF), and capillary gel electrophoresis (CGE), providing alternative separation mechanism that makes CE an ideal instrument for separation of a variety of compounds.[4] The further miniaturization of electrophoresis leads to the development of microchip electrophoresis (MCE), which is promising for the use as point-of-care (POC) devices. [5] In chapter II, the separation of steroids with CE was studied. The author expects that this experiment would provide the fundamental knowledge of CE that can be used for further development of MCE and POC devices.

1.2 Point of care testing

POC testing is defined as a diagnostic instrument that performs *in vitro* analysis on patients, providing rapid test results without trained laboratory personnel, performed in a wide variety of locations: in a home, in ambulances, at an accident site and at hospitals.[6] The POC testing is conducted with portable devices and stationary benchtop tools that enable to conduct an analytical test, deliver clear and concise results, as well as manage and operate the platform. According to the World Health Organization (WHO), ASSURED is an acronym for the criteria of POC devices, which stands for affordable, sensitive, specific, user-friendly, rapid and robust, equipment-free, and deliverable to end-users.[7] In recent years, POC devices have become increasingly popular as replacements of the traditional equipment found in central laboratories, which is often bulky, requires skilled personnel to operate, and takes a long time to deliver an analytic result (Figure 1).[8] Moreover, the traditional equipment is costly. Therefore, developing POC devices is necessary for the rapid diagnosis.

In order to develop efficient POC devices, many aspects need to be considered, such as device platforms, recognition elements, signal transducers, and so on.[9] The detection method is one of the essential aspects to be considered by researchers for designing suitable devices. The detection can be used to answer qualitative, quantitative, or both questions depending on the goal of the work. Many types of detection methods, such as colorimetric,[10–12] fluorescence,[13,14] electrochemistry,[8,15,16] and so on, have been used in

POC devices. Although they have been used in developing POC devices, most detection methods require additional electric instruments to read the signal. Therefore, the detection methods without any further instrument or equipment-free detection have been investigated in the past few years.[17] Optical detection like the naked eye has great potential for developing equipment-free detection methods. The color/fluorescence change reaction between analytes and reagents has been widely used to realize the presence of analytes. Moreover, the color intensity can be used to quantify analyte concentrations which can be detected with naked eyes or a camera and a computer software to capture images and process the data.[18] Many optical sensors for environmental and biomedical applications have been published.

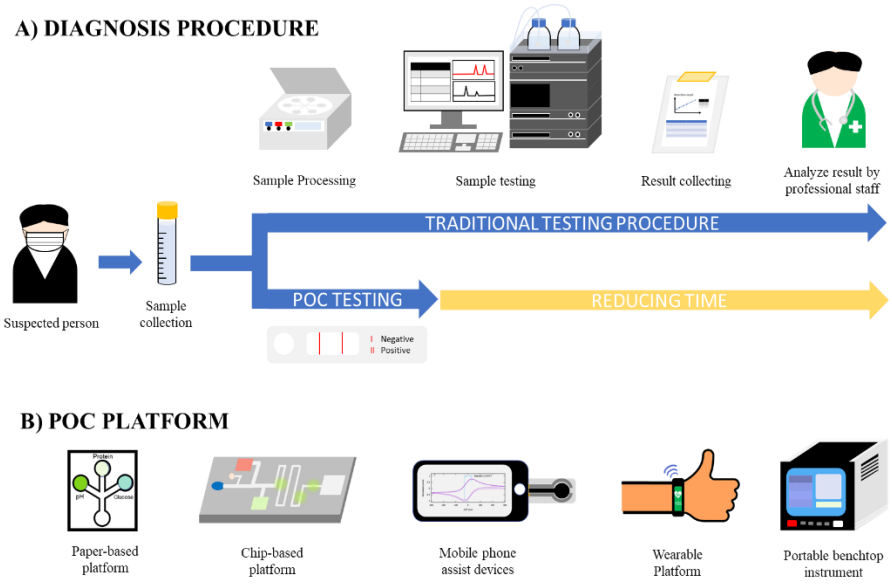

Figure 1. A) Schematic illustrations of medical diagnosis using conventional methods relied on centralized laboratories and POC testing approaches. B) Difference platforms for POC testing.

Optical intensity-based detection shows many promising features, although some people might see the color differently depending on the light, time of the day, the weather, and seasons.[17] Because of the novel signal transformation design in device platforms, especially paper-based devices with colorimetric detection, equipment-free quantitative strategies have already been introduced, such as distance-based,[20,21]

counting-based,[22] time-based,[23] and text-based strategies.[24] Here, the author developed detection devices for biomolecules to further investigate POC testing. The development of hydrogel as the distance-based detection of trypsin was reported in chapter III, and the fluorescence sensor for cytochrome c was reported in chapter V.

1.3 Hydrogels

A hydrogel is one type of material formed by hydrophilic polymers with 3D networks. This material can swell and hold a large amount of aqueous solution due to the hydrophilic properties of polymers.[25] Hydrogels are found in nature (gelatin and collagen as examples) or synthesized in the laboratory. The enormous versatility of commercially available monomers allows the researchers to prepare hydrogels with various interactions (Figure 2) and have physical and chemical properties suitable to their objective applications. Nowadays, hydrogels have been used in many applications, such as separation membranes,[26] biosensors,[27,28] adsorbing materials,[29,30] and drug delivery systems.[31,32] Considering hydrogel in biomedical or pharmaceutical applications, hydrogel shows many advantages such as biocompatibility, physical or chemical responsive properties, and biodegradability, resulting in many publications developing hydrogels for these fields of application.

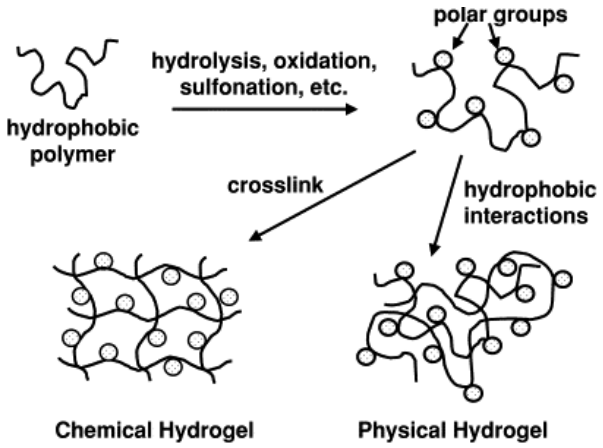

Figure 2. Schematic methods for forming hydrogels by chemical modification of hydrophobic polymers.[33] Figure is reproduced with permission from Elsevier.

1.3.1 Poly(ethylene glycol) based hydrogel

A poly(ethylene glycol) (PEG) is a polyether that is also known as polyethylene oxide (PEO) or polyoxyethylene (POE). Oxygen in the monomer unit makes PEG hydrophilic.[34] The variety of chain lengths and geometries (linear, branched, star, etc.) (Figure 3) available in the market allow researchers to use PEG in many kinds of applications.[34] The PEG-based hydrogel can be synthesized from different types of monomers as the main network structure. Besides, other types of functional monomers can be co-polymerized into the PEG network to adjust PEG hydrogel's physical or chemical properties.

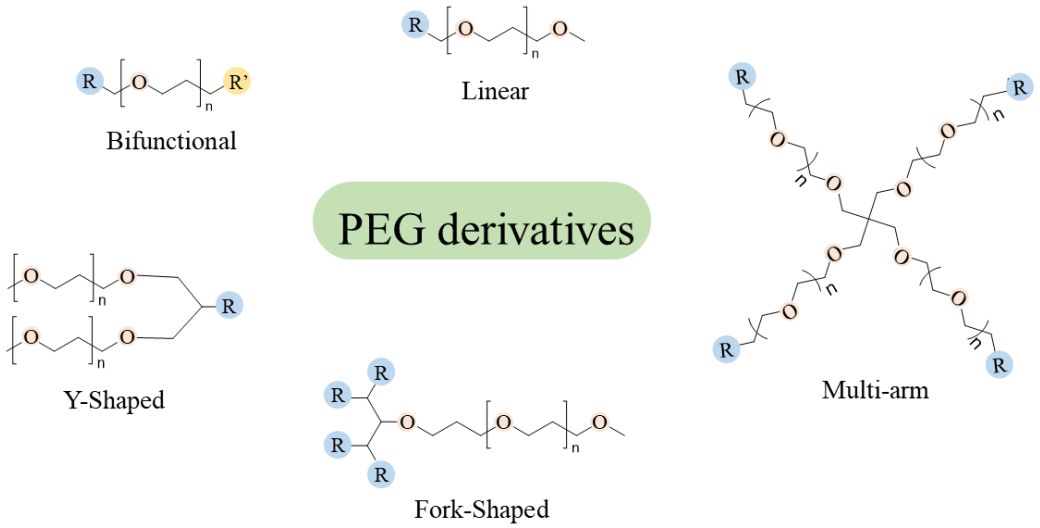

Figure 3. PEG with different geometry structures.

The PEG is widely used for biological applications due to its well-known property as a biocompatible material evidenced by its inability to provoke an immune response or promote cell death.[34] Consequently, the publications that use PEG to modify therapeutic proteins and peptides,[35,36] to coat drug delivery carriers,[37] and to use as scaffold for *in vivo* cell culture,[38] have been reported. Considering PEG in the analytical chemistry aspect, the PEG polymer is suitable for analyzing biomolecules because of its biocompatibility and less unspecific hydrogel interaction. PEG hydrogel can be used as an adsorbent material in the preconcentration,[39] sieving matrix in the separation,[40] and a recognition element in the

determination step.[41] In this thesis, PEG hydrogels were prepared for various analyses and detections of biomolecules, reported in chapters III - V.

1.4 Molecularly imprinted polymer

Molecular imprinting is one of the essential techniques for creating and designing materials that mimic natural receptors. Since the molecularly imprinting technique was introduced for the first time by Wulff and co-workers more than 40 years ago, it is still the recent trend for developing novel materials.[42,43] The principle of creating molecular imprinting typically involves the copolymerization of a functional monomer or series of functional monomers, a cross-linker, and an initiator in the presence of template molecules. In the polymer solution, the functional monomer possesses special functional groups to bind with the template molecules. After polymerization, molecularly imprinted polymers (MIPs) are created around the templates, and subsequent removal of template molecules will leave cavities with complementary size, shape, and chemical moieties to the template (Figure 4).[42] These cavities can recognize and reversibly interact with the template molecules, resulting in selectively recognized materials that can be applied to various applications.

One application of molecular imprinting technology is affinity-based separations for biomedical,[44] environmental,[45,46] and food analysis.[47,48] The use of MIP in the sample preconcentration and treatment can facilitate the adsorption performance with its recognition cavities. Only the target analyte remain while other interferences are removed. The use of MIPs as the materials in solid-phase extraction,[49] solid-phase microextraction,[50] and magnetic stir bar sorption[50] have been studied and published by several publications. Moreover, the use of MIPs as packing materials and stationary phases for separating template analytes in HPLC, capillary electrochromatography (CEC), or thin layer chromatography systems has also been reported.[51,52] Another application of molecularly imprinted materials is to use them as chemical and biological sensors. In the MIP-based sensor, MIPs not only act as the recognition element for the target analytes but also have elements that can generate output signals in the form of optical, electrochemical, or

piezoelectric detection. These output signals allow MIPs to be utilized in fluorescence, electrochemical, chemiluminescence, and UV-Vis sensing for various analytes, from small molecules to large biomolecules.[53–55]

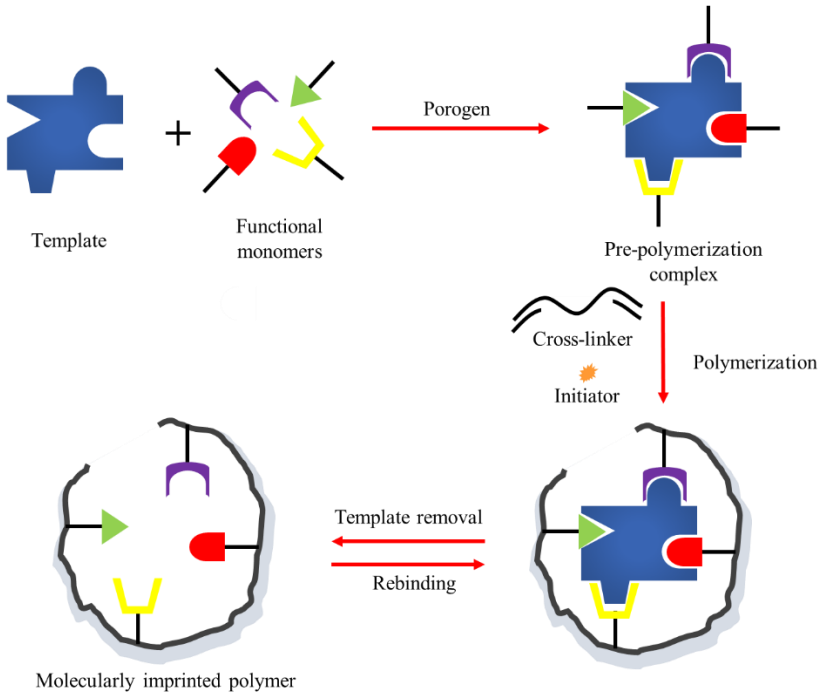

Figure 4. Principle of MIP preparation.

The traditional MIPs are prepared in the form of bulky materials that are further ground into smaller pieces, which may damage the recognition site. Besides, the traditional MIPs are hard to apply with the large template molecules due to the difficulty in template removal and adsorption processes. In order to expand the application and overcome the limitation of traditional MIPs, many novel techniques to prepare MIPs have been developed in recent years, such as precipitation polymerization,[56] emulsion polymerization,[57] and surface imprinting.[58] Besides, the incorporation of MIP techniques with other materials, such as magnetic nanoparticles,[59,60] and metal-covalent organic framework[61,62] have been reported. The preparation of MIPs in the form of hydrogels shows a promise for preparing the imprinting

polymers of biomolecules. This reason is that hydrogel contains fewer organic solvents, which help biomolecules maintain their natural form. Besides, the loose network polymer shows a flexible structure that allows large biomolecules to penetrate and release. However, there are few fundamental studies regarding MIP hydrogels for biomolecules, thus, the preparation of MIP hydrogels using PEG polymers and their applications to separation/detection for proteins are examined in chapters IV and V.

2. Contents of this thesis

The contents of this thesis are the fundamental studies of biomedical analysis, from the conventional analytical instrument to the development of the miniaturized detection method for point-of-care testing. In detail, chapter II focuses on developing a separation method for steroid analysis with capillary electrophoresis with UV spectrophotometry and mass spectrometry detection. Steroids were online preconcentrated and separated using transient trapping (tr-trapping) in the MEKC mode. Chapters III - V focus on preparing PEG hydrogels and their application for point-of-care testing. Chapter III demonstrates the use of PEG hydrogel as the distance and fluorescence intensity detection for trypsin detection. The result showed promise of using PEG hydrogel as the porous material for distance-based measurement of biomolecules. The improvement of selectivity in hydrogels was further studied in chapters IV and V in the form of MIPs. In chapter IV, molecularly imprinting hydrogels for lysozyme were prepared with a microfluidic dispensing device, and parameters affecting lysozyme adsorption were investigated. The multivariate data on the adsorption capacity of lysozyme was successfully acquired. The hydrogels provided a high imprinting factor, and adsorption specificity toward lysozyme were obtained. Finally, the molecularly imprinting hydrogel as a fluorescence sensor for cytochrome c determination was prepared in chapter V. The obtained MIP hydrogel showed specific fluorescence quenching toward cytochrome c.

References

(1) World Health Organization. *Global Health Observatory*. Choice Reviews Online. https://www.who.int/gho/mortality_burden_disease/causes_death/top_10/en/ (accessed 2020-04-11).

(2) Organization, W. H.; Safety, I. P. on C. Biomarkers in Risk Assessment : Validity and Validation. World Health Organization: Geneva PP - Geneva 2001.

(3) Cheng, Q. J. Grand Challenges and Perspectives in Biomedical Analysis and Diagnostics. *Front. Anal. Sci.* **2021**, *1*, 700386

(4) Nimse, S. B.; Sonawane, M. D.; Song, K.-S.; Kim, T. Biomarker Detection Technologies and Future Directions. *Analyst* **2016**, *141* (3), 740–755.

(5) Hassan, S. Microchip Electrophoresis. *Encyclopedia* . **2021**, *1* (1), 30-41

(6) Gubala, V.; Harris, L. F.; Ricco, A. J.; Tan, M. X.; Williams, D. E. Point of Care Diagnostics: Status and Future. *Anal. Chem.* **2012**, *84* (2), 487–515.

(7) Kosack, C. S.; Page, A. L.; Klatser, P. R. A Guide to Aid the Selection of Diagnostic Tests. *Bull. World Health Organ.* **2017**, *95* (9), 639–645.

(8) Ruiz-Vega, G.; Arias-Alpízar, K.; de la Serna, E.; Borgheti-Cardoso, L. N.; Sulleiro, E.; Molina, I.; Fernàndez-Busquets, X.; Sánchez-Montalvá, A.; del Campo, F. J.; Baldrich, E. Electrochemical POC Device for Fast Malaria Quantitative Diagnosis in Whole Blood by Using Magnetic Beads, Poly-HRP and Microfluidic Paper Electrodes. *Biosens. Bioelectron.* **2020**, *150*.

(9) Shrivastava, S.; Trung, T. Q.; Lee, N.-E. Recent Progress, Challenges, and Prospects of Fully Integrated Mobile and Wearable Point-of-Care Testing Systems for Self-Testing. *Chem. Soc. Rev.* **2020**, *49* (6), 1812–1866.

(10) Sun, Y.; Zhao, C.; Niu, J.; Ren, J.; Qu, X. Colorimetric Band-Aids for Point-of-Care Sensing and Treating Bacterial Infection. *ACS Cent. Sci.* **2020**, *6* (2), 207–212.

(11) Yetisen, A. K.; Moreddu, R.; Seifi, S.; Jiang, N.; Vega, K.; Dong, X.; Dong, J.; Butt, H.; Jakobi, M.; Elsner, M.; Koch, A. W. Dermal Tattoo Biosensors for Colorimetric Metabolite Detection. *Angew. Chemie - Int. Ed.* **2019**, *58* (31), 10506–10513.

(12) Ammanath, G.; Yeasmin, S.; Srinivasulu, Y.; Vats, M.; Cheema, J. A.; Nabilah, F.; Srivastava, R.; Yildiz, U. H.; Alagappan, P.; Liedberg, B. Flow-through Colorimetric Assay for Detection of Nucleic Acids in Plasma. *Anal. Chim. Acta* **2019**, *1066*, 102–111.

(13) Zhou, J.; Yu, C.; Li, Z.; Peng, P.; Zhang, D.; Han, X.; Tang, H.; Wu, Q.; Li, L.; Huang, W. A Rapid and Highly Selective Paper-Based Device for High-Throughput Detection of Cysteine with Red Fluorescence Emission and a Large Stokes Shift. *Anal. Methods* **2019**, *11* (10), 1312–1316.

(14) Gong, Y.; Zheng, Y.; Jin, B.; You, M.; Wang, J.; Li, X. J.; Lin, M.; Xu, F.; Li, F. A Portable and Universal Upconversion Nanoparticle-Based Lateral Flow Assay Platform for Point-of-Care Testing. *Talanta* **2019**, *201* (March), 126–133.

(15) Lu, J.; Ge, S.; Ge, L.; Yan, M.; Yu, J. Electrochemical DNA Sensor Based on Three-Dimensional Folding Paper Device for Specific and Sensitive Point-of-Care Testing. *Electrochim. Acta* **2012**, *80*, 334–341.

(16) Kong, F. Z.; Jahan, S.; Zhong, R.; Cao, X. Y.; Li, W. L.; Wang, Y. X.; Xiao, H.; Liu, W. W.; Cao, C. X. Electrophoresis Titration Model of a Moving Redox Boundary Chip for a Point-of-Care Test of an Enzyme-Linked Immunosorbent Assay. *ACS Sensors* **2019**, *4* (1), 126–133.

(17) Tian, T.; Li, J.; Song, Y.; Zhou, L.; Zhu, Z.; Yang, C. J. Distance-Based Microfluidic Quantitative Detection Methods for Point-of-Care Testing. *Lab Chip* **2016**, *16* (7), 1139–1151.

(18) Li, Z.; You, M.; Bai, Y.; Gong, Y.; Xu, F. Equipment-Free Quantitative Readout in Paper-Based Point-of-Care Testing. *Small Methods* **2020**, *4* (4).

(19) Cheng, Y. H.; Tang, H.; Jiang, J. H. Enzyme Mediated Assembly of Gold Nanoparticles for Ultrasensitive Colorimetric Detection of Hepatitis C Virus Antibody. *Anal. Methods* **2017**, *9* (25), 3777–3781.

(20) Yamada, K.; Henares, T. G.; Suzuki, K.; Citterio, D. Distance-Based Tear Lactoferrin Assay on Microfluidic Paper Device Using Interfacial Interactions on Surface-Modified Cellulose. *ACS Appl. Mater. Interfaces* **2015**, *7* (44), 24864–24875.

(21) Ma, Y.; Mao, Y.; Huang, D.; He, Z.; Yan, J.; Tian, T.; Shi, Y.; Song, Y.; Li, X.; Zhu, Z.; Zhou, L.; Yang, C. J. Portable Visual Quantitative Detection of Aflatoxin B1 Using a Target-Responsive Hydrogel and a Distance-Readout Microfluidic Chip. *Lab Chip* **2016**, *16* (16), 3097–3104.

(22) Hu, J.; Choi, J. R.; Wang, S.; Gong, Y.; Feng, S.; Pingguan-Murphy, B.; Lu, T. J.; Xu, F. Multiple Test Zones for Improved Detection Performance in Lateral Flow Assays. *Sensors Actuators B Chem.* **2017**, *243*, 484–488.

(23) Lewis, G. G.; Robbins, J. S.; Phillips, S. T. A Prototype Point-of-Use Assay for Measuring Heavy Metal Contamination in Water Using Time as a Quantitative Readout. *Chem. Commun.* **2014**, *50* (40), 5352–5354.

(24) Yamada, K.; Suzuki, K.; Citterio, D. Text-Displaying Colorimetric Paper-Based Analytical Device. *ACS Sensors* **2017**, *2* (8), 1247–1254.

(25) Bahram, M. An Introduction to Hydrogels and Some Recent Applications; Mohseni, N., Ed.; IntechOpen: Rijeka, 2016; p Ch. 2.

(26) Alele, N.; Ulbricht, M. Membrane-Based Purification of Proteins from Nanoparticle Dispersions: Influences of Membrane Type and Ultrafiltration Conditions. *Sep. Purif. Technol.* **2016**, *158*, 171–182.

(27) Cheubong, C.; Yoshida, A.; Mizukawa, Y.; Hayakawa, N.; Takai, M.; Morishita, T.; Kitayama, Y.; Sunayama, H.; Takeuchi, T. Molecularly Imprinted Nanogels Capable of Porcine Serum Albumin Detection in Raw Meat Extract for Halal Food Control. *Anal. Chem.* **2020**, *92* (9), 6401–6407.

(28) Wang, C.; Javadi, A.; Ghaffari, M.; Gong, S. A PH-Sensitive Molecularly Imprinted Nanospheres/Hydrogel Composite as a Coating for Implantable Biosensors. *Biomaterials* **2010**, *31* (18), 4944–4951.

(29) Jing, G.; Wang, L.; Yu, H.; Amer, W. A.; Zhang, L. Recent Progress on Study of Hybrid Hydrogels for Water Treatment. *Colloids Surfaces A Physicochem. Eng. Asp.* **2013**, *416* (1), 86–94.

(30) Van Tran, V.; Park, D.; Lee, Y.-C. Hydrogel Applications for Adsorption of Contaminants in Water and Wastewater Treatment. *Environ. Sci. Pollut. Res.* **2018**, *25* (25), 24569–24599.

(31) Scrivano, L.; Parisi, O. I.; Iacopetta, D.; Ruffo, M.; Ceramella, J.; Sinicropi, M. S.; Puoci, F. Molecularly Imprinted Hydrogels for Sustained Release of Sunitinib in Breast Cancer Therapy.

Polym. Adv. Technol. **2019**, *30* (3), 743–748.

(32) Mortensen, N.; Toews, P.; Bates, J. Crosslinking-Dependent Drug Kinetics in Hydrogels for Ophthalmic Delivery. *Polymers (Basel).* **2022**, *14* (2), 248.

(33) Gull, N.; Khan, S. M.; Islam, A.; Butt, M. T. Z. Hydrogels Used for Biomedical Applications. *Bio Monomers Green Polym. Compos. Mater.* **2019**, *54*, 175–199.

(34) Zarrintaj, P.; Saeb, M. R.; Jafari, S. H.; Mozafari, M. Chapter 18 - Application of Compatibilized Polymer Blends in Biomedical Fields; A.R., A., Thomas, S. B. T.-C. of P. B., Eds.; Elsevier, 2020; pp 511–537.

(35) Kinstler, O.; Molineux, G.; Treuheit, M.; Ladd, D.; Gegg, C. Mono-N-Terminal Poly(Ethylene Glycol)–Protein Conjugates. *Adv. Drug Deliv. Rev.* **2002**, *54* (4), 477–485.

(36) Alconcel, S. N. S.; Baas, A. S.; Maynard, H. D. FDA-Approved Poly(Ethylene Glycol)–Protein Conjugate Drugs. *Polym. Chem.* **2011**, *2* (7), 1442–1448.

(37) Knop, K.; Hoogenboom, R.; Fischer, D.; Schubert, U. S. Poly(Ethylene Glycol) in Drug Delivery: Pros and Cons as Well as Potential Alternatives. *Angew. Chemie Int. Ed.* **2010**, *49* (36), 6288–6308.

(38) Zhu, J. Bioactive Modification of Poly(Ethylene Glycol) Hydrogels for Tissue Engineering. *Biomaterials* **2010**, *31* (17), 4639–4656.

(39) Kubo, T.; Arimura, S.; Tominaga, Y.; Naito, T.; Hosoya, K.; Otsuka, K. Molecularly Imprinted Polymers for Selective Adsorption of Lysozyme and Cytochrome c Using a PEG-Based Hydrogel: Selective Recognition for Different Conformations Due to PH Conditions. *Macromolecules* **2015**, *48* (12), 4081–4087.

(40) Liu, C.; Kubo, T.; Naito, T.; Otsuka, K. Controllable Molecular Sieving by Copoly (Poly(Ethylene Glycol) Acrylate/Poly(Ethylene Glycol) Diacrylate)-Based Hydrogels via Capillary Electrophoresis for DNA Fragments . *ACS Appl. Polym. Mater.* **2020**, *2* (9), 3886–3893.

(41) Sawayama, J.; Takeuchi, S. Long-Term Continuous Glucose Monitoring Using a Fluorescence-Based Biocompatible Hydrogel Glucose Sensor. *Adv. Healthc. Mater.* **2021**, *10* (3), 2001286.

(42) Li, R.; Feng, Y.; Pan, G.; Liu, L. Advances in Molecularly Imprinting Technology for Bioanalytical Applications. *Sensors (Switzerland)* **2019**, *19* (1).

(43) Wulff, G.; Sarhan, A. Über Die Anwendung von Enzymanalog Gebauten Polymeren Zur Racemattrennung. *Angew. Chemie* **1972**, *84* (8), 364.

(44) Owens, P. K.; Karlsson, L.; Lutz, E. S. M.; Andersson, L. I. Molecular Imprinting for Bio- and Pharmaceutical Analysis. *TrAC Trends Anal. Chem.* **1999**, *18* (3), 146–154.

(45) Azizi, A.; Bottaro, C. S. A Critical Review of Molecularly Imprinted Polymers for the Analysis of Organic Pollutants in Environmental Water Samples. *J. Chromatogr. A* **2020**, *1614*, 460603.

(46) Ji, Y.; Yin, J.; Xu, Z.; Zhao, C.; Huang, H.; Zhang, H.; Wang, C. Preparation of Magnetic Molecularly Imprinted Polymer for Rapid Determination of Bisphenol A in Environmental Water and Milk Samples. *Anal. Bioanal. Chem.* **2009**, *395* (4), 1125–1133.

(47) de Sá, I. P.; Higuera, J. M.; Costa, V. C.; Costa, J. A. S.; da Silva, C. M. P.; Nogueira, A. R. A. Determination of Trace Elements in Meat and Fish Samples by MIP OES Using Solid-Phase Extraction. *Food Anal. Methods* **2020**, *13* (1), 238–248.

(48) Song, X.; Xu, S.; Chen, L.; Wei, Y.; Xiong, H. Recent Advances in Molecularly Imprinted Polymers

in Food Analysis. *J. Appl. Polym. Sci.* **2014**, *131* (16).

(49) Qiao, F.; Sun, H.; Yan, H.; Row, K. H. Molecularly Imprinted Polymers for Solid Phase Extraction. *Chromatographia* **2006**, *64* (11), 625–634.

(50) Sarafraz-Yazdi, A.; Razavi, N. Application of Molecularly-Imprinted Polymers in Solid-Phase Microextraction Techniques. *TrAC Trends Anal. Chem.* **2015**, *73*, 81–90.

(51) Zheng, C.; Huang, Y.-P.; Liu, Z.-S. Recent Developments and Applications of Molecularly Imprinted Monolithic Column for HPLC and CEC. *J. Sep. Sci.* **2011**, *34* (16–17), 1988–2002.

(52) Song, Z.; Li, J.; Lu, W.; Li, B.; Yang, G.; Bi, Y.; Arabi, M.; Wang, X.; Ma, J.; Chen, L. Molecularly Imprinted Polymers Based Materials and Their Applications in Chromatographic and Electrophoretic Separations. *TrAC Trends Anal. Chem.* **2022**, *146*, 116504.

(53) Ahmad, O. S.; Bedwell, T. S.; Esen, C.; Garcia-Cruz, A.; Piletsky, S. A. Molecularly Imprinted Polymers in Electrochemical and Optical Sensors. *Trends Biotechnol.* **2019**, *37* (3), 294–309.

(54) Piletsky, S. A.; Turner, A. P. F. Electrochemical Sensors Based on Molecularly Imprinted Polymers. *Electroanalysis* **2002**, *14* (5), 317–323.

(55) Shimizu, K. D.; Stephenson, C. J. Molecularly Imprinted Polymer Sensor Arrays. *Curr. Opin. Chem. Biol.* **2010**, *14* (6), 743–750.

(56) Lu, Y.; Zhu, Y.; Zhang, Y.; Wang, K. Synthesizing Vitamin e Molecularly Imprinted Polymers via Precipitation Polymerization. *J. Chem. Eng. Data* **2019**, *64* (3), 1045–1050.

(57) Zhao, G.; Liu, J.; Liu, M.; Han, X.; Peng, Y.; Tian, X.; Liu, J.; Zhang, S. Synthesis of Molecularly Imprinted Polymer via Emulsion Polymerization for Application in Solanesol Separation. *Appl. Sci.* **2020**, *10* (8), 2868.

(58) Dong, C.; Shi, H.; Han, Y.; Yang, Y.; Wang, R.; Men, J. Molecularly Imprinted Polymers by the Surface Imprinting Technique. *Eur. Polym. J.* **2021**, *145* (September 2020), 110231.

(59) Ansari, S.; Karimi, M. Recent Configurations and Progressive Uses of Magnetic Molecularly Imprinted Polymers for Drug Analysis. *Talanta* **2017**, *167* (February), 470–485.

(60) Sanadgol, N.; Wackerlig, J. Developments of Smart Drug-Delivery Systems Based on Magnetic Molecularly Imprinted Polymers for Targeted Cancer Therapy: A Short Review. *Pharmaceutics* **2020**, *12* (9), 1–31.

(61) Guo, Z.; Florea, A.; Jiang, M.; Mei, Y.; Zhang, W.; Zhang, A.; Săndulescu, R.; Jaffrezic-Renault, N. Molecularly Imprinted Polymer/Metal Organic Framework Based Chemical Sensors. *Coatings* **2016**, *6* (4), 42.

(62) Qian, K.; Fang, G.; Wang, S. A Novel Core-Shell Molecularly Imprinted Polymer Based on Metal-Organic Frameworks as a Matrix. *Chem. Commun.* **2011**, *47* (36), 10118–10120.

Chapter II

Development of transient trapping micellar electrokinetic chromatography coupled with mass spectrometry for steroids analysis

Abstract

An online sample preconcentration technique based on transient trapping (tr-trapping) in micellar electrokinetic chromatography (MEKC) was applied for steroid detection with UV (tr-trapping-UV) and electrospray ionization mass spectrometry detection (tr-trapping-ESI-MS). ESI-MS was used to improve the sensitivity in MEKC. The MEKC separation was carried out using volatile ammonium formate as a background solution to facilitate the coupling with ESI-MS. The partial introduction of a sodium dodecyl sulfate (SDS) micellar solution before the introduction of a sample solution to the capillary provided the effective preconcentration of analytes. At the same time, the SDS micelle would not enter the ESI-MS system, so that its interference in ESI-MS detection was suppressed. Six steroids, including androsterone, cortisone, estradiol (with α-, β- stereoisomers), hydrocortisone, progesterone, and testosterone, were analyzed by the developed method. In tr-trapping-ESI-MS, an acidic condition of pH 3.5 was employed to suppress the electroosmotic flow, which can avoid micellar solution migrating to the MS instrument. The developed method showed that the micellar solution requires a 2-fold slower time than the sample to migrate along the column, which can prohibit the cause of the problem with the MS instrument and interference signal of SDS in the steroid's detection. The tr-trapping-ESI-MS protocol showed up to 540-fold enhancements of the peak intensity and 50-fold improvement of the limit of detection compared with capillary zone electrophoresis using androsterone as a model sample. This simple and sensitive

preconcentration technique provides a possibility for the detection of trace compounds that are difficult to detect with the UV-vis and fluorescence instruments.

1. Introduction

Capillary electrophoresis (CE) is a popular separation technique in various analytical fields due to its advantages, such as low reagent/sample consumption, high resolution, and ability to separate the sample with various interaction/modes. Generally, CE can separate analytes based on the charges and sizes of analytes that migrate through the capillary tube under an applied voltage.[1] Besides, adding some materials into the background solution (BGS) can mimic a stationary phase providing molecular interactions to separate analytes. By adding an ionic surfactant micelle into the BGS, a mode of micellar electrokinetic chromatography (MEKC) can be achieved, where the micelle serves as a pseudo-stationary phase for separating neutral analytes based on the partition mechanism between the micelle and BGS. MEKC provides a wide range of separation applications for biomolecules and pharmaceutical substances.[2,3]

In the case of biological samples, however, the sample usually contains lower analyte concentrations than the detection limit of the system, and it is one of the problematic issues. To improve the sensitivity, various off-line or on-line sample preconcentration techniques have been developed and applied to CE. Examples of on-line sample preconcentration techniques include isotachophoresis[4], field-amplified sample stacking (FASS)[5,6], large-volume sample stacking with an electroosmotic flow pump (LVSEP)[7–9], and sweeping[10]. Transient trapping (tr-trapping) is also one of the on-line sample preconcentration techniques in MEKC that was firstly described by Sueyoshi et al.[11,12] In tr-trapping, the micellar solution is injected into the capillary prior to the introduction of the sample solution. When the voltage is applied, the micelle begins to migrate toward the anode, and the analytes are accumulated and trapped at the sample/micelle boundary for a few seconds. After the preconcentration, the micelle concentration slowly decreases at the sample/micelle boundary, which allows the trapped analytes to release

based on their interaction with the micelle.[12] The studies on tr-trapping with UV[13] and fluorescent[11,14] detection methods were recently reported.

Even though UV and fluorescent detections are commonly used in CE, they also have limitations since not all samples have chromophore or fluorophore in their structures. In addition, some derivatizing processes for introducing chromophore/fluorophore in the sample structure are time-consuming and complicated. Mass spectrometry (MS) is an informative analytical technique that measures the mass-to-charge ratio (*m/z*) of molecules present in samples, which can overcome the limitation of UV and fluorescent detections. The *m/z* property of each analyte obtained from the MS measurement can be used for both quantitative and qualitative analysis.[15] However, mass spectrum is sometimes hindered by the restricted conditions for sample quality. To avoid interference from impurities, a pre-separation of crude sample is usually required before MS analysis. So far, CE coupled with MS (CE-MS), in which an electrospray ionization (ESI) interface is usually employed, has been recognized as an important tool for the analysis of biological compounds in various fields.[16] It has been demonstrated that CE-MS can offer high sensitivity and selectivity for both chiral and achiral compounds. Besides, it can separate isotope compounds.[16] Different from normal CE separations, CE-MS protocols usually employ specific buffer systems to facilitate the downflow ionization of targets. For example, when considering MEKC, the surfactants are poorly compatible with MS detection for many reasons, such as being unable to evaporate, making the electrospray unstable, and lowering the sensitivity of MS detection.[16–19] Thus, strategies to guarantee both the CE and MS sections work well are required.

In this study, we demonstrated the method that uses the tr-trapping-MEKC technique combined with ESI-MS (tr-trapping-ESI-MS) for analyzing biological samples. This study was firstly optimized for the chemical conditions and instrument parameters that might affect tr-trapping-ESI-MS. Steroid compounds were selected as the analytes since they are an important group of compounds that can be found in the body and can be used as biomarkers.[20] The illegal use of steroids among body-builder and athletes is prohibited in many competitions and sport-events.[21] The improper use of steroid compounds is also found

in agriculture, and releasing these compounds into the water can cause an environmental problem.[22,23] Six steroids, including androsterone, cortisone, estradiol (with α- and β-stereoisomer), hydrocortisone, progesterone, and testosterone, were tested with the optimized condition and separation efficiency. Firstly, tr-trapping-MEKC using UV detection (tr-trapping-UV) was employed for the separation of steroids, and then the condition was further optimized for tr-trapping-ESI-MS. Finally, the separation of steroids with tr-trapping-ESI-MS was demonstrated.

2. Material and methods

2.1 Chemical and reagents

Androsterone, cortisone, hydrocortisone, and progesterone were purchased from Sigma-Aldrich (Tokyo, Japan), sodium dodecyl sulfate (SDS) and thiourea were from Wako Pure Chemical Industries (Kyoto, Japan), α-Estradiol, Sudan R, and testosterone were from Tokyo Chemical Industry (Tokyo, Japan), β-Estradiol, ammonium formate (NH_3COOH), ethanol (EtOH), formic acid (HCOOH), ammonium hydroxide, and deionized water were from Nacalai Tesque (Kyoto, Japan). All reagents were of analytical or HPLC grade, and the structures of all steroids used in this work are shown in Figure 1. Electrolyte solutions were prepared with the prescribed amount of each buffer component and its pH was measured with a pH meter (F-53 model, Horiba, Kyoto, Japan). Stock solutions of samples were prepared by dissolving the sample with EtOH and kept at 4 ^{o}C before use. Sample solutions were prepared by diluting the stock solution with the BGS. All the solutions were filtered through a membrane filter (0.45 μm pore size) prior to use.

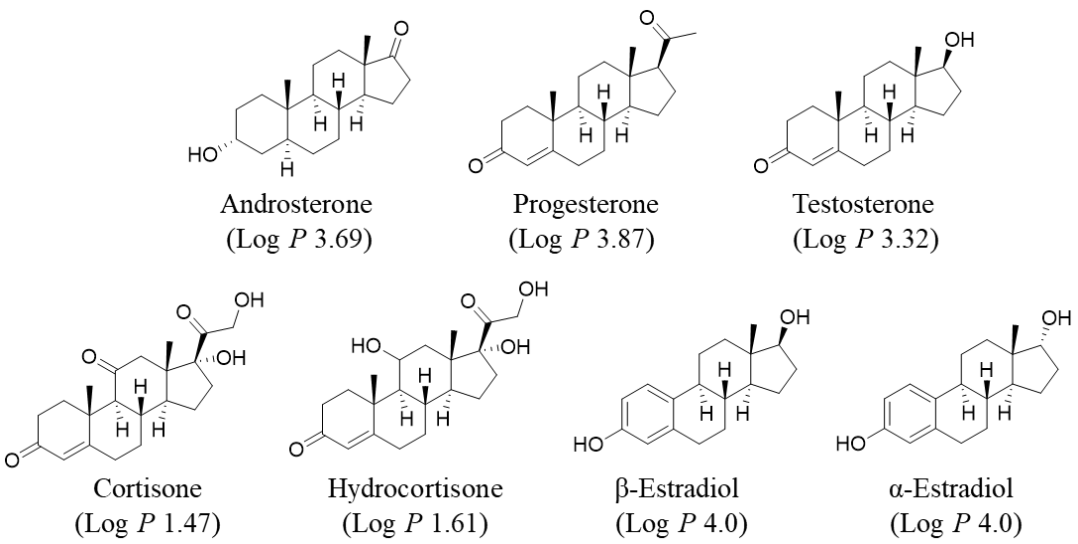

Figure 1. Structures of tested steroids and their Log *P* values. The Log *P* values are obtained from PubChem database.[24]

2.2 Apparatus

CE experiments were performed with a P/ACE MDQ system (Beckman Coulter, Fullerton, CA, USA). For UV detection, a photodiode array (PDA) UV detection system was employed. For the MS detection, the outlet of the CE system was connected with a 3200 Q TRAP mass spectrometer system (Sciex, Framingham, MA, USA). A fused-silica capillary (50 μm i.d., 375 mm o.d.) was purchased from Polymicro Technologies (Phoenix, AZ, USA).

2.3 Procedure

In a tr-trapping-UV procedure, the capillary column with a total length of 50 cm was used. 20% EtOH in 20 mM ammonium formate (pH 7.0) was used as a BGS. Next, 50 mM SDS dissolved in BGS as the micellar solution was injected with 0.5 psi for 90 s. Then, the steroid samples prepared in BGS were

introduced at 2.5 psi for 10 s. The separation was performed at 30.0 kV at 25 ºC. After each measurement, the capillary was washed with 1 M NaOH, water, and BGS for 3, 3, and 3 min, respectively.

In the tr-trapping-ESI-MS procedure, the capillary column with a total length of 120 cm was used. As a BGS, 30 mM ammonium formate (pH 3.5) was used, while 25 mM SDS dissolved in 10 mM ammonium formate (pH 3.5) was employed as the micellar solution. The schematics of the tr-trapping-ESI-MS operation are illustrated in Figure 2. Firstly, the capillary was filled with the BGS. After the partial injection of the micellar solution at 1.5 psi for 20 s, the sample solution was further introduced into the capillary with pressure injection at 5.0 psi for 180 s. Then, a 30.0 kV separation voltage with 0.5 psi as an auxiliary pressure was applied to both ends of the capillary at 25 ºC. For MS detection, 5.0 kV was applied to introduce the sample into the detector. 10 mM formic acid and 50% MeOH was used as the sheath solution with a flow rate of 5.0 µL/min. The nebulizer gas pressure was 20 psi. After each measurement, the capillary was washed with 1 M NaOH, water, and BGS for 3, 3, and 3 min, respectively.

2.4 Principle of tr-trapping–ESI-MS

The fundamental mechanism of tr-trapping was studied and described in the previous papers.[11,12] In Figure 2, a process of tr-trapping-ESI-MS was briefly explained. After the micellar solution (M) is partially introduced into the capillary filled with a BGS without micelle (Figure 2a), a sample solution (S) is then injected into the capillary. Depending on their hydrophobicity, the analytes would be incorporated into the micelle and are trapped nearby the boundary between the S and M zones (S/M boundary) during the injection process and the initial stage of electrophoresis as shown in Figure 2b. The trapped sample is concentrated rather than broadened since the sample band cannot penetrate into the micelle plug at the initial stage. After applying the voltage, the M zone slowly moves along the capillary channel and resulting in the broadening of the M zone with the gradually decreased micelle concentration which generates a micelle gradient. At the same time, the analytes migrate in the M zone, get separated based on partitioning

between the micelle and solution, and then get released from the M zone (Figure 2c). After the sample release from the M zone, the samples migrate towards the MS instrument. During this stage, the analyte's velocity is determined by the electroosmotic flow (EOF) and pressure. The micelle migrates much slower than or even opposite direction to the sample since the negatively charged micelle contributes a negative velocity to the M zone (Figure 2d). Therefore, the sample would migrate to the MS instrument prior to the micelle and SDS cannot interfere with the signal of the mass spectrum (Figure 2e).

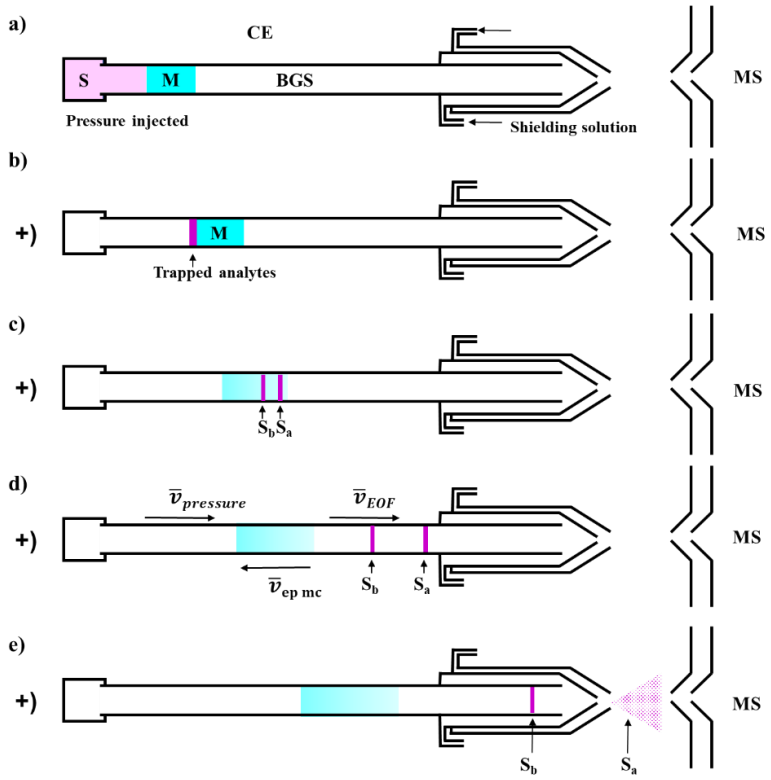

Figure 2. Schematics of tr-trapping-ESI-MS. (a) Initial condition, (b) preconcentration of analytes due to the trap mechanism, (c) separation of analytes due to the difference in release timings due to their hydrophobicity, (d) sample released from M zone and migrate to MS instrument, and (e) sample was injected to MS instrument for detection. M, micellar solution; S, sample solution without the micelle; $\bar{v}_{EOF}$, $\bar{v}_{pressure}$, $\bar{v}_{ep,\ mc}$ are the velocity of the EOF, pressure, and electrophoretic mobility of SDS, respectively. The hydrophobicity of S_a is smaller than that of S_b.

3. Results and discussion

3.1 Detection of steroids with tr-trapping-UV

As a starting point, the tr-trapping-UV protocol was developed. Most steroids are neutral compounds that cannot be separated with typical capillary zone electrophoresis (CZE). Therefore, as reported by many works, MEKC showed its ability to separate and quantify steroids.[17,25–31] From the previous literature, the separation of steroids can be done in a wide pH range from acidic to basic conditions.[25] SDS was the most common surfactant used as a micelle forming agent.[25,30,31] While many bile salts, such as sodium cholate and sodium taurocholate, were also used as the micelle forming agents in the main micellar solution or a mixed micellar solution of other surfactants.[17,26,27] Various additives, such as cyclodextrin[28], urea[25], and organic solvent[29], were also used to modify the aqueous phase for improving the separation efficiency. In this study, ammonium formate was selected as the buffer for steroid separation since it is volatile. EtOH was selected as the organic solvent for steroid stock preparation and used as a mixing solvent in BGS, 20%EtOH in 20 mM ammonium formate pH 7.0. The use of EtOH can improve the separation by reducing the hydrophilicity of the solvent phase. However, too high ratio of EtOH can cause the breakdown of the micellar structure and should be avoided. Moreover, EtOH also improves the solubility of steroids at a high concentration because most steroids can dissolve in water only at a low level. Although many previous papers showed that the mix of SDS and bile salt could improve the steroid separation efficiency, the use of the mixed micelle solution can cause the problem when applied to MS detection. Therefore, only SDS was used as a micelle forming agent in this study. After adjusting the condition of micellar solution introduction, the optimal condition regarding both sensitivity and resolution were obtained when applied 50 mM SDS in 20% EtOH in 20 mM ammonium formate at 0.5 psi for 90 s. The large volume of sample was introduced at 2.5 psi for 10 s as the optimal injection time.

Six steroids, including androsterone, cortisone, estradiol, hydrocortisone, progesterone, and testosterone, were separated with tr-trapping-UV. Two stereoisomers (α-, β-) of estradiol were also examined. With this condition, 5 types of steroids showed the signal within 15 min of separation. Cortisone,

hydrocortisone, progesterone, and testosterone can be measured at 254 nm while estradiol can be measured at 200 nm. Androsterone cannot be detected with UV due to the lack of a strong chromophore in its structure. The migration sequence from earliest to latest was cortisone/hydrocortisone > testosterone > estradiol > progesterone (Figure 3). According to the separation mechanism of tr-trapping described previously, after the sample was trapped in the sample/micelle boundary, the compounds can be separated based on the releasing of the trapped compound off the micelle gradient similar to the normal MEKC principle.[32] Since the separation principle of MEKC is based on the differential partition of analytes between the micelle and BGS. It is expected that the compounds with less hydrophobic would migrate faster than compounds with more hydrophobic ones. The migration order agreed with the hydrophobic property (Log *P*) of steroids except for estradiol. The reason that cortisone and hydrocortisone cannot be separated might be because SDS is not a good micellar agent for the separation of corticosteroids.[27] Interestingly, even cortisone and hydrocortisone cannot be completely separated with this condition, α- and β-estradiol show a different migration time.

The developed method was validated and the calibration curves between peak area and steroids concentration were plotted, as shown in Table 1. The linear relationship between peak area and steroids concentration between 2 – 60 ppm can be observed with the R^2 value between 0.990 – 0.999. The value of %RSD of the migration time of the analyte was in the range of 1.88 – 5.38% (n = 3 at 20 ppm) demonstrating good reproducibility of the analysis.

Table 1. Calibration curves of steroids with the tr-trapping-UV method.

Compound	Migration time (min)	Linear range (ppm)	Equation[a]	R^2
Cortisone	6.6	2 - 60	$A = 525.4 \times C_s - 1286.8$	0.990
Testosterone	8.8	2 - 60	$A = 571.3 \times C_s - 697.0$	0.999
α-Estradiol	9.7	2 - 40	$A = 1490.0 \times C_s + 1719.6$	0.995
β-Estradiol	10.2	2 - 60	$A = 1842.4 \times C_s - 589.4$	0.991
Progesterone	12.3	2 - 40	$A = 469.7 \times C_s + 56.9$	0.998

[a] The abbreviations A and C_s mean peak area and analyte concentration, respectively.

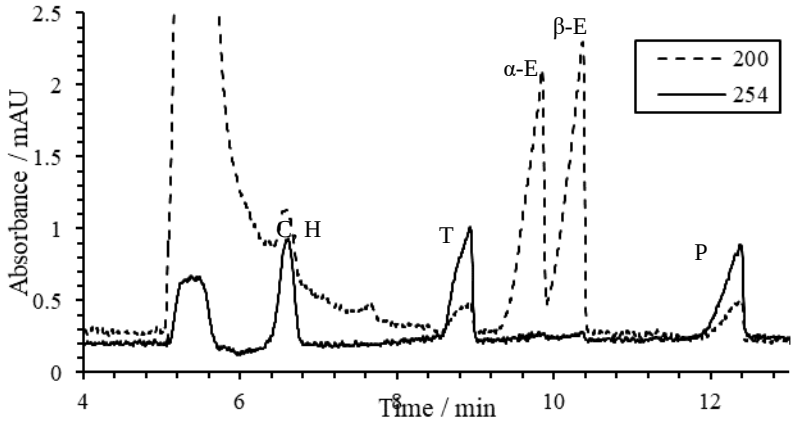

Figure 3. Electropherogram of 5 steroids using the tr-trapping-UV analysis. Dashed line: 200 nm, solid line: 254 nm. Analytical condition: the micellar solution injection, 0.5 psi, 90 s; sample solution injection, 2.5 psi, 10 s; sample concentration, 20 ppm each. The letters above the peaks represent the abbreviations of steroids: C = cortisone, E = estradiol, H = hydrocortisone, P = progesterone, and T = testosterone.

3.2 Strategies for optimization condition of tr-trapping-ESI-MS

As shown in the previous section, UV can be used as the detection scheme for some steroids. Although some steroids have a chromophore in their structures[33], many steroid hormones provide low absorbance and it is difficult to directly detect with UV at the real concentration in human samples. MS provides another approach to this issue by measuring the *m/z* ratio of ions, which shows a specific detection for each molecule based on a characteristic defragment pattern.[15] Here, the condition for detecting with MS was carefully controlled to avoid interference from electrolyte molecules. To specify, efforts were made to avoid the surfactant SDS, which was used in the tr-trapping analysis, entering the MS system.

Firstly, the migration of the surfactant SDS was considered. Ammonium formate was continued to use as the buffer since it was compatible for both CE separation and MS detection. In order to apply the tr-trapping method to the ESI-MS analysis, the condition which suppresses migrating SDS toward the MS detector as much as possible and can send the analytes for ionizing with ESI needs to be considered. As one of the most important factors influencing the velocity of the analyte, the electroosmotic mobility (μ_{EOF}) was investigated and optimized to control the migration of SDS. As the negatively charged SDS contributes a migration velocity of the analyte that directs from the cathode to anode. The EOF affects the velocity and even alters the migration direction of SDS. The μ_{EOF} and $\mu_{ep,mc}$ values can be measured and calculated using the equation and relation below:

$$\mu_{EOF} = \frac{v_{EOF}}{E} = \frac{L_d/t_m}{V/L_t} \quad (1)$$

$$\bar{v}_{total} = \bar{v}_{EOF} + \bar{v}_{ep,mc} = (\mu_{EOF} + \mu_{ep,mc})E \quad (2)$$

where $\bar{v}$ is the velocity, E is the electric field strength, L_d is the effective capillary length, t_m is the migration time, V is the applied voltage, and L_t is the total capillary length.

The measurement of μ_{EOF} and $\mu_{ep,mc}$ values was firstly carried out with the P/ACE MDQ system with UV detection (L_t = 50 cm). Here, the μ_{EOF} was measured with a neutral molecule, thiourea, as an EOF

marker, and $\mu_{ep,mc}$ was measured with Sudan R as a micelle marker. Based on eqs. (1) and (2), the electrophoretic mobility of SDS in the form of micelles and free-molecule were calculated approximately -3.7×10^{-4} and -2.5×10^{-4} $cm^2V^{-1}s^{-1}$, respectively. To limit SDS migrating to the outlet of the capillary, μ_{EOF} needs to be below these values. It is well-known that the pH of the BGS dramatically affects μ_{EOF}. When pH is above 3, the EOF will migrate with a direction towards the anode. At higher pH, μ_{EOF} increases velocity and provides the possibility for the micellar solution to migrate toward the outlet port. Therefore, μ_{EOF} from 17 mM ammonium buffer pH 3.5 - 6.4 was investigated and the result is shown in Table 2. The result showed that at pH 3.5, The value of μ_{EOF} was 1.97×10^{-4} $cm^2V^{-1}s^{-1}$. When pH was above 4, μ_{EOF} was higher than 2.71×10^{-4} $cm^2V^{-1}s^{-1}$ which was unable to be used. Therefore, pH 3.5 was selected as the optimum pH in CE conditions.

Table 2. μ_{EOF} values at different pHs.

pH	6.4	5.0	4.0	3.5
μ_{EOF} (cm^2 V^{-1} s^{-1})	4.42×10^{-4}	4.15×10^{-4}	2.71×10^{-4}	1.97×10^{-4}

In the CE-MS equipment, the 120 cm capillary length was used for steroids separation. At the interface of the capillary outlet and ESI sheath, the pressure was applied for the ionization. For stabilizing the ESI, the pressure of the auxiliary gas of 0.5 psi was applied during the CE separation. The effect of auxiliary gas pressure on the CE-MS devices was studied. When applying the analytes to migrate to the detector with only pressure at 0.5 psi, the signal of the sample was observed at 75.4 min, which can be calculated velocity as 0.26 mm/s. When applying voltage at 250 V/cm (30 kV/120 cm), the velocities of the EOF (at pH 3.5) and free-SDS can be calculated as 0.49 mm/s and -0.63 mm/s, respectively. Therefore, the SDS molecule was moved toward the outlet side at a total speed of 0.12 mm/s. From these obtained values, the SDS molecules could reach the ESI interface at approximately 100 min after the start of migration under the tr-trapping-ESI-MS optimized condition.

3.3 Detection of steroids with tr-trapping-ESI-MS

After optimizing the condition, the obtained method was used for simultaneous detection of 5 steroid hormones that commonly found in human; briefly, androsterone (M_w = 290.44), cortisone (M_w = 360.44), hydrocortisone (M_w = 362.47), progesterone (M_w = 314.47), and testosterone (M_w = 288.42). As a demonstration of the separation efficiency of the tr-trapping method, the samples were also tested without injection the M zone, *i.e.*, the CZE mode. It was found that in the CZE mode, all the samples migrated at the same time (~ 33 min), which was due to all the analytes having a neutral charge in this pH condition. Therefore, no separation based on the charge-to-mass ratio was observed for these analytes and resulted in all analytes migrating along with the EOF. In the tr-trapping-ESI-MS mode, the peak of each steroid was resolved and can be confirmed with each m/z value and migration time, as shown in Table 3. The peaks of the analytes can be observed at the migration time between 23.3 – 38.4 min, which leaves time to stop the separation before the SDS reaches the MS instrument. The peak before 20 min might come from the impurity from androsterone and hydrocortisone (data not shown here). When considering the migration order of the analyte, the migration sequence was testosterone/cortisone > androsterone > progesterone > hydrocortisone. The migration order of the steroids from tr-trapping-ESI-MS was different from tr-trapping-UV which might be the difference in the separation condition (pH, pressure, etc.). The migration sequence of androsterone, progesterone, and testosterone were agreed with their hydrophobic properties. Interestingly, hydrocortisone which has more hydrophilic functional in its structure than the previous three steroids was the last compound that come to the detection window. The reason for that is still unclear but it indicated that another interaction occurs during the separation.

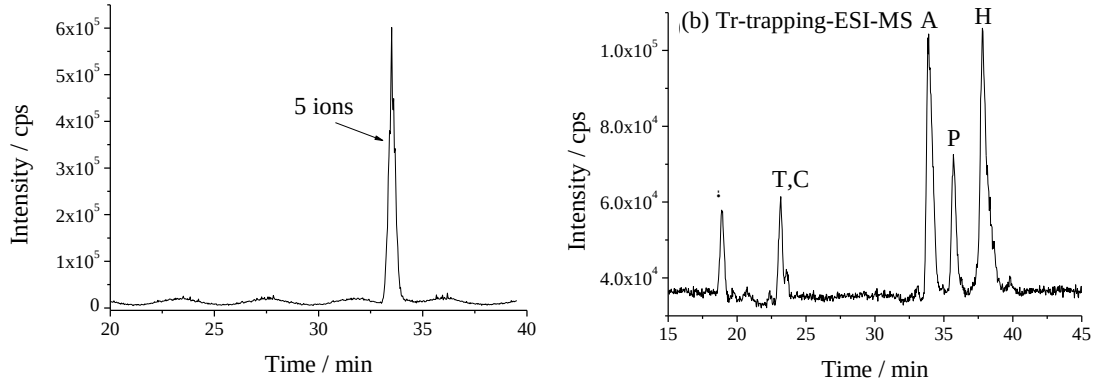

Figure 4. Total ion electropherogram in (a) CZE, (b) tr-trapping-ESI-MS analysis of 5 steroids. Analytical condition: the micellar solution injection, (a) none, (b) 1.5 psi, 20 s; sample solution injection, (a) 5.0 psi, 5 s, (b) 5.0 psi, 180 s; sample concentration, (a) 10 ppm, (b) 25 ppb each. The letters in the figure represent the steroids similar to Fig. 3 with the addition of A = androsterone.

To validate the tr-trapping-ESI-MS method, the %RSD of the migration time was studied. The %RSD of the migration time of the analytes was in the range of 1.13 - 1.83% (Table 3), demonstrating good reproducibility in the analysis process. The androsterone was selected as the model to establish the calibration curve. A good linear relationship between the peak height and androsterone concentration in the range of 1 - 300 ppb with the $R^2 = 0.992$ was obtained (Figure 5). The limit of detection (LOD) can be as low as 1 ppb which is 50 times lower than the CZE mode (LOD_{CZE} = 50 ppb) and more than 1000 times lower than tr-trapping-UV that can be detected on ppm level. In addition, the sensitivity enhancement factor (SEF) was calculated using the following equation:

$$\text{SEF} = \text{Dilution factor x } \frac{\text{Peak height form Tr-trap-ESI-MS}}{\text{Peak height from CZE}} \quad (3)$$

From the calculation, a maximum SEF as high as 540 times can be achieved. This result shows the good sensitivity of steroid detection of the developed method.

Table 3. Validation data of steroids with the tr-trapping-ESI-MS method.

Compound	*m/z*	Migration time (min)	%RSD (n = 3)	Plate number (*N*) (at 50 ppb)
Testosterone	289.2	23.3	1.71%	54250
Androsterone	308.3	34.2	1.70%	23034
Progesterone	315.4	36.2	1.83%	33200
Cortisone	361.4	23.3	1.13%	55148
Hydrocortisone	363.4	38.4	1.64%	31797

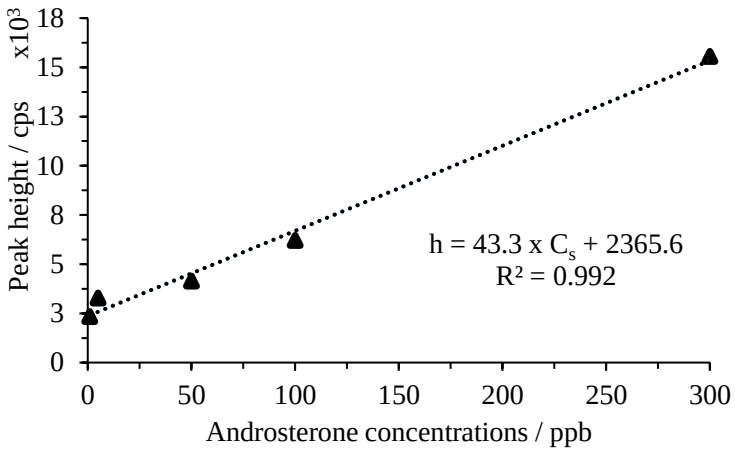

Figure 5. Calibration plot between the peak height and androsterone concentration under the optimized tr-trapping-ESI-MS condition. The abbreviations h and C_s in the equation are the mean peak height and analyte concentration, respectively.

The method to analyze steroids has been usually developed with HPLC and CG[34,35], whereas there are plenty of approaches to determine steroid hormone by CE that have been recently developed.[36–40] This work demonstrated the possibility to use the tr-trapping technique for sample preparation with the MS instrument without the interference of micelle molecule. The tr-trapping-ESI-MS procedure is simple since

it can be automatically programmed the injection and separation in one instrument. Although the developed method required 50 min to operate the separation, this method can guarantee that SDS would not cause the problem with the MS instrument because it requires around 2-fold of time to migrate through the capillary channel.

4. Conclusions

In this work, the application of the tr-trapping technique in combination with UV and MS detections was successfully demonstrated. The developed conditions can be used for the separation of steroids for both UV and MS detection. The result of tr-trapping-UV showed the possibility to use SDS to separate steroids and their stereoisomer without the use of any chiral agents. The separation in the tr-trapping-ESI-MS provides the LOD as low as 1.0 ppb, which is 1000-fold lower than tr-trap-UV and 50-fold lower than the CZE-MS technique. The possibility to use the tr-trapping technique with MS detection provides the possibility to use CE to separate and detect the neutral compounds that are normally difficult to detect with UV or fluorescent detection. In addition, the optimization strategy for tr-trapping-ESI-MS also provides the idea to use this method with other surfactants and bile salts, which can give other possibilities for tr-trapping-ESI-MS. For example, the use of surfactants with chiral structure might be able to preconcentration and separation of chiral compounds.

References

(1) See, H. H.; Ali, N. A. *Electrophoresis | Capillary Electrophoresis: Principles of Capillary*, Third Edit.; Elsevier, 2019; Vol. 2.

(2) Hancu, G.; Simon, B.; Rusu, A.; Mircia, E.; Gyéresi, Á. Principles of Micellar Electrokinetic Capillary Chromatography Applied in Pharmaceutical Analysis. *Adv. Pharm. Bull.* **2013**, *3* (1), 1–8.

(3) Voeten, R. L. C.; Ventouri, I. K.; Haselberg, R.; Somsen, G. W. Capillary Electrophoresis: Trends and Recent Advances. *Anal. Chem.* **2018**, *90* (3), 1464–1481.

(4) Hjalmarsson, S. G.; Baldesten, A. Capillary Isotachophoresis. *C R C Crit. Rev. Anal. Chem.* **1981**, *11* (4), 261–352.

(5) Sueyoshi, K.; Kitagawa, F.; Otsuka, K. Effect of a Low-Conductivity Zone on Field-Amplified Sample Stacking in Microchip Micellar Electrokinetic Chromatography. *Anal. Sci.* **2013**, *29* (1), 133–138.

(6) Wang, L.; Xu, H.; Ye, H.; Yu, L.; Lin, Z.; Liu, X.; Chen, G. Field-Amplified Sample Stacking in Capillary Electrophoresis for the Determination of Alkaloids in *Sinomenium Acutum*. *Anal. Methods* **2013**, *5* (19), 5267–5271.

(7) Kawai, T.; Koino, H.; Sueyoshi, K.; Kitagawa, F.; Otsuka, K. Highly Sensitive Chiral Analysis in Capillary Electrophoresis with Large-Volume Sample Stacking with an Electroosmotic Flow Pump. *J. Chromatogr. A* **2012**, *1246*, 28–34.

(8) Kawai, T.; Watanabe, M.; Sueyoshi, K.; Kitagawa, F.; Otsuka, K. Highly Sensitive Oligosaccharide Analysis in Capillary Electrophoresis Using Large-Volume Sample Stacking with an Electroosmotic Flow Pump. *J. Chromatogr. A* **2012**, *1232*, 52–58.

(9) Pieckowski, M.; Kowalski, P.; Bączek, T. Combination of Large Volume Sample Stacking with Polarity Switching and Cyclodextrin Electrokinetic Chromatography (LVSS-PS-CDEKC) for the Determination of Selected Preservatives in Pharmaceuticals. *Talanta* **2020**, *211*, 120673.

(10) Quirino, J. P.; Kim, J. B.; Terabe, S. Sweeping: Concentration Mechanism and Applications to High-Sensitivity Analysis in Capillary Electrophoresis. *J. Chromatogr. A* **2002**, *965* (1–2), 357–373.

(11) Sueyoshi, K.; Kitagawa, F.; Otsuka, K. On-Line Sample Preconcentration and Separation Technique Based on Transient Trapping in Microchip Micellar Electrokinetic Chromatography. *Anal. Chem.* **2008**, *80* (4), 1255–1262.

(12) Breadmore, M. C.; Quirino, J. P.; Thormann, W. Insight into the Mechanism of Transient Trapping in Micellar Electrokinetic Chromatography. *Electrophoresis* **2011**, *32* (5), 542–549.

(13) Sueyoshi, K.; Koino, H.; Kitagawa, F.; Otsuka, K. Sensitive Enantioseparation by Transient Trapping-Cyclodextrin Electrokinetic Chromatography. *J. Chromatogr. A* **2012**, *1269*, 366–371.

(14) Sueyoshi, K.; Hashiba, K.; Kawai, T.; Kitagawa, F.; Otsuka, K. Hydrophobic Labeling of Amino Acids: Transient Trapping-Capillary/Microchip Electrophoresis. *Electrophoresis* **2011**, *32* (10), 1233–1240.

(15) Urban, P. L. Quantitative Mass Spectrometry: An Overview. *Philos. Trans. R. Soc. A Math. Phys. Eng. Sci.* **2016**, *374* (2079).

(16) Shamsi, S. A.; Miller, B. E. Capillary Electrophoresis-Mass Spectrometry: Recent Advances to the Analysis of Small Achiral and Chiral Solutes. *Electrophoresis* **2004**, *25* (23–24), 3927–3961.

(17) Amundsen, L. K.; Kokkonen, J. T.; Sirén, H. Comparison of Partial Filling MEKC Analyses of Steroids with Use of ESI-MS and UV Spectrophotometry. *J. Sep. Sci.* **2008**, *31* (5), 803–813.

(18) Cheng, H. L.; Tseng, M. C.; Tsai, P. L.; Her, G. R. Analysis of Synthetic Chemical Drugs in Adulterated Chinese Medicines by Capillary Electrophoresis/Electrospray Ionization Mass Spectrometry. *Rapid Commun. Mass Spectrom.* **2001**, *15* (16), 1473–1480.

(19) Hommerson, P.; Khan, A. M.; de Jong, G. J.; Somsen, G. W. Capillary Electrophoresis-Atmospheric Pressure Chemical Ionization-Mass Spectrometry Using an Orthogonal Interface: Set-up and System Parameters. *J. Am. Soc. Mass Spectrom.* **2009**, *20* (7), 1311–1318.

(20) Lehmann, C.; Sharawy, N.; Zhou, J.; Pavlovic, D. Metabolomic Analysis as Biomarker to Study Steroid Hormone Administration in Sepsis. *Med. Hypotheses* **2012**, *79* (3), 329–330.

(21) Basaria, S. Androgen Abuse in Athletes: Detection and Consequences. *J. Clin. Endocrinol. Metab.* **2010**, *95* (4), 1533–1543.

(22) Shargil, D.; Gerstl, Z.; Fine, P.; Nitsan, I.; Kurtzman, D. Impact of Biosolids and Wastewater Effluent Application to Agricultural Land on Steroidal Hormone Content in Lettuce Plants. *Sci. Total Environ.* **2015**, *505*, 357–366.

(23) Scott, A. P. Do Mollusks Use Vertebrate Sex Steroids as Reproductive Hormones? Part I: Critical Appraisal of the Evidence for the Presence, Biosynthesis and Uptake of Steroids. *Steroids* **2012**, *77* (13), 1450–1468.

(24) Kim, S.; Chen, J.; Cheng, T.; Gindulyte, A.; He, J.; He, S.; Li, Q.; Shoemaker, B. A.; Thiessen, P. A.; Yu, B.; Zaslavsky, L.; Zhang, J.; Bolton, E. E. PubChem in 2021: New Data Content and Improved Web Interfaces. *Nucleic Acids Res.* **2021**, *49* (D1), D1388–D1395.

(25) Kartsova, L. A.; Bessonova, E. A. Determination of Steroids in Biological Samples by Micellar Electrokinetic Chromatography. *J. Anal. Chem.* **2007**, *62* (1), 68–75.

(26) Sirén, H.; Seppänen-Laakso, T.; Orešič, M. Capillary Electrophoresis with UV Detection and Mass Spectrometry in Method Development for Profiling Metabolites of Steroid Hormone Metabolism. *J. Chromatogr. B Anal. Technol. Biomed. Life Sci.* **2008**, *871* (2), 375–382.

(27) Nishi, H.; Fukuyama, T.; Matsuo, M.; Terabe, S. Separation and Determination of Lipophilic Corticosteroids and Benzothiazepin Analogues by Micellar Electrokinetic Chromatography Using Bile Salts. *J. Chromatogr. A* **1990**, *513* (C), 279–295.

(28) Nishi, H.; Matsuo, M. Separation of Corticosteroids and Aromatic Hydrocarbons by Cyclodextrin-Modified Micellar Electrokinetic Chromatography. *J. Liq. Chromatogr.* **1991**, *14* (5), 973–986.

(29) Kobayashi, Y.; Matsui, J.; Watanabe, F. Simultaneous Separation of Free and Conjugated Steroids by Micellar Electrokinetic Chromatography and Its Clinical Application. *Biol. Pharm. Bull.* **1995**, *18* (11), 1614–1616.

(30) Chien, R. L.; Burgi, D. S.; Landers, J. P. Electrokinetic Stacking Injection of Neutral Analytes under Continuous Conductivity Conditions. *Anal. Chem.* **2002**, *74* (15), 3929–3931.

(31) Jumppanen, J. H.; Wiedmer, S. K.; Sirén, H.; Riekkola, M. -L; Haario, H. Optimized Separation of Seven Corticosteroids by Micellar Electrokinetic Chromatography. *Electrophoresis* **1994**, *15* (1), 1267–1272.

(32) Terabe, S.; Kim, J. B. Micellar Electrokinetic Chromatography. *Encycl. Anal. Sci. Second Ed.* **2004**, 1–10.

(33) Dorfman, L. Ultraviolet Absorption of Steroids. *Chem. Rev.* **1953**, *53* (1), 47–144.

(34) Görög, S.; See, H. H.; Ali, N. A.; Breadmore, M. C.; Quirino, J. P.; Thormann, W. Recent Advances in the Analysis of Steroid Hormones and Related Drugs. *Electrophoresis* **2011**, *32* (5), 767–782.

(35) Harrison, C. R. Role of Capillary Electrophoresis in the Fight against Doping in Sports. *Anal. Chem.* **2013**, *85* (15), 6982–6987.

(36) Kravchenko, A. V.; Kolobova, E. A.; Kartsova, L. A. Usage of 3-Methyl-1-β-Cyclodextrinimidazole Tosylate for Electrophoretic Separation and Preconcentration of Corticosteroids by Capillary Electrophoresis. *Monatshefte fur Chemie* **2021**, *152* (9), 1067–1074.

(37) Botello, I.; Borrull, F.; Calull, M.; Aguilar, C. Simultaneous Determination of Weakly Ionizable Analytes in Urine and Plasma Samples by Transient Pseudo-Isotachophoresis in Capillary Zone Electrophoresis. *Anal. Bioanal. Chem.* **2011**, *400* (2), 527–534.

(38) Wang, C. C.; Cheng, S. F.; Cheng, H. L.; Chen, Y. L. Analysis of Anabolic Androgenic Steroids in Urine by Full-Capillary Sample Injection Combined with a Sweeping CE Stacking Method. *Anal. Bioanal. Chem.* **2013**, *405* (6), 1969–1976.

(39) Wang, C. C.; Chen, J. L.; Chen, Y. L.; Cheng, H. L.; Wu, S. M. A Novel Stacking Method of Repetitive Large Volume Sample Injection and Sweeping MEKC for Determination of Androgenic Steroids in Urine. *Anal. Chim. Acta* **2012**, *744*, 99–104.

(40) Kukusamude, C.; Srijaranai, S.; Quirino, J. P. Stacking and Separation of Neutral and Cationic Analytes in Interface-Free Two-Dimensional Heart-Cutting Capillary Electrophoresis. *Anal. Chem.* **2014**, *86* (6), 3159–3166.

Chapter III

Protein determination by distance and color change via PEG-based hydrogels

Abstract

Equipment-free detection devices are attractive for point-of-care analysis, especially in resource-limited regions. Distance-based detection is the measurement of color change along the detection path related to the concentration of analytes. Hydrogels are three-dimensional crosslinked polymer networks with tunable properties and may be suitable for the distance-based sensors. But, in the previous studies, only small ions have been used as the targets. In this work, we demonstrated the possibility of using hydrogel as the distance-based measurement of large biomolecules such as proteins. The hydrogel was prepared with a poly(ethylene glycol) diacrylate and a fluorescein derivative as the fluorescent detection probe. The fluorescence alteration in the presence of a target protein, trypsin can be observed in both intensity-based and distance-based detection. It was found that the effect of the concentration of a fluorescence reagent was not significantly impacted in distance-based detection, while it is essential in intensity-based detection. The relationship between the distance change and trypsin concentration in the range of 0.5 – 5 mM can be observed. The result showed the possibility of using hydrogel for the distance-based detection for large biomolecules.

1. Introduction

The development of point-of-care testing (POCT) has been a recent trend in the scientific community. POCT aims to replace traditional laboratory tests that usually require large instruments, high-skilled staff, and a long operation time.[1] According to the World Health Organization (WHO) standard, an ideal POC diagnostic must meet the ASSURED standard, which stands for affordable, sensitive, specific, user-friendly, rapid/robust, equipment-free, and deliverable to end-users.[2] Microfluidic is one of the popular platforms for fabricating POC devices to reduce reagent/sample consumption, instrument size, and operation time.[3] Moreover, multiple materials have been used to construct microfluidic devices, including glass, silicone, polydimethylsiloxane (PDMS), paper, and thread.[4–6] The early devices were made in chip platforms that allow the solution to flow inside the microfluidic channel. In contrast, paper and thread-based microfluidics allow the solution to flow inside the porous materials.

Although microfluidics has been introduced for application in limited resources, other instruments are usually required as detection instruments. These detection instruments can detect analytes based on colorimetric,[7] fluorescence,[8,9] chemiluminescence,[10] electro-chemistry,[11] or electrochemi-luminescence.[12] These instruments might be challenging to operate in locations without supply of electricity. Therefore, the development of POC devices with equipment-free quantitative readout becomes one of the recent trends.[13] Distance-based measurement is an alternative method for equipment-free readout. In this detection method, the target analyte is introduced into the devices with long paths containing reagents. When the target analytes move along the paths, the reaction between analytes and reagents causes the generation of color or fluorescence, which can be seen with naked eye. The generation of color/fluorescence along the path in proportion to target concentration makes determination the target, similar to reading a thermometer quantitatively.[14] Thus, a variety of distance-based microfluidic platforms have been developed in recent years.[15–18]

Among different microfluidic materials, microfluidic paper-based analytical devices (μPADs) are one of the popular platforms for making distance-based devices. Paper, which commonly contains cellulose

as the main material, can allow the solution to flow inside the porous spontaneously without any external pumping systems.[19]

As another platform of a distance-based device, we focus on hydrogels. Hydrogels are three-dimensional (3D) crosslinked polymer networks that contain a large amount of water.[20] Normally, hydrogel properties can be tunable based on the selection of monomers and preparation methods. Due to the variation of hydrogels, they have been applied in various scientific applications, from water treatment to tissue engineering.[21,22] Besides, as one of unique applications, the use of hydrogel for distance-based sensors have been published.[23–25] However, only small ions have been used as the targets. For practical usages, the detection in bio-related samples such as urine, blood, and salivary, especially for the biomolecules. In this work, we tried to study the possibility of using hydrogel as the distance-based sensor for large biomolecules like proteins. Poly(ethylene glycol) (PEG) diacrylates were employed for the preparation of hydrogels and trypsin as a target protein. The quenching reaction between trypsin and a synthesized fluorescence monomer made it possible to see the change in both color/fluorescence intensity and their distance.

2. Material and methods

2.1 Chemicals and reagents

PEG diacrylate (23G' where the number represents the repeat unit) was kindly donated by Shin-Nakamura Chemical (Wakayama, Japan) and utilized as received. 2,2′-azobis[2-(2-imidazolin-2-yl)propane] (AIYP) were from Wako Pure Chemical Industries (Osaka, Japan).; fluorescein 5-isothiocyanate (FITC), 2-acrylamido-2-methylpropane sulfonic acid (AMPS), and allylamine (AA) were purchased from Tokyo Chemical Industry (Tokyo, Japan).; lysozyme chloride from egg white, cytochrome c from equine heart, trypsin from the bovine pancreas, and bovine serum albumin (BSA) from Sigma-Aldrich (Tokyo, Japan); and other reagents were from Nacalai Tesque (Kyoto, Japan). All reagents were of analytical or HPLC grade.

2.2 Instruments

The synthesized monomer was characterized by JNM-ECA500 (JEOL, Japan) as an NMR spectrometer and Nicolet iS5 ATR (Thermo Fisher Scientific, USA) as an FT-IR spectrometer. The absorbance of chemicals was measured using UV-2450 (Shimadzu, Japan) as a UV-Vis spectrophotometer. The fluorescence was measured using RF-5300PC (Shimadzu) as a fluorescence spectrometer. The absorbance and fluorescence of hydrogel were also measured using a SpectraMax iD3 plate reader (Molecular Devices, Tokyo, Japan).

2.3 Synthesis of a fluorescent monomer (FITC-AA)

A FITC-AA was used as a fluorescent monomer and synthesized following our previously reported method.[26] In brief, FITC and AA were dissolved in tetrahydrofuran and stirred at room temperature overnight. After the reaction was completed, the solvent was separated by evaporating with the evaporator. Then products were purified by silica gel column chromatography using *n*-hexane/ethyl acetate/methanol = 15/85/1 as an elution solvent. Then, the isolated compound was dried in a vacuum and reconfirmed the structure by FT-IR and ^{1}H-NMR.

2.4 Preparation of the hydrogel and protein measurement

The hydrogels were prepared in two different containers for measuring by fluorescence intensity and distance change. For fluorescence measurement, the hydrogel was prepared by mixing the polymerization composition as shown in Table 1 and stirred for 30 min. Then, the mixing solution was purged with nitrogen gas for 30 min. Then, the polymerization solution of 100 µL was transferred to a well of the 96-wells microplate. After transferring the solution to the well, the polymer solution was polymerized using a UV lamp at 365 nm for 3 h. After polymerization, 100 mM Tris-HCl buffer of 100 µL was added to each well several times to wash the unreacted reagents until the washing solution showed no UV

absorbance peak. The obtained hydrogel was used for trypsin detection based on fluorescence intensity. For fluorescent detection, trypsin of 40 µL at different concentrations were added to the microplate wells and shaken with a shaking apparatus for 3 h. Fluorescence intensity were measured with a microplate reader (λ_{ex} = 450 nm, λ_{em} = 550 nm).

Table 1. Composition of hydrogels for intensity-based and distance-based detection

	Fluorescence monomer	Monomer	Cross-linker	Initiator	Solvent
H1	FITC-AA, 0.57 µmol	AMPS 20.5 µmol	23G' 215 µmol	AIYP 4.29 mg	1.0 mM Tris–HCl buffer (pH 7.4), 2.1 mL; MeOH, 0.9 mL
H2	FITC-AA, 0.06 µmol				

For the distance-based hydrogel preparation, polymerization solution of 200 µL was transferred to a glass container (25 mm in length, 6 mm in diameter, two open-end) sealed with parafilm at the bottom. Then, the top of the tubes was sealed again and polymerized using a UV lamp at 365 nm for 3 h. When the polymerization process was completed, the parafilm was removed from the top and bottom of the tube, and the glass tube was put in a 15 mL tube. Then, 100 mM Tris-HCl buffer of 10 mL was added into the tube and shaken with a shaking apparatus to wash the hydrogel. After washing, the hydrogel was stored in 1 mM Tris-HCl buffer pH 7.4 before use.

For protein detection with distance-based measurement, tubes were first sealed at the bottom of the tube with the parafilm. Then, trypsin solution of 40 µL was added to the tube and waited for the reaction between FITC-AA and trypsin to occur for 3 h. The picture of color change was taken every 30 minutes. Then, the photos were analyzed with the ImageJ program to precisely measure the distance change.

3. Results and discussion

3.1 Interaction between FITC-AA and trypsin

FITC-AA was synthesized and characterized based on our previous method. After the success in the synthesis process, UV-Vis and fluorescent spectra of FITC-AA with the interaction of trypsin was examined. FITC is a commercially available dye used as a fluorescent tracer for tagging proteins via the isothiocyanate group of FITC and the amine group of proteins. However, FITC can be quenched by other chemicals and experimental conditions. It was also well-known that the adsorption spectrum of FITC can be changed with pH conditions. Under acidic condition, FITC-AA was converted to a non-fluorescent form. Therefore, Tris-HCl buffer pH 7.4 was used for all experiments to activate FITC-AA. The UV-Vis spectrophotometer measurement showed that λ_{max} of FITC-AA is around 490 nm. When we employed trypsin solution with FITC-AA, the absorbance shift to the shorter wavelength was observed when the amount of trypsin increases (Figure 1). This result indicated that the complexation between trypsin and FITC-AA occurred. For fluorescence measurement, the relationship between fluorescence quenching at 520 nm and trypsin concentrations was observed, showing the possibility of using FITC-AA as the colorimetric or fluorescence probe for trypsin detection.

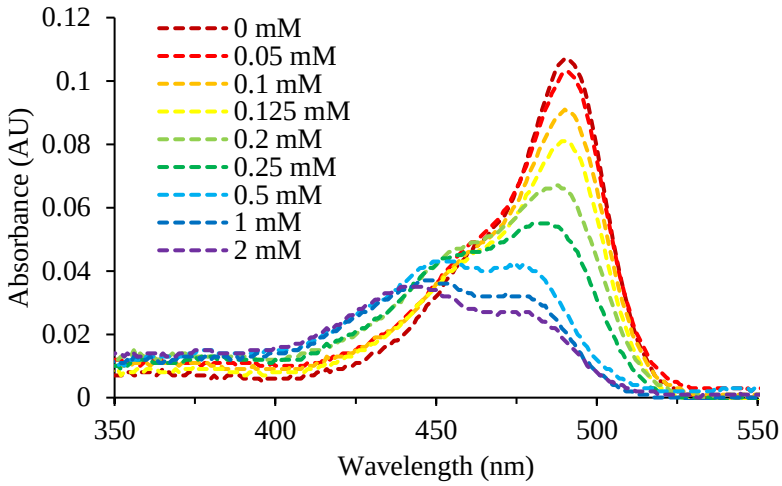

Figure 1. UV-Vis absorption spectra of FITC-AA with different concentrations of trypsin. The absorption spectra were obtained in a sample tube of 1.0 mL. The mixture of 1000 µL of 2 µM FITC-AA and 100 µL trypsin solution in 1 mM Tris-HCl pH 7.4 was firstly mixed before the absorption measurement.

3.2 Hydrogels with fluorescence detection

After the interaction between FITC-AA and trypsin in the solution was examined, the hydrogels using FITC-AA as a fluorescence probe for trypsin detection were prepared. In order to measure the fluorescence intensity, the hydrogels were prepared in a 96-well microplate. The hydrogels were prepared with two concentrations of FITC-AA (0.06 and 0.60 µmol) to study the effect of FITC-AA concentrations on fluorescence detection. Observing with the naked eye, the obtained hydrogel showed yellowish-green color when using 0.60 µmol FITC-AA, while they were almost colorless with 0.06 µmol FITC-AA. However, both hydrogels showed green fluorescent under UV light. By adding trypsin at different concentrations into the well, the alteration of fluorescence intensity was observed as shown in Figure 2. Comparing these two hydrogels showed that the hydrogel prepared with 0.6 µmol FITC-AA gave higher sensitivity than that with 0.06 µmol FITC-AA. This result indicated that the concentration of FITC-AA affected the detection sensitivity for the fluorescence intensity-based detection method.

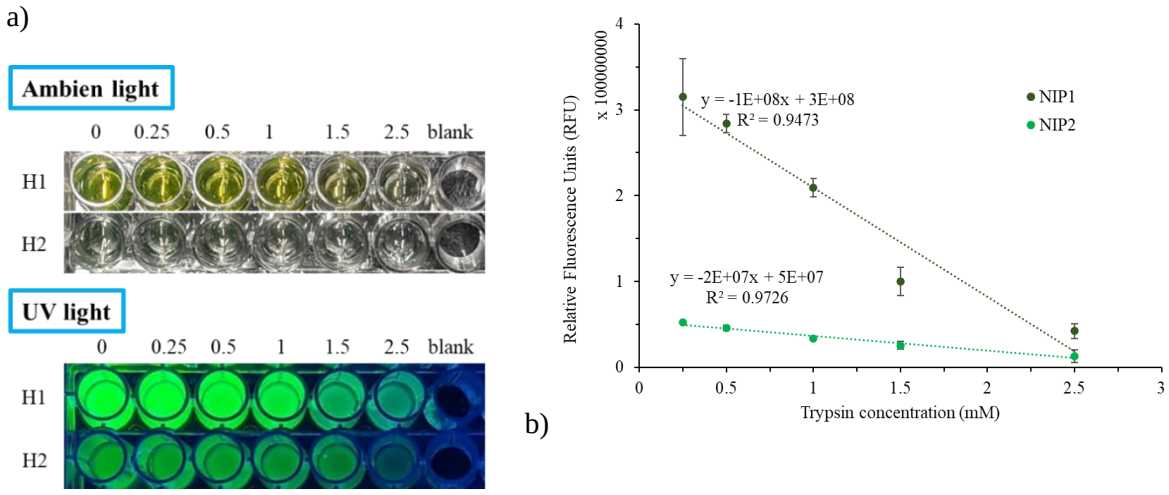

Figure 2. a) Photo of the hydrogels under the ambient and UV light with different trypsin concentrations. b) The relationship between fluorescence intensity and trypsin concentrations. Trypsin solution of 40 µl was added to the wells and shaken for 3 h before fluorescence measurement. Fluorescence was measured at 550 nm with excitation at 450 nm.

3.3 Hydrogels with distance-based detection

After the fluorescence intensity measurement, the possibility of using hydrogel as the distance-based detection was examined. The hydrogels were prepared into the tube, and the average length of obtained hydrogels was 14.84 ± 0.55 mm with %RSD = 3.74%. This consistency in hydrogel length shows good precision in the preparation process. The obtained hydrogel showed yellowish-green color that can be seen by the naked eyes. By adding the trypsin solution into the tube and letting it permeate into the hydrogel, it was found that the color and fluorescence change from the top of the hydrogel surface to the bottom was observed. This result was seen from both ambient and UV light (360 nm). Under the ambient light, hydrogel changed from yellowish-green color to colorless, while the difference in green fluorescence intensity was seen under UV light (Figure 3). The distance gradually changed over 3 h and was measured with the ImageJ program. Besides, the relationship between distance change and trypsin concentration from 0.5 – 5 mM

was observed with %RSD in the range of 4.72 – 7.36 (Figure 4). This result showed the possibility of using this hydrogel as the distance-based measurement for proteins.

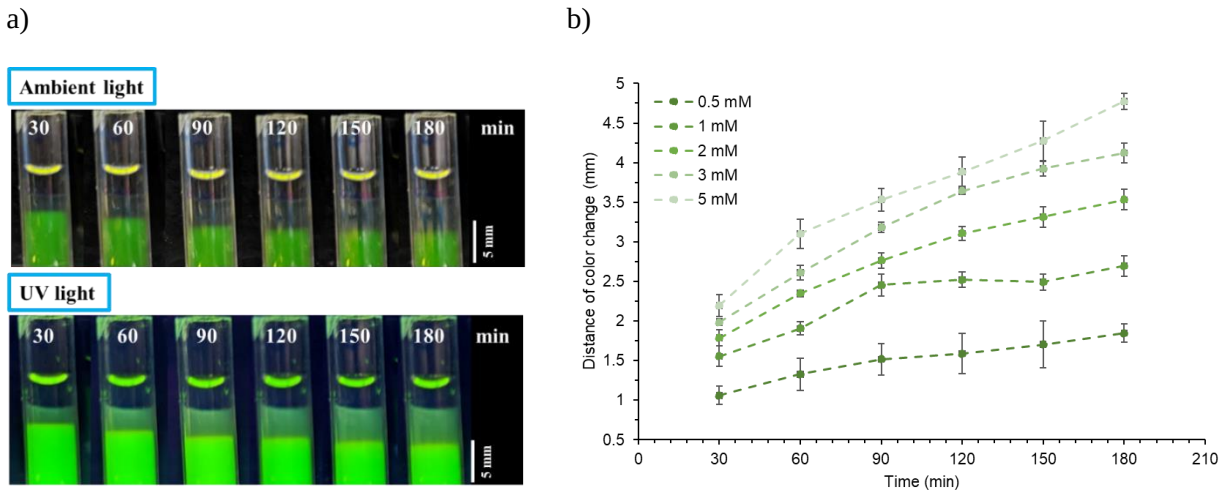

Figure 3. a) Photos of the hydrogel with the color/fluorescence change under the ambient and UV light after adding 3 mM trypsin solution of 40 µL at different times. b) The distance-change of hydrogels over 3 h after adding different trypsin concentrations.

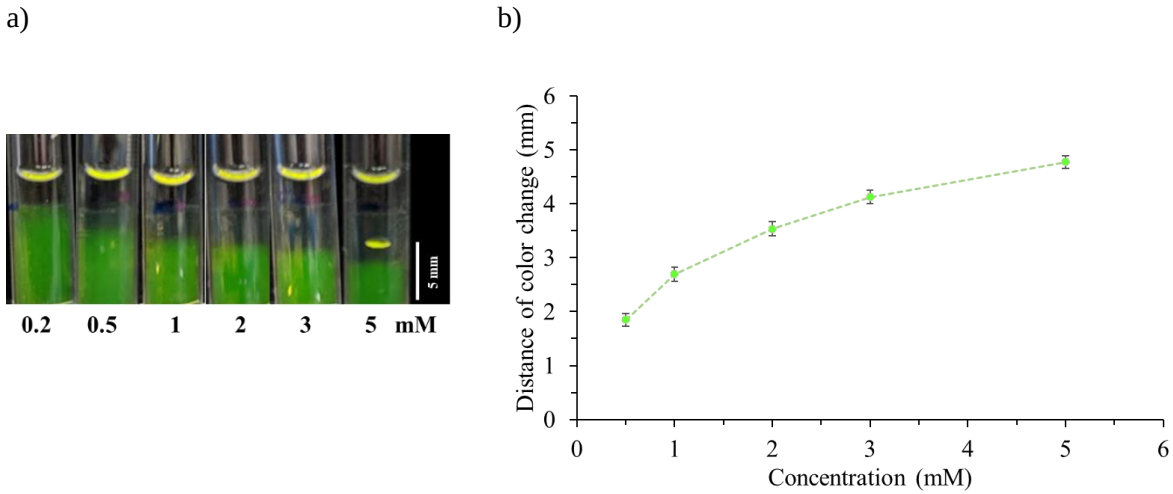

Figure 4. a) Photos of the hydrogel with the color change under ambient light after adding trypsin solution of 40 µL at different concentrations for 3 h. b) The relationship between distance change and trypsin concentration at 3 h.

Two types of hydrogels prepared with different FITC-AA concentrations were used to study the effect of FITC-AA concentrations, similar to fluorescence intensity-based measurement. It was found that the distance of color change between these two hydrogels was almost same, but the color/fluorescence change was slightly different. This result indicated that the concentration of FITC-AA did not affect the detection sensitivity, unlike the intensity-based detection. Also, it indicated that the transportation of analyte along the porous hydrogel is more critical than reagent concentration. Therefore, the adjustment of porous hydrogel for solution transportation is the factor that needs to be investigated to reduce detection time.

3.4 Evaluation of distance-based with other proteins

The selectivity of hydrogels over other proteins, including cytochrome c, lysozyme, and BSA was tested. It was found that there was no color change was observed for lysozyme and BSA at 2 mM concentration. The result indicated a higher sensitivity toward trypsin than other proteins on the prepared hydrogel. The elongation of the red color from cytochrome c solution was observed, which shows the possibility of using a hydrogel for other protein detection (Figure 5). In order to prepare the hydrogel specifically for only one protein, further optimizations to reduce the effect of other interference need to be incorporated.

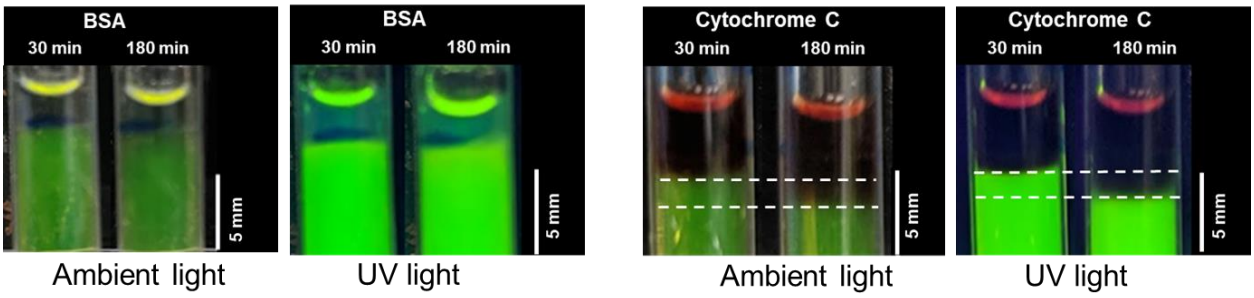

Figure 5. Photos of the hydrogel with the color change under ambient and UV light after adding 2 mM BSA and cytochrome c of 40 µL.

To know the general reaction of the prepared hydrogels, smaller molecules on the hydrogel was also studied by evaluating the quenching of FITC-AA in the presence of proton, H^+. After adding HCl solution into the tube, it was found that the distance change was clearly observed within 5 min after injecting HCl solution., which is much faster than that of trypsin, 3 h for the measurement. This phenomenon might be because the proton is much smaller than trypsin, resulting in faster transportation into the hydrogel. This result showed that the composition of hydrogel allowing large biomolecules to transport faster needs to be investigated.

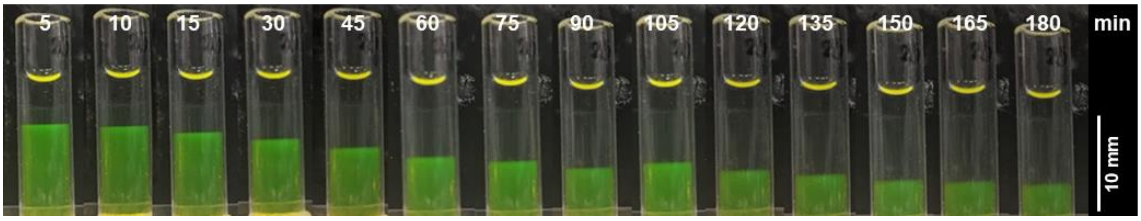

Figure 6. Photos of the hydrogel with the color change under ambient light after adding 25 mM HCl solution of 40 µL at different concentrations for 3 h.

4. Conclusions

In conclusion, the possibility of using hydrogel as a distance-based sensor for trypsin detection was successfully demonstrated. The result showed that the effect of fluorescence reagent in intensity-based and distance-based detection is different. While the concentration of FITC-AA affected the sensitivity in intensity-based detection, the FITC-AA concentration seems to have a lower impact than solution transportation in distance-based measurement. The relationship between distance change and trypsin concentrations could be observed. Furthermore, the distance change over time was observed in other proteins, which showed the promise of distance-based hydrogel sensors for large biomolecules detection. Moreover, compared with a small ion, proton, trypsin transported slower than the proton, resulting in a

more extended detection time. In order to achieve more practical with the actual application, the hydrogel compositions that allow large molecules to transport inside faster and reduce detection time need to be investigated.

References

(1) Ruiz-Vega, G.; Arias-Alpízar, K.; de la Serna, E.; Borgheti-Cardoso, L. N.; Sulleiro, E.; Molina, I.; Fernàndez-Busquets, X.; Sánchez-Montalvá, A.; del Campo, F. J.; Baldrich, E. Electrochemical POC Device for Fast Malaria Quantitative Diagnosis in Whole Blood by Using Magnetic Beads, Poly-HRP and Microfluidic Paper Electrodes. *Biosens. Bioelectron.* **2020**, *150*.

(2) Kosack, C. S.; Page, A. L.; Klatser, P. R. A Guide to Aid the Selection of Diagnostic Tests. *Bull. World Health Organ.* **2017**, *95* (9), 639–645.

(3) Jung, W.; Han, J.; Choi, J. W.; Ahn, C. H. Point-of-Care Testing (POCT) Diagnostic Systems Using Microfluidic Lab-on-a-Chip Technologies. *Microelectron. Eng.* **2015**, *132*, 46–57.

(4) Nayak, S.; Sridhara, A.; Melo, R.; Richer, L.; Chee, N. H.; Kim, J.; Linder, V.; Steinmiller, D.; Sia, S. K.; Gomes-Solecki, M. Microfluidics-Based Point-of-Care Test for Serodiagnosis of Lyme Disease. *Sci. Rep.* **2016**, *6* (September), 1–9.

(5) Hu, J.; Wang, S.; Wang, L.; Li, F.; Pingguan-murphy, B.; Jian, T.; Xu, F. Advances in Paper-Based Point-of-Care Diagnostics. *Biosens. Bioelectron.* **2014**, *54*, 585–597.

(6) Weng, X.; Kang, Y.; Guo, Q.; Peng, B.; Jiang, H. Recent Advances in Thread-Based Microfluidics for Diagnostic Applications. *Biosens. Bioelectron.* **2019**, *132* (March), 171–185.

(7) Kannan, B.; Jahanshahi-Anbuhi, S.; Pelton, R. H.; Li, Y.; Filipe, C. D. M.; Brennan, J. D. Printed Paper Sensors for Serum Lactate Dehydrogenase Using Pullulan-Based Inks to Immobilize Reagents. *Anal. Chem.* **2015**, *87* (18), 9288–9293.

(8) Zhou, J.; Yu, C.; Li, Z.; Peng, P.; Zhang, D.; Han, X.; Tang, H.; Wu, Q.; Li, L.; Huang, W. A Rapid and Highly Selective Paper-Based Device for High-Throughput Detection of Cysteine with Red Fluorescence Emission and a Large Stokes Shift. *Anal. Methods* **2019**, *11* (10), 1312–1316.

(9) Ge, S.; Ge, L.; Yan, M.; Song, X.; Yu, J.; Liu, S. A Disposable Immunosensor Device for Point-of-Care Test of Tumor Marker Based on Copper-Mediated Amplification. *Biosens. Bioelectron.* **2013**, *43* (1), 425–431.

(10) Wang, Y.; Wang, S.; Ge, S.; Wang, S.; Yan, M.; Zang, D.; Yu, J. Ultrasensitive Chemiluminescence Detection of DNA on a Microfluidic Paper-Based Analytical Device. *Monatshefte fur Chemie* **2014**, *145* (1), 129–135.

(11) Pan, D.; Khan, M. S.; Misra, S. K.; Wang, Z.; Daza, E.; Schwartz-Duval, A. S.; Kus, J. M.; Pan, D. Paper-Based Analytical Biosensor Chip Designed from Graphene-Nanoplatelet-Amphiphilic-Diblock-Co-Polymer Composite for Cortisol Detection in Human Saliva. *Anal. Chem.* **2017**, *89* (3), 2107–2115.

(12) Chen, L.; Zhang, C.; Xing, D. Paper-Based Bipolar Electrode-Electrochemiluminescence (BPE-ECL) Device with Battery Energy Supply and Smartphone Read-out: A Handheld ECL System for Biochemical Analysis at the Point-of-Care Level. *Sensors Actuators, B Chem.* **2016**, *237*, 308–317.

(13) Fu, E. Enabling Robust Quantitative Readout in an Equipment-Free Model of Device Development. *Analyst* **2014**, *139* (19), 4750–4757.

(14) Tian, T.; Li, J.; Song, Y.; Zhou, L.; Zhu, Z.; Yang, C. J. Distance-Based Microfluidic Quantitative Detection Methods for Point-of-Care Testing. *Lab Chip* **2016**, *16* (7), 1139–1151.

(15) Chen, Y. T.; Yang, J. T. Detection of an Amphiphilic Biosample in a Paper Microchannel Based on

Length. *Biomed. Microdevices* **2015**, *17* (3).

(16) Song, Y.; Zhang, Y.; Bernard, P. E.; Reuben, J. M.; Ueno, N. T.; Arlinghaus, R. B.; Zu, Y.; Qin, L. Multiplexed Volumetric Bar-Chart Chip for Point-of-Care Diagnostics. *Nat. Commun.* **2012**, *3*, 1–9.

(17) Li, Y.; Xuan, J.; Song, Y.; Qi, W.; He, B.; Wang, P.; Qin, L. Nanoporous Glass Integrated in Volumetric Bar-Chart Chip for Point-of-Care Diagnostics of Non-Small Cell Lung Cancer. *ACS Nano* **2016**, *10* (1), 1640–1647.

(18) Yamada, K.; Henares, T. G.; Suzuki, K.; Citterio, D. Distance-Based Tear Lactoferrin Assay on Microfluidic Paper Device Using Interfacial Interactions on Surface-Modified Cellulose. *ACS Appl. Mater. Interfaces* **2015**, *7* (44), 24864–24875.

(19) Martinez, A. W.; Phillips, S. T.; Whitesides, G. M.; Carrilho, E. Diagnostics for the Developing World: Microfluidic Paper-Based Analytical Devices. *Anal. Chem.* **2010**, *82* (1), 3–10.

(20) Yazdi, M. K.; Vatanpour, V.; Taghizadeh, A.; Taghizadeh, M.; Ganjali, M. R.; Munir, M. T.; Habibzadeh, S.; Saeb, M. R.; Ghaedi, M. Hydrogel Membranes: A Review. *Mater. Sci. Eng. C* **2020**, *114* (April), 111023.

(21) Basak, S.; Nandi, N.; Paul, S.; Hamley, I. W.; Banerjee, A. A Tripeptide-Based Self-Shrinking Hydrogel for Waste-Water Treatment: Removal of Toxic Organic Dyes and Lead (Pb2+) Ions. *Chem. Commun.* **2017**, *53* (43), 5910–5913.

(22) Rahimnejad, M.; Zhong, W. Mussel-Inspired Hydrogel Tissue Adhesives for Wound Closure. *RSC Adv.* **2017**, *7* (75), 47380–47396.

(23) Du, X.; Zhai, J.; Zeng, D.; Chen, F.; Xie, X. Distance-Based Detection of Calcium Ions with Hydrogels Entrapping Exhaustive Ion-Selective Nanoparticles. *Sensors Actuators, B Chem.* **2020**, *319* (March), 128300.

(24) Du, X.; Xie, X. Non-Equilibrium Diffusion Controlled Ion-Selective Optical Sensor for Blood Potassium Determination. *ACS Sensors* **2017**, *2* (10), 1410–1414.

(25) Wang, R.; Du, X.; Zhai, J.; Xie, X. Distance and Color Change Based Hydrogel Sensor for Visual Quantitative Determination of Buffer Concentrations. *ACS Sensors* **2019**, *4* (4), 1017–1022.

(26) Kubo, T.; Arimura, S.; Naito, T.; Sano, T.; Otsuka, K. Competitive ELISA-like Label-Free Detection of Lysozyme by Using a Fluorescent Monomer-Doped Molecularly Imprinted Hydrogel. *Anal. Sci.* **2017**, *33* (11), 1311–1315.

Chapter IV

Development of a microfluidic dispensing device for multivariate data acquisition and application in molecularly imprinting hydrogel preparation

Abstract

Molecularly imprinted polymer (MIP) is the recent advanced material with molecular recognition ability that can be used in various applications. In order to get high specificity recognition for target molecules, optimization of polymerization conditions is crucial. However, this process is time and labor-consuming. The advance in the microfluidic field enables the researchers to control the flow rate and divide the solution based on the design of microfluidic devices to acquire multivariate data by simultaneously preparing the samples with different conditions. In this chapter, we fabricated microfluidic dispensing devices with different flow path widths that can give the solution of different flow rates. The accuracy of the flow rate was compared with the simulation value. The obtained flow rate data showed almost the same data as the simulation value, and a dispensing volume ratio showed high reproducibility. Besides, the multivariate data from mixing fluorescence and protein solutions prepared by this dispensing device and a micropipette showed no significant difference giving the possibility of using this device to replace traditional laboratory equipment. Finally, the dispensing device was used for preparing MIP hydrogels for lysozyme as a template protein. We successfully acquired multivariate data on the adsorption capacity of proteins, as a result, the hydrogels provided a high imprinting factor and adsorption specificity toward lysozyme.

1. Introduction

Molecular imprinting is one of the most important techniques for producing and designing materials that mimic natural receptors.[1] The principle of imprinting is included template molecules with other polymer components during the synthesis process. When the templates were removed, the cavities corresponding to the template size were generated inside of the polymer network that can provide a specific recognition to the template.[1] Recently, molecularly imprinted polymers (MIPs) have been widely studied and applied as artificial molecular recognition materials for selective adsorption and/or concentration of target compounds.[2,3] Generally, the technique of MIP has been applied to small molecules. However, the applications for macromolecules of biomolecules can lead to practical studies as the tools to construct antibodies and enzymes artificially. On the other hand, we could find a few examples of the application of MIP toward biomolecules of proteins,[4,5] viruses,[6,7] and whole cells,[8] and there are still some challenges to be solved. For example, we have to deal with the problems such as (1) the instability of protein in the polymerization solution, (2) the difficulty in the completion of the template removal, and (3) the nonspecific adsorption caused by the polymer backbone on the study of MIP targeting proteins.

To overcome the limitation of the traditional MIPs, many novel techniques have been developed in recent years, such as emulsion polymerization,[9] precipitation polymerization,[10] and surface imprinting.[11] Besides, the incorporating MIP techniques with other types of materials, such as metal-covalent organic framework,[12,13] and magnetic nanoparticle[14,15] open up the new possibility for improving MIPs performance in various applications. MIPs based on hydrogels are one of the recent preparation techniques that have attracted attention for preparing the imprinting polymers of biomolecules. A hydrogel is a soft material with a loose polymer network that provides many advantages, such as stimulus responsiveness, permeability, elasticity, and water-absorbing properties.[16] Hydrogels have been used as separation membranes,[17] biosensors,[18,19] adsorbing materials,[20,21]and drug delivery systems.[22,23] Considering proteins as the templates, hydrogels show better performance than rigid MIPs due to their properties, such as (1) higher protein stability since hydrogels contain fewer organic solvents than bulk MIPs, and (2) flexible structure that

allows macromolecules to penetrate and release. Several studies have been reported on the MIPs hydrogel for proteins.[24,25] Polyacrylamide-based and poly(ethylene glycol) (PEG)-based cross-linker MIP hydrogels have been reported. In comparison with polyacrylamide and PEG, PEG is superior to polyacrylamide in biocompatibility and low toxicity properties, which can be a promising application in the biological and medical fields. At the same time, acrylamide usually shows nonspecific adsorption biomolecules. Even though many MIP hydrogels have been reported by our group[26,27] and other researchers, [28–30] there are still many problems of developing protein MIP hydrogels to be solved .

In order to obtain good quality of MIPs, the optimization of MIP compositions is required. The optimization of conditions usually changes one type of variable. Since many chemical compositions were included in the polymerization process, a huge number of experiments need to be done to obtain the necessary data. These optimization processes are time consuming and labor and cost intensive. Here, microfluidic is the field that studies the behavior of fluids on a small scale and is applied in multidisciplinary areas involving engineering, physics, chemistry, biochemistry, nanotechnology, and biotechnology.[31] We focus on the advantages of the microfluidic system over the macroscale analytical system, such as reducing the sample size and reagent consumption. As a result, it contributes to the reduction of energy and the cost for operating the experiment.[31] Many microfluidic devices have been exploited for various biomedical,[32] environmental,[33] and pharmaceutical applications.[34,35] Most of the microfluidic studies have been carried out using polydimethylsiloxane (PDMS),[36] transparent and soft elastomer, as the substrate to fabricate the microfluidic system, and a lot of microfluidic designs have also been developed.[37,38] The versatility in design allows microfluidic systems to mix and distribute solutions in difficult and complex systems so that we can reduce the time and labor of experiments.

In this work, we fabricated a new microfluidic system that can offer solutions from a single inlet to multiple outlets at different distribution ratios. The microfluidic device was fabricated with PDMS as the substrates. We evaluated its distribution performance and reproducibility. Finally, we demonstrated the

possibility of using the device to obtain the multivariate data of the MIP hydrogel preparation for a target protein, lysozyme.

2. Material and methods

2.1 Chemicals and reagents

PEG 600 dimethacrylate (14G where the number represents the repeat unit) was kindly donated from Shin-Nakamura Chemical (Wakayama, Japan) and utilized as received. Sylgard® 184 Silicone Elastomer Base (prepolymer) and curing agent were purchased from Dow Corning Toray (Tokyo, Japan). Fluoresbrite® Polychromatic Red Microspheres 1.0 µm (fluorescent microbeads) was from Polysciences Inc. (Warrington, PA, USA). S–CLEAN S–24 was from Sasaki Chemical (Kyoto, Japan). Lysozyme chloride from egg white, bovine serum albumin (BSA), sodium p-styrenesulfonate (SS), fluorescein, and 2,2′-azobis[2-(2-imidazolin-2-yl)propane] (AIYP) were from Wako Pure Chemical Industries (Osaka, Japan). 2-acrylamido-2-methylpropane sulfonic acid (AMPS), sodium allylsulfonate (AS), and 8-anilino-1-naphthalenesulfonic acid (ANS) were from Tokyo Chemical Industry (Tokyo, Japan). Cytochrome c from the equine heart and trypsin from the bovine pancreas were from Sigma-Aldrich Japan (Tokyo, Japan), and other reagents were from Nacalai Tesque (Kyoto, Japan). All solvents were analytical or HPLC grade.

2.2 Instruments

A laser direct drawing device DWL2000 model (Heidelberg Instruments, Germany) was used for patterning the chrome mask. A DELTA80 T3/VP SPEC–KU (SÜSS MicroTec SE, Germany) was used for spin coating the polymer. A KSC–150CBU (Kanamex, Kanagawa, Japan) was used for cleaning the wafer. The wafer and mask were aligned by an MA6 BSA SPEC – KU/3 (SÜSS MicroTec SE). The microfluidic pattern was checked and polymerized by an Olympus IX51 fluorescence microscope (Tokyo, Japan). An

As One DO-300 (Osaka, Japan) was used for drying and baking at constant temperatures. A Thinky ARE–300 (Tokyo, Japan) was used for mixing and removing air bubbles in PDMS solution. A Cute-1MP (Femto Science, Gyeonggi, Korea) was used for the vacuum plasma process.

The solution in dispensing device was transferred by a PHD ULTRA syringe pump (Harvard Apparatus, Holliston, MA, USA). The absorbance of chemicals was measured using a UV-2450 (Shimadzu, Kyoto, Japan) as a UV-Vis spectrophotometer. The fluorescence was measured using an RF-5300PC (Shimadzu) as a fluorescence spectrometer. The absorbance and fluorescence were also measured using a SpectraMax iD3 plate reader (Molecular Devices, Tokyo, Japan). A Shimadzu Nexera X3 HPLC system was used for the measurement of proteins in the mixture solution.

2.3 Preparation of microfluidic dispensing device

The structure and dimension of a microfluidic channel were designed and drawn in the AutoCAD program. The picture of the design device used in this experiment and the flow path structure is shown in Figure 1. The SU-8 mold of the flow path pattern was drawn and developed on a chrome mask using a Direct-Write Laser System. After the pattern was developed, the chrome mask was carefully washed and dried with deionized (DI) water, acetone and finally cleaned with a mixing solution of sulfonic acid and hydrogen peroxide (ratio 5:1). Then, SU-8 3050 photo-resist polymer was spin-coated on a silicon substrate, and the wafer was soft-baked at 65 ^{o}C and 95 ^{o}C for 5 and 10 min, respectively. The chrome mask was then installed with the silicon wafer and irradiated with UV light for polymerization. After polymerization, post-exposer bake was done at 65 ^{o}C and 95 ^{o}C for 1 and 4 min, respectively. The SU-8 mold was further immersed in the developer for 3 min twice to remove uncured SU-8, soaked in isopropyl alcohol with shaking for 1 min, and then air-dried. Finally, the silicon substrate with trichloro (3,3,4,4,5,5,6,6,7,7,8,8,8-tridecafluorooctyl)silane was dropped on the surface, and the prepared SU-8 mold was put in a vacuum desiccator for 120 min.

After the SU-8 mold was fabricated, a PDMS microfluidic dispensing device was made by mixing Sylgard® 184 silicone elastomer base and curing agent in a ratio of 10: 1 (w/w). The PDMS mixing solution was stirred and defoamed with an ARE-300. Then, the PDMS mixing solution was spread on the SU-8 mold and allowed to stand in a vacuum desiccator until air bubbles in the PDMS solution disappeared. After heating the PDMS solution at 100 ºC for 30 min, the PDMS was removed from the SU-8 mold. The holes were created at both ends of the microfluidic channel. Next, the PDMS was placed on the glass slide and treated with plasma to join the surface between the PDMS and a glass slide for 120 s. Finally, the PDMS and slide were heated at 100 ºC for 10 min to connect the surface completely.

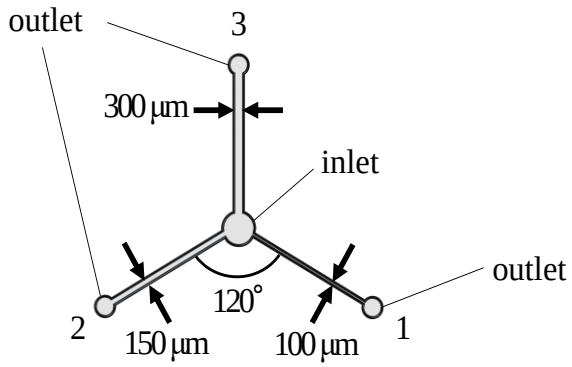

Figure 1. The design of the dispensing device using AutoCAD software.

2.4 Evaluation of microfluidic dispensing devices

The flow rate near the discharge port of the microfluidic dispensing device was measured by using a syringe and a syringe pump. Fluorescent microbeads dispersed in DI water were sent to the dispensing device. A fluorescence microscope image was taken in the terminal region of the flow path using a digital camera. The moving distance of the fluorescent beads in a fixed frame was measured. The movement speed was calculated from the movement distance and the number of frames. The average movement speeds of 50 fluorescent beads were evaluated as the average flow velocity. The value obtained by multiplying the average flow velocity by the cross-sectional area of the flow path was assessed as the flow rate.

The actual dispensing volume of the device was evaluated by the following procedure. First, a certain amount of pure water was sent to the device using a syringe and a syringe pump. Next, a constant concentration of fluorescein solution was diluted with DI water from each outlet. Finally, the dilution rate was calculated from the fluorescence intensity of the diluted fluorescein solution, and the amount of dispensed DI water was determined.

The reaction of ANS and BSA was used to compare the performance of dispensing devices with a commercial micropipette. First, ANS and BSA with the known concentrations were transferred to a microtube in different concentrations using dispensing device or micropipette (Table 4) by controlling the dispensing volume of ANS and BSA solution. Then, after both ANS and BSA solutions were added to the microtube, the solution volume was adjusted and transferred to a 96-well plate for the fluorescence intensity measurement.

2.5 Preparation of the imprinted hydrogel using microfluidic dispensing devices

The MIP components, including the cross-linker, functional monomer, template protein, and initiator, were dissolved in a solution. Then, these solutions with the variable parameters were transferred to a 200 μL-microtube using the microfluidic dispensing devices with the control volume, while the other control parameters were manually transferred with micropipettes (the composition of each component in all gel was shown in Tables 1 – 3). Then, the total volume of the polymerization solution was adjusted to 100 μL in each microtube with a micropipette. The polymerization composition was mixed and shaken for 30 min. Then, the mixing solution was under a vacuum for degassing. The photopolymerization was carried out under 365 nm for 3 h. After polymerization, the hydrogel was washed for 24 h with a 1 M NaCl solution (Scheme 1). Non-imprinted polymers (NIPs) were also prepared without any templates. After the preparation and

washing process, hydrogels were directly used or stored no more than one week before the protein adsorption test.

2.6 Batch adsorption test for proteins

The adsorption test for prepared hydrogel was carried out using 20 μM protein solutions in 1.0 mM Tris-HCl buffer pH 7.1 with 50 mM NaCl. The adsorbed amount of proteins was estimated from the remaining concentration in the adsorption solution after 24 h at room temperature with a shaking apparatus. The adsorption ratio (AR) was defined as follows:

$$\mathrm{AR}\ (\%) = P_{\mathrm{adsorb}} / P_{\mathrm{theo}} \times 100 \quad (1)$$

Where P_{adsorb} is the amount of adsorbed protein to the gels (w/v) and P_{theo} is the theoretical amount of absorbable proteins estimated from the preparation compositions. Here, the P_{theo} of NIP was the same as that of MIP. Furthermore, the imprinting factor (IF) was calculated as follows:

IF = the amount of adsorbed protein toward MIP / the amount of adsorbed protein toward NIP (2)

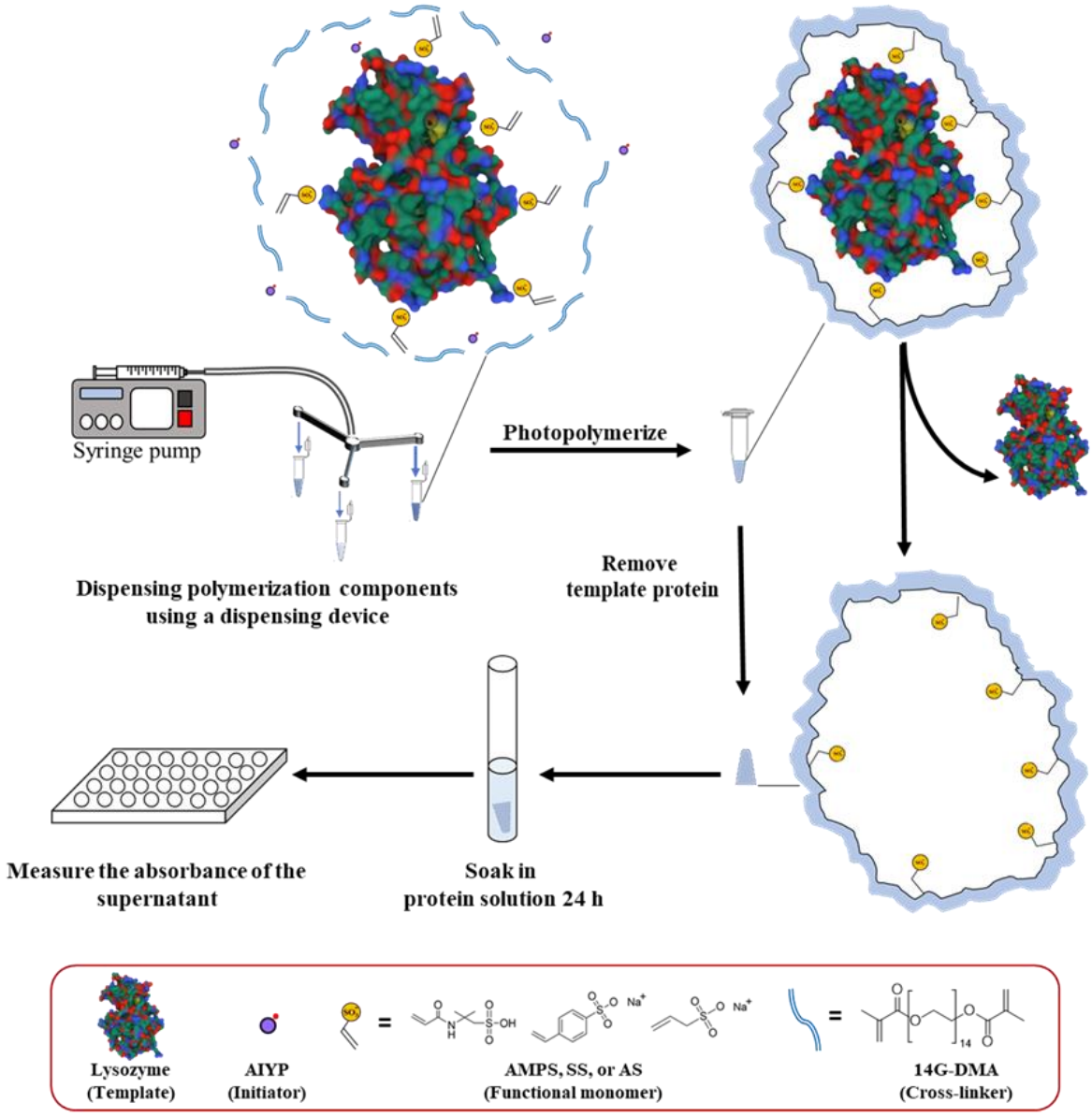

Scheme 1. Preparation of a protein imprinted hydrogel and protein adsorption procedures.

Table 1. Composition of MIP hydrogel #1-32.

Gel #	AMPS (μmol)	AIYP (wt.% vs 14G)	Cross-linker, template, solvent
1	1.9	0.58	14G, 80.7 μmol; Lysozyme, 0.38 μmol; 1.0 mM Tris-HCl buffer (pH 7.0), 1.0 ml
2		1.2	
3		1.5	
4		2.1	
5		2.6	
6		3.0	
7		5.4	
8		6.7	
9	3.9	0.58	
10		1.2	
11		1.5	
12		2.1	
13		2.6	
14		3.0	
15		5.4	
16		6.7	
17	6.9	0.58	
18		1.2	
19		1.5	
20		2.1	
21		2.6	
22		3.0	
23		5.4	
24		6.7	
25	8.6	0.58	
26		1.2	
27		1.5	
28		2.1	
29		2.6	
30		3.0	
31		5.4	
32		6.7	

Table 2. Composition of MIP hydrogel #33-56.

Gel #	AMPS (μmol)	SS (μmol)	AS (μmol)	Cross-linker, initiator, template, solvent
33	6.8			
34		6.8		
35			6.8	
36	2.0	4.8		
37	2.6	4.3		
38	2.8	4.0		
39	3.4	3.4		
40	4.0	2.8		
41	4.3	2.6		
42	4.8	2.0		
43	2.0		4.8	14G, 80.7 μmol;
44	2.6		4.3	AIYP, 2.5 wt.% vs. 14G;
45	2.8		4.0	Lysozyme, 0.38 μmol;
46	3.4		3.4	1.0 mM Tris-HCl buffer (pH 7.0), 1.0 ml
47	4.0		2.8	
48	4.3		2.6	
49	4.8		2.0	
50		4.8	2.0	
51		4.3	2.6	
52		4.0	2.8	
53		3.4	3.4	
54		2.8	4.0	
55		2.6	4.3	
56		2.0	4.8	

Table 3. Composition of MIP hydrogel #57-77.

Gel #	AMPS (μmol)	SS (μmol)	AS (μmol)	Cross-linker, initiator, template, solvent
57	6.8			14G, 80.7 μmol; AIYP, 1.0 wt.% vs. 14G; Lysozyme, 0.38 μmol; 1.0 mM Tris-HCl buffer (pH 7.0), 1.0 ml
58		6.8		
59			6.8	
60	5.3	1.5		
61	4.7	2.1		
62	3.6	3.2		
63	3.2	3.6		
64	2.1	4.7		
65	1.5	5.3		
66		5.3	1.5	
67		4.7	2.1	
68		3.6	3.2	
69		3.2	3.6	
70		2.1	4.7	
71		1.5	5.3	
72	1.5		5.3	
73	2.1		4.7	
74	3.2		3.6	
75	3.6		3.2	
76	4.7		2.1	
77	5.3		1.5	

3. Results and discussion

3.1 The fabrication and evaluation of microfluidic dispensing devices

After the fabrication process, the flow rate and actual discharge of the microfluidic dispensing device were evaluated. The flow rate of each flow path was also calculated by the simulation software (COMSOL Multiphysics 5.4, COMSOL, Stockholm, Sweden) to compare the accuracy in the fabrication process. The result shows that the flow rate ratio from the simulation and the experiment was almost identical at each outlet (Figure 2a). Moreover, the result shows high reproducibility, indicating the reusability of fabricating devices. However, the difference between the flow rate and the dispensing amount can be observed. This reason was due to the difference in measurement techniques. The flow rate was measured inside the dispensing device, and the obtained data are similar to the simulation value. In contrast,

dispensing volume was measured after the solution was released from the outlet. Therefore, when dropping elution from the device to the container, the flow rate might be slightly changed, resulting in a difference in the actual dispensing amount. The above result showed the success in the fabrication process and the application of the microfluidic for dispensing the solution with sufficient distribution ratios to realize different conditions simultaneously.

Table 4. Conditions of [1] and [BSA] mixing solution using the dispensing device and a micropipette.

ANS (μM)	BSA (μM)	ANS (μM)	BSA (μM)
4.5	2.2	14.8	2.4
6.2	3.0	15.4	4.5
6.8	2.6	15.7	4.9
7.3	2.1	15.9	2.9
7.4	2.3	16.0	2.1
7.8	1.9	16.4	4.1
9.3	3.5	16.6	2.4
9.8	4.8	16.7	1.7
10.0	2.9	19.6	3.1
10.0	2.0	20.5	4.2
10.1	3.2	21.1	2.8
10.6	2.6	22.0	2.3
10.9	2.5	22.0	5.0
11.9	2.2	23.8	4.4
12.4	1.8	24.8	3.7
13.5	2.8	28.6	4.6
14.4	5.5	30.6	4.0
14.7	3.3	31.8	3.3

The performance of microfluidic dispensing devices to acquire multivariate data was also compared with the performance of a commercially available pipette by using the fluorescence reaction between ANS and BSA. Since the fluorescence intensity was affected by both concentrations of ANS and BSA,[39,40] the multi-data result was obtained by varying both ANS and BSA concentrations, as shown in Table 4. The dispensing device and micropipette results showed no significant difference at a 95% confidence interval

(Figure 2b). This result provides the possibility to use these devices to transfer the solution with the same performance as a micropipette but with less labor and time to operate more complex conditions.

a) b)

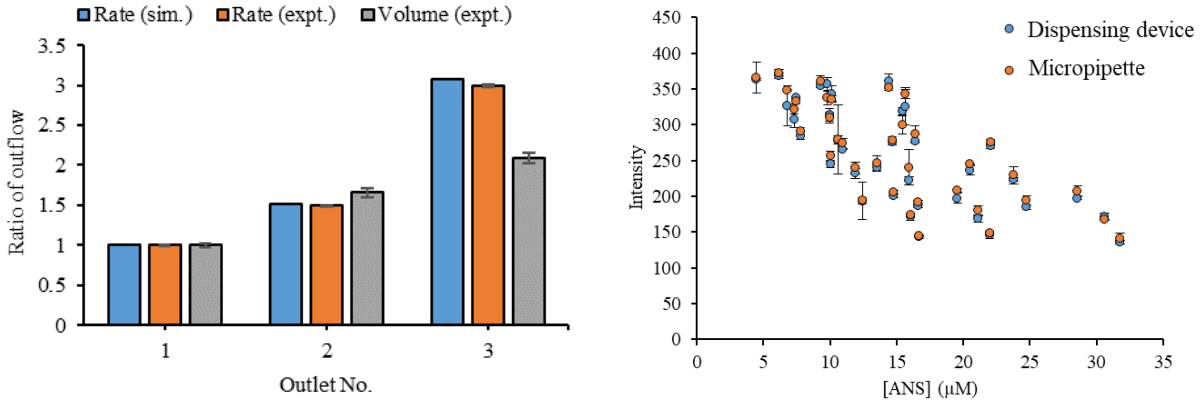

Figure 2. a) Ratio of outflow rate or volume by each outlet from the dispensing device from the simulation (sim.) and experimental data (expt.). b) Fluorescence intensity of ANS using the dispensing device and a micropipette to transfer the solution. The mixing condition of ANS and BSA is shown in Table 4.

3.2 Optimization conditions for lysozyme MIP hydrogel polymerization using microfluidic dispensing devices

In order to demonstrate the application of dispensing devices, multivariate data on the polymerization solution composition of the MIP hydrogel was acquired. The compositions of polymerization solution were known to affect the adsorption performance. Therefore, the hydrogel prepared with different monomer concentrations, amount of initiator, and types of monomers were investigated. Lysozyme was used as a template protein in this study.

3.2.1 The effect of initiator and monomer and their relationship

In the first multivariate study, the hydrogels with different AIYP/14G (wt%) (0.58 – 6.75) and AMPS/lysozyme molar ratios (5.07 – 22.9) were synthesized. The results showed that the adsorption on

MIP hydrogels increased when the ratio of AMPS/lysozymes increased from 5.07 to 22.9 (Figure 3). It can be explained that hydrogels having more functional monomers showed strong electrostatic interaction with protein. Whereas adsorption on MIP hydrogels gradually decreased as the AIYP/14G ratio increased. This tendency indicates that large molecules were hampered to permeant into hydrogels because cross-link increased by associating with the increase of AIYP, and it led to a decrease of polymerized chain length. Hence, using a relatively small amount of initiator is important to let proteins smoothly permeant into hydrogels. Consequently, we can obtain higher adsorbed amount and adsorption selectivity. When the regression equation is structured by using surface methodology regarding the relation between AIYP ratio toward cross-linking agents (wt.%), AMPS ratio toward proteins, and the adsorption rate, each rate is considered as a dependent variable, and the determination coefficient is indicated as $R^2 = 0.827$ which can be calculated according to the following equation:

$$y = 0.98x_1^2 - 6.70x_1 - 0.22x_1x_2 + 1.25x_2 + 6.53 \quad (3)$$

Where y is the adsorption rate, x_1 is the amount of AIYP for the cross-linking agent (wt.%), and x_2 is the molar ratio of AMPS to the protein.

The equation shows that the amount of AIYP gives a negative effect, while the molar ratio of AMPS toward the protein can provide a positive effect on lysozyme adsorption. Besides, the dependence effect of AMPS on the amount of AIYP can be observed by the equation.

a)

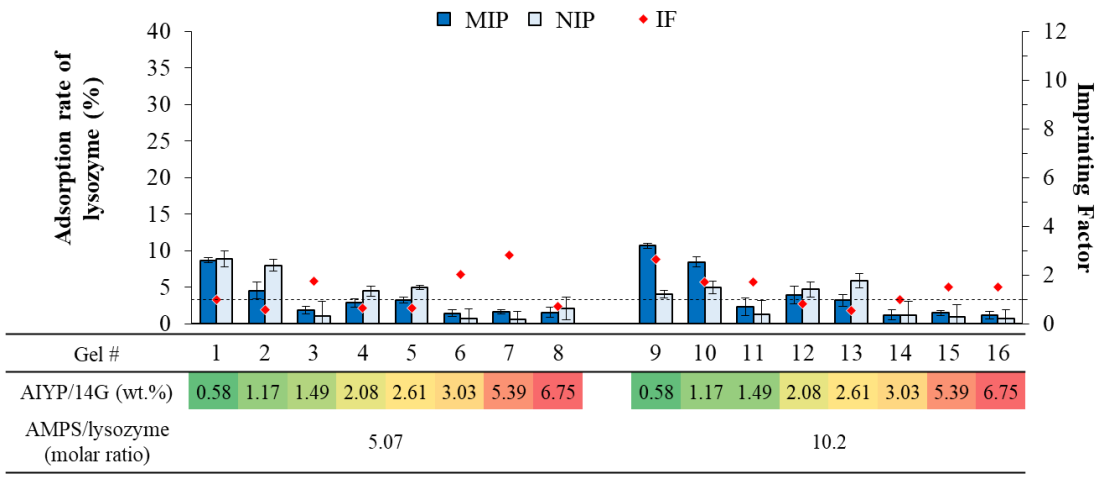

b)

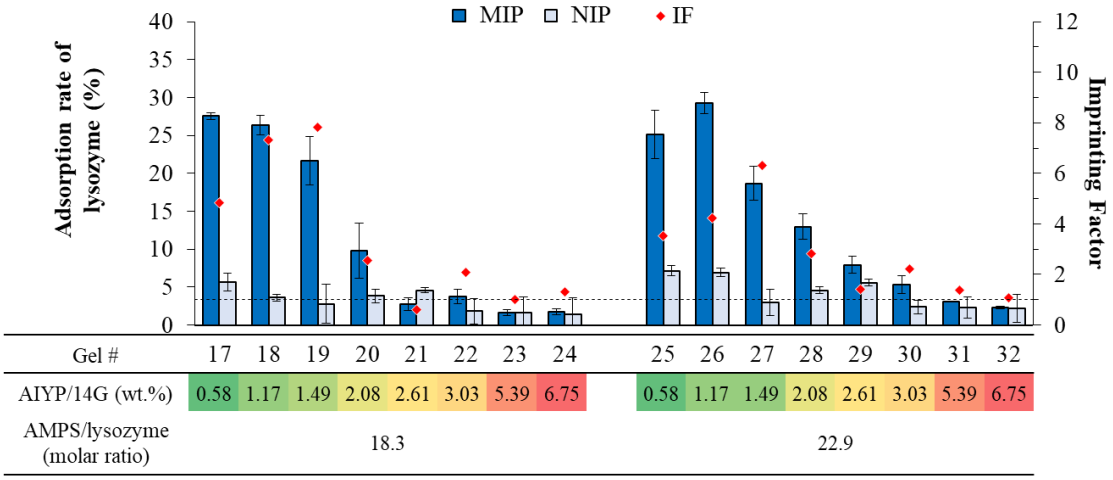

Figure 3. Adsorption rate of lysozyme in each lysozyme MIP and NIP hydrogels prepared with different AIYP/14G and AMPS/lysozyme ratios. The lysozyme and 14G concentrations for every hydrogel in the preparation process were 0.38 mM and 80.6 mM, respectively. Adsorption condition: gel size, 100 μL; solution volume, 2.5 mL; concentration of lysozyme, 0.02 mM; concentration of NaCl, 50 mM; solvent, 1.0 mM Tris-HCl buffer (pH 7.1).

3.2.2 The effect of types of sulfonate monomers

We also investigated the preparation of MIP hydrogels using different sulfonated monomers (AMPS, AS, and SS) (Scheme 1). The investigation implies that these different monomers may have different electrostatic interactions with lysozyme depending on each different structure. Then, we prepared the hydrogel with three sulfonated monomers and the hydrogel combined with two different sulfonated monomers. Furthermore, the synthesis of hydrogels with different amounts of AIYP was conducted at the same time (2.5% for gels #33-56 and 1.0% for gels #57-77). The hydrogel with two sulfonate monomers showed higher IF than the hydrogel with one simple sulfonate monomer indicating IF which was approximately 1 described in Table 2 (Figure 4a). Especially when using AMPS and SS, we confirmed that they tended to show higher IF than other combinations.

Interestingly, as shown in Table 3 (Figure 4b), we observed a different trend when altering the AIYP proportion to 1.0 wt%. Regarding AMPS and SS, the higher adsorption was found even though they are one sulfonated monomer. On the basis of these results, we constructed the regression equation. Consequently, the determination coefficient $R^2 = 0.967$ was obtained, and the following high correlativity equation was obtained:

$$y = 1.03x_2 - 0.09x_2 x_3 - 0.1x_2x_4 + 2.45x_3 - 0.16x_3 x_4 + 4.16 \quad (4)$$

Where y is the adsorption rate, x_2 - x_3 -x_4 are the molar ratio toward proteins of AMPS, SS, and AS, respectively.

According to these results, SS is presumed to contribute to the most effective adsorption. SS is the only monomer having an aromatic ring, considering each construction of monomers. Therefore, in addition to the electrostatic interactions, we can conclude that the aromatic ring of SS interacts with the hydrophobic region inside of lysozymes each other.

a)

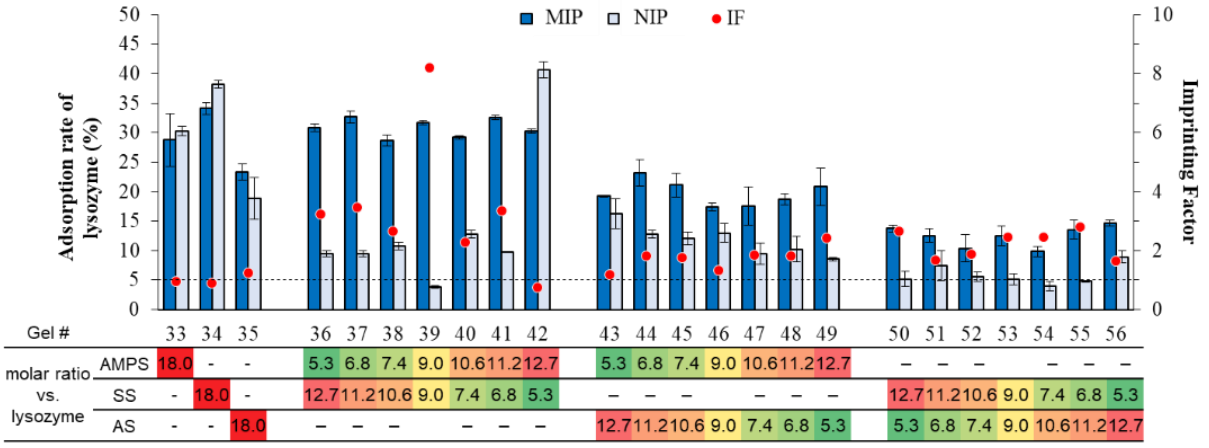

b)

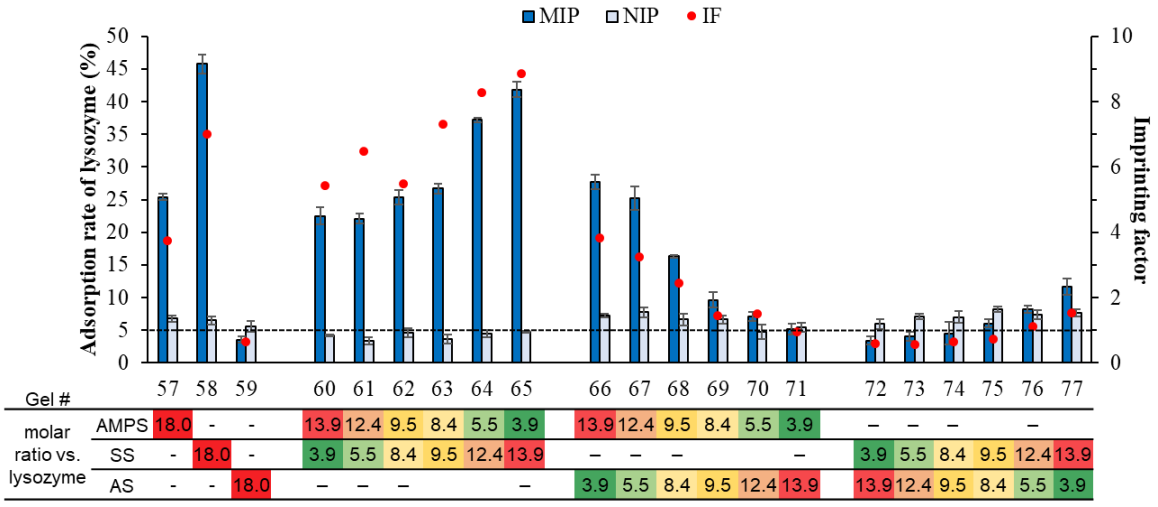

Figure 4. a) and b) Adsorption rate of lysozyme in each lysozyme MIP and NIP gels prepared with different combinations of sulfonate monomers. The concentrations of lysozyme, 14G, and AIYP in every hydrogel in the preparation process were 0.38 mM, 80.6 mM, 2.5 wt% (#33-56) or 1.0 wt% (#57-77) vs. 14G, respectively. Adsorption condition: gel size, 100 µL; solution volume, 2.5 mL; concentration of lysozyme, 0.02 mM; concentration of NaCl, 50 mM; solvent, 1.0 mM Tris-HCl buffer (pH 7.1).

Through these results, we successfully realized the simple optimization of synthetic MIP by using the microfluidic dispensing device that we invented. From both sections 3.2.1 and 3.2.2, it can be seen that the effect of the amount of initiator, the ratio of template/functional monomers, and types of sulfonate monomer can affect the adsorption performance in different ways and equations that show the relation between these parameters and adsorption performance were established. However, the single equation that combines all of these parameters cannot be obtained from these data sets, as seen in Figure 4 that changing only one parameter can lead to a different adsorption behavior of other parameters. To make the single equation possible, larger data sets need to be done and using only microfluidic dispensing devices to variate these parameters is impossible. Even though the microfluidic dispensing device can reduce the time in MIP hydrogel preparation process, the other processes in this work, such as hydrogel washing and protein adsorption, also require numerous labor works. Therefore, other high-throughput instruments that can reduce labor work on other processes would provide the data for a better understanding MIP and need to be developed.

3.2.3 Selectivity of MIP toward lysozyme

After obtaining the adsorption data by varying the condition of MIP polymerization solutions, MIP hydrogels were further used for testing the specificity toward lysozyme with the other proteins. First, the performance of lysozyme adsorption was compared with trypsin adsorption in the single protein adsorption (Figure 5). It was found that all MIP hydrogels can adsorb trypsin lower than 15%, which was lower than lysozyme adsorption in most conditions except for MIP hydrogels prepared with low ratios of sulfonate monomer (gels #1 - 16) or high amount of AIYP (gels #32-24, 30-32). Moreover, the MIP hydrogel was used for the adsorption test in the lysozyme mixing solution with cytochrome c and BSA to study the selectivity in mixing conditions (trypsin cannot be performed in this condition due to the degradation effect when mixing with other proteins). The result from MIP hydrogel #37, as an example, showed that MIP hydrogel has higher specificity toward lysozyme than the other two proteins at all initial concentrations

(Figure 6). Furthermore, these results showed that the MIP composition highly specific to lysozyme protein was successfully obtained by using dispensing devices to acquire multivariate data.

a)

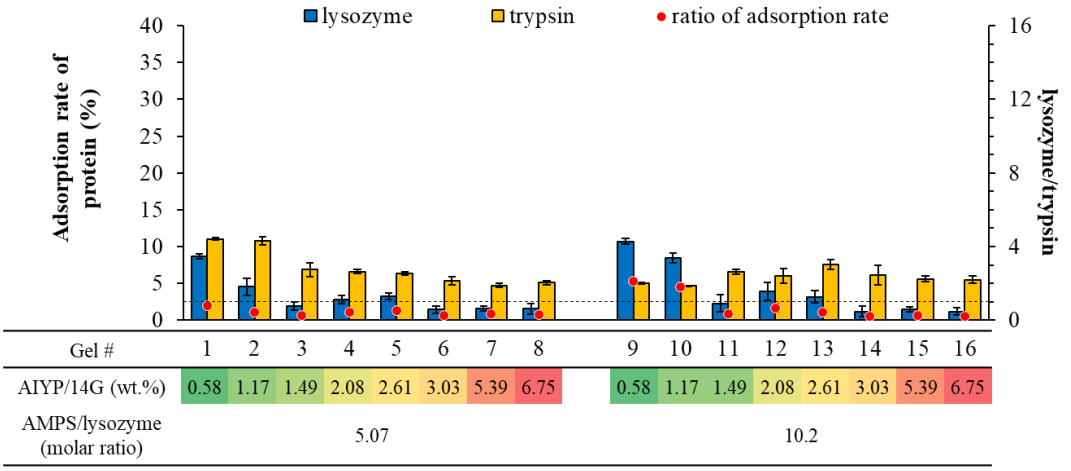

b)

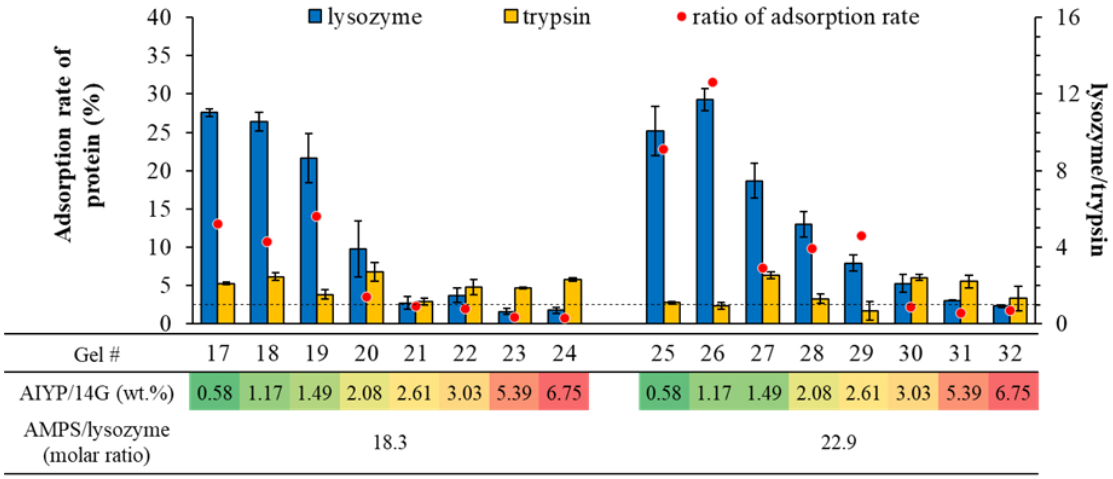

c)

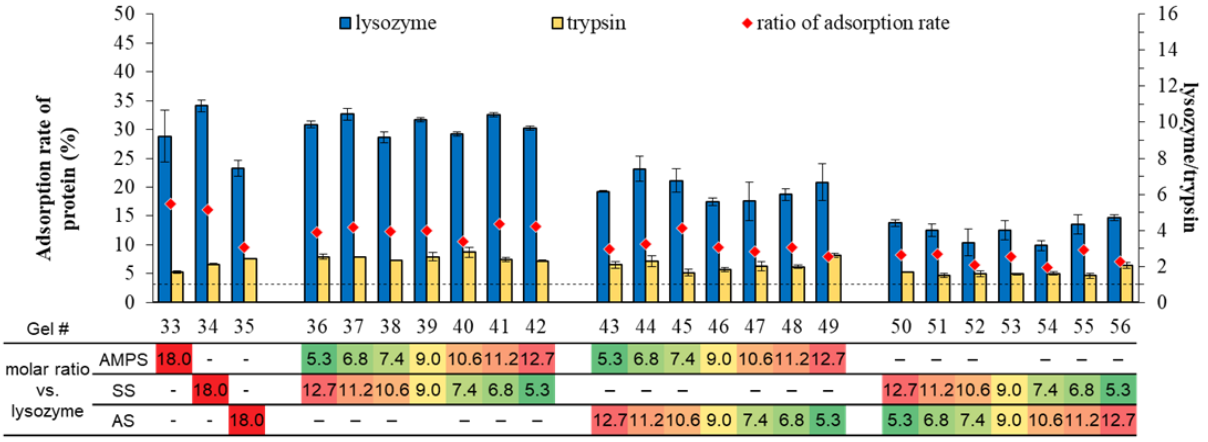

d)

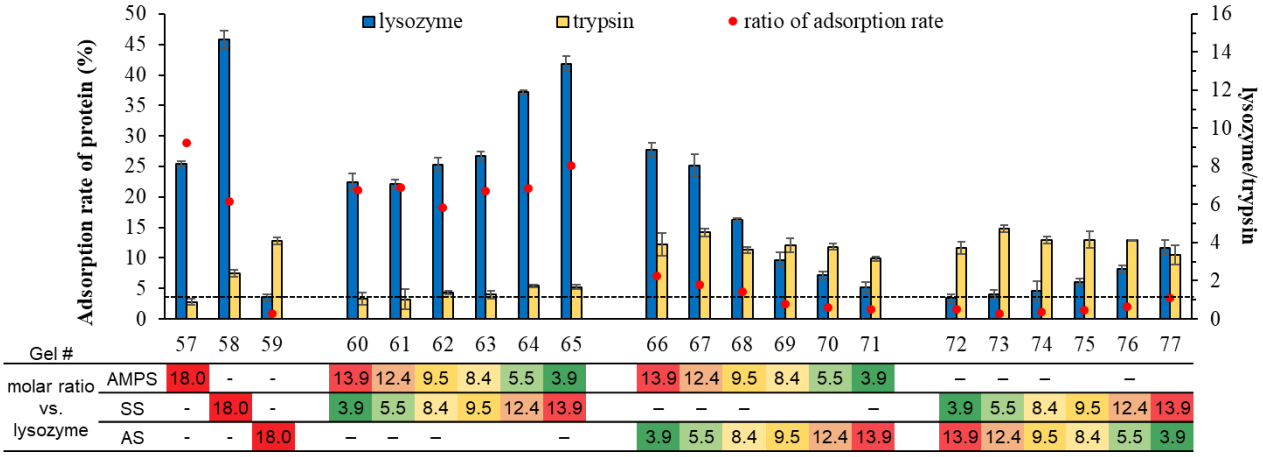

Figure 5. Adsorption performance toward lysozyme and trypsin of MIP hydrogels #1-77. Adsorption condition: gel size, 100 μL; solution volume, 2.5 mL; concentration of protein, 0.02 mM; concentration of NaCl, 50 mM; solvent, 1.0 mM Tris-HCl buffer (pH 7.1).

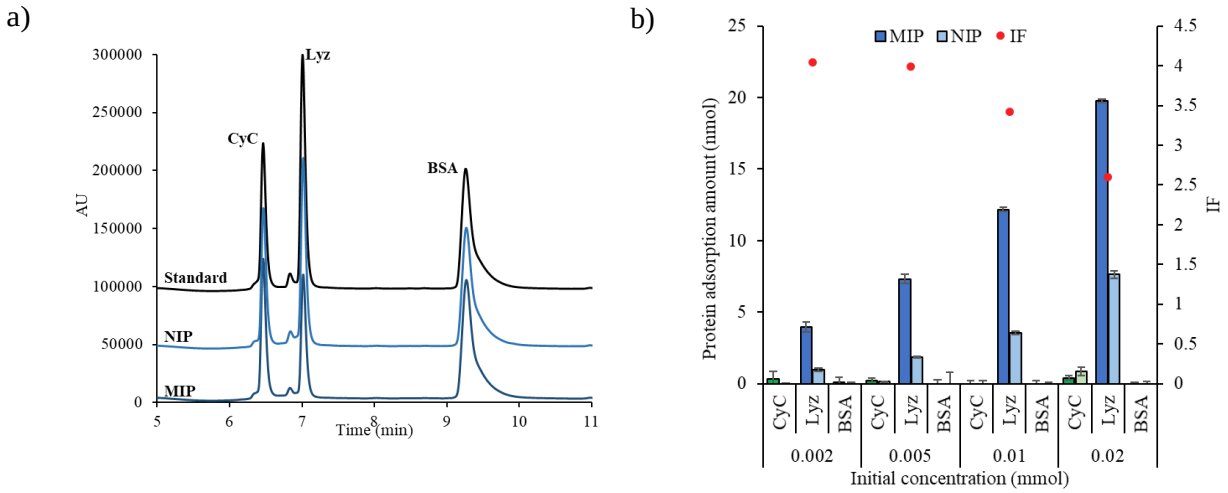

Figure 6. a) Chromatograms of the standard protein solution after immersing in NIP and MIP at 0.01 mM of each protein concentration. b) Adsorption performance of #37 MIP and NIP in the mixing protein solution at different initial concentrations. Adsorption condition: gel size, 100 µL; solution volume, 2.5 mL; concentration of proteins, 0.002 – 0.02 mM; concentration of NaCl, 50 mM; solvent, 1.0 mM Tris-HCl buffer (pH 7.1). The abbreviation for proteins; Cyc = cytochrome c, Lyz = lysozyme, and BSA = Bovine serum albumin.

4. Conclusions

In this work, we successfully developed a microfluidic device that can transfer solutions with a different flow rate to acquire multivariate data. The performance of the fabricated device was evaluated by comparing experimental data with the simulation value. It was confirmed that experimental data obtained from the devices could distribute the solution at almost the same flow rate ratio as the simulation result. We also evaluated the amount of dispensed liquid, and the result confirmed that it could be distributed with high reproducibility. The performance of the dispensing device was also compared with a commercially available pipette for transferring solutions to acquire multivariate data between the reaction of ANS and BSA. The result shows no significant difference in the fluorescence intensity of the data obtained from

dispensing devices and micropipettes, demonstrating the use of dispensing devices to get complex data with less labor and time to vary the variation condition.

Finally, we demonstrated the use of this dispensing device for preparing the MIP hydrogel by varying polymerization solution composition for the lysozyme imprinted hydrogel. It was shown that each polymerization component could affect the adsorption performance differently. Besides, the hydrogel with high specificity adsorption toward lysozyme can be obtained. These results show the possibility of acquiring multivariate data using a dispensing device for the analysis and consideration of optimization conditions by simultaneously preparing samples under different conditions.

To acquire the multivariate data, not only the preparation process that labor work needs to be reduced, but also other processes in this experiment. Even though the microfluidic dispensing device can reduce the time in MIP hydrogel preparation step, processes that are time and labor-intensive still remain. Therefore, we hope that other high-throughput instruments to utilize MIP research will be developed in the future.

References

(1) Culver, H. R.; Peppas, N. A. Protein-Imprinted Polymers: The Shape of Things to Come? *Chem. Mater.* **2017**, *29* (14), 5753–5761.

(2) Li, X.; Husson, S. M. Adsorption of Dansylated Amino Acids on Molecularly Imprinted Surfaces: A Surface Plasmon Resonance Study. *Biosens. Bioelectron.* **2006**, *22* (3), 336–348.

(3) Cantarella, M.; Carroccio, S. C.; Dattilo, S.; Avolio, R.; Castaldo, R.; Puglisi, C.; Privitera, V. Molecularly Imprinted Polymer for Selective Adsorption of Diclofenac from Contaminated Water. *Chem. Eng. J.* **2019**, *367* (February), 180–188.

(4) Matsunaga, T.; Takeuchi, T. Crystallized Protein-Imprinted Polymer Chips. *Chem. Lett.* **2006**, *35* (9), 1030–1031.

(5) Takeuchi, T.; Goto, D.; Shinmori, H. Protein Profiling by Protein Imprinted Polymer Array. *Analyst* **2007**, *132* (2), 101–103.

(6) Jenik, M.; Schirhagl, R.; Schirk, C.; Hayden, O.; Lieberzeit, P.; Blaas, D.; Paul, G.; Dickert, F. L. Sensing Picornaviruses Using Molecular Imprinting Techniques on a Quartz Crystal Microbalance. *Anal. Chem.* **2009**, *81* (13), 5320–5326.

(7) Altintas, Z.; Pocock, J.; Thompson, K. A.; Tothill, I. E. Comparative Investigations for Adenovirus Recognition and Quantification: Plastic or Natural Antibodies? *Biosens. Bioelectron.* **2015**, *74*, 996–1004.

(8) Zhang, J.; Wang, Y.; Lu, X. Molecular Imprinting Technology for Sensing Foodborne Pathogenic Bacteria. *Anal. Bioanal. Chem.* **2021**, *413* (18), 4581–4598.

(9) Zhao, G.; Liu, J.; Liu, M.; Han, X.; Peng, Y.; Tian, X.; Liu, J.; Zhang, S. Synthesis of Molecularly Imprinted Polymer via Emulsion Polymerization for Application in Solanesol Separation. *Appl. Sci.* **2020**, *10* (8), 2868.

(10) Lu, Y.; Zhu, Y.; Zhang, Y.; Wang, K. Synthesizing Vitamin e Molecularly Imprinted Polymers via Precipitation Polymerization. *J. Chem. Eng. Data* **2019**, *64* (3), 1045–1050.

(11) Dong, C.; Shi, H.; Han, Y.; Yang, Y.; Wang, R.; Men, J. Molecularly Imprinted Polymers by the Surface Imprinting Technique. *Eur. Polym. J.* **2021**, *145* (September 2020), 110231.

(12) Guo, Z.; Florea, A.; Jiang, M.; Mei, Y.; Zhang, W.; Zhang, A.; Săndulescu, R.; Jaffrezic-Renault, N. Molecularly Imprinted Polymer/Metal Organic Framework Based Chemical Sensors. *Coatings* **2016**, *6* (4), 42.

(13) Qian, K.; Fang, G.; Wang, S. A Novel Core-Shell Molecularly Imprinted Polymer Based on Metal-Organic Frameworks as a Matrix. *Chem. Commun.* **2011**, *47* (36), 10118–10120.

(14) Ansari, S.; Karimi, M. Recent Configurations and Progressive Uses of Magnetic Molecularly Imprinted Polymers for Drug Analysis. *Talanta* **2017**, *167* (February), 470–485.

(15) Sanadgol, N.; Wackerlig, J. Developments of Smart Drug-Delivery Systems Based on Magnetic Molecularly Imprinted Polymers for Targeted Cancer Therapy: A Short Review. *Pharmaceutics* **2020**, *12* (9), 1–31.

(16) Yazdi, M. K.; Vatanpour, V.; Taghizadeh, A.; Taghizadeh, M.; Ganjali, M. R.; Munir, M. T.; Habibzadeh, S.; Saeb, M. R.; Ghaedi, M. Hydrogel Membranes: A Review. *Mater. Sci. Eng. C* **2020**,

114 (April), 111023.

(17) Alele, N.; Ulbricht, M. Membrane-Based Purification of Proteins from Nanoparticle Dispersions: Influences of Membrane Type and Ultrafiltration Conditions. *Sep. Purif. Technol.* **2016**, *158*, 171–182.

(18) Cheubong, C.; Yoshida, A.; Mizukawa, Y.; Hayakawa, N.; Takai, M.; Morishita, T.; Kitayama, Y.; Sunayama, H.; Takeuchi, T. Molecularly Imprinted Nanogels Capable of Porcine Serum Albumin Detection in Raw Meat Extract for Halal Food Control. *Anal. Chem.* **2020**, *92* (9), 6401–6407.

(19) Wang, C.; Javadi, A.; Ghaffari, M.; Gong, S. A PH-Sensitive Molecularly Imprinted Nanospheres/Hydrogel Composite as a Coating for Implantable Biosensors. *Biomaterials* **2010**, *31* (18), 4944–4951.

(20) Jing, G.; Wang, L.; Yu, H.; Amer, W. A.; Zhang, L. Recent Progress on Study of Hybrid Hydrogels for Water Treatment. *Colloids Surfaces A Physicochem. Eng. Asp.* **2013**, *416* (1), 86–94.

(21) Van Tran, V.; Park, D.; Lee, Y.-C. Hydrogel Applications for Adsorption of Contaminants in Water and Wastewater Treatment. *Environ. Sci. Pollut. Res.* **2018**, *25* (25), 24569–24599.

(22) Scrivano, L.; Parisi, O. I.; Iacopetta, D.; Ruffo, M.; Ceramella, J.; Sinicropi, M. S.; Puoci, F. Molecularly Imprinted Hydrogels for Sustained Release of Sunitinib in Breast Cancer Therapy. *Polym. Adv. Technol.* **2019**, *30* (3), 743–748.

(23) Mortensen, N.; Toews, P.; Bates, J. Crosslinking-Dependent Drug Kinetics in Hydrogels for Ophthalmic Delivery. *Polymers (Basel).* **2022**, *14* (2), 248.

(24) Venkataraman, A. K.; Clegg, J. R.; Peppas, N. A. Polymer Composition Primarily Determines the Protein Recognition Characteristics of Molecularly Imprinted Hydrogels. *J. Mater. Chem. B* **2020**, *8* (34), 7685–7695.

(25) Qi, M.; Zhao, K.; Bao, Q.; Pan, P.; Zhao, Y.; Yang, Z.; Wang, H.; Wei, J. Adsorption and Electrochemical Detection of Bovine Serum Albumin Imprinted Calcium Alginate Hydrogel Membrane. *Polymers (Basel).* **2019**, *11* (4), 622.

(26) Kubo, T.; Arimura, S.; Tominaga, Y.; Naito, T.; Hosoya, K.; Otsuka, K. Molecularly Imprinted Polymers for Selective Adsorption of Lysozyme and Cytochrome c Using a PEG-Based Hydrogel: Selective Recognition for Different Conformations Due to PH Conditions. *Macromolecules* **2015**, *48* (12), 4081–4087.

(27) Kubo, T.; Arimura, S.; Naito, T.; Sano, T.; Otsuka, K. Competitive ELISA-like Label-Free Detection of Lysozyme by Using a Fluorescent Monomer-Doped Molecularly Imprinted Hydrogel. *Anal. Sci.* **2017**, *33* (11), 1311–1315.

(28) Morishita, T.; Yoshida, A.; Hayakawa, N.; Kiguchi, K.; Cheubong, C.; Sunayama, H.; Kitayama, Y.; Takeuchi, T. Molecularly Imprinted Nanogels Possessing Dansylamide Interaction Sites for Controlling Protein Corona in Situ by Cloaking Intrinsic Human Serum Albumin. *Langmuir* **2020**, *36* (36), 10674–10682.

(29) Adrus, N.; Ulbricht, M. Molecularly Imprinted Stimuli-Responsive Hydrogels for Protein Recognition. *Polymer (Guildf).* **2012**, *53* (20), 4359–4366.

(30) Reddy, S. M.; Sette, G.; Phan, Q. Electrochemical Probing of Selective Haemoglobin Binding in Hydrogel-Based Molecularly Imprinted Polymers. *Electrochim. Acta* **2011**, *56* (25), 9203–9208.

(31) Whitesides, G. M. The Origins and the Future of Microfluidics. *Nature* **2006**, *442* (7101), 368–373.

(32) Perestrelo, A.; Águas, A.; Rainer, A.; Forte, G. Microfluidic Organ/Body-on-a-Chip Devices at the Convergence of Biology and Microengineering. *Sensors* **2015**, *15* (12), 31142–31170.

(33) Li, H. F.; Lin, J. M. Applications of Microfluidic Systems in Environmental Analysis. *Anal. Bioanal. Chem.* **2009**, *393* (2), 555–567.

(34) Lee, J. B.; Sung, J. H. Organ-on-a-Chip Technology and Microfluidic Whole-Body Models for Pharmacokinetic Drug Toxicity Screening. *Biotechnol. J.* **2013**, *8* (11), 1258–1266.

(35) Wu, M.-H.; Huang, S.-B.; Lee, G.-B. Microfluidic Cell Culture Systems for Drug Research. *Lab Chip* **2010**, *10* (8), 939.

(36) Ng, J. M. K.; Gitlin, I.; Stroock, A. D.; Whitesides, G. M. Components for Integrated Poly(Dimethylsiloxane) Microfluidic Systems. *Electrophoresis* **2002**, *23* (20), 3461–3473.

(37) Chen, P. C.; Chen, Y. C.; Tsai, C. M. Microfluidic Chip for Rapid Mixing and Uniform Distribution of Multiple Reagents Using Commercial Pipettes. *Microelectron. Eng.* **2016**, *150*, 57–63.

(38) Chen, Y.; Sun, W.; Luo, P.; Zhang, M.; Wang, Y.; Zhang, H.; Hu, P. A New Circular-Shape Microfluidic Network for Generating Gradients of Multiple Substances -Design, Demonstration and Application. *Sensors Actuators, B Chem.* **2019**, *283*, 247–254.

(39) Gasymov, O. K.; Glasgow, B. J. ANS Fluorescence: Potential to Augment the Identification of the External Binding Sites of Proteins. *Biochim. Biophys. Acta - Proteins Proteomics* **2007**, *1774* (3), 403–411.

(40) Rosen, C. G.; Weber, G. Dimer Formation from 1-Anilino-8-Naphthalenesulfonate Catalyzed by Bovine Serum Albumin. Fluorescent Molecule with Exceptional Binding Properties. *Biochemistry* **1969**, *8* (10), 3915–3920.

Chapter V

Specific adsorption and fluorescence detection of cytochrome c using molecularly imprinted PEG-hydrogel

Abstract

Quantification of certain proteins is usually essential requirement for clinical, biomedical, environmental, and food quality control applications. Protein imprinting polymer is one type of the molecularly imprinted polymers (MIPs) that can be used as artificial antibodies to replace the natural antibodies, which are usually expensive and low physical/chemical stability. Moreover, preparation of MIPs with signal probes allows the use for the sensor with specific recognition cavities for target molecules. In this work, a fundamental study on the preparation of MIP hydrogel as the fluorescence sensor for protein detection was investigated. Cytochrome c was selected as a model template, and a fluorescein derivative (FITC-AA) was used as a fluorescent probe. We suppose that fluorescence quenching can be observed when cytochrome is adsorbed inside the MIP hydrogel. Various parameters affecting adsorption performance and fluorescence intensity were investigated. Under the optimal conditions, the MIP hydrogel showed high selective adsorption and sensitive fluorescent response for cytochrome c. Furthermore, the specificity of MIP hydrogel toward cytochrome c with other proteins was also investigated. The results showed that the MIP hydrogel provided higher selectivity when comparing adsorption performance with larger-size proteins (trypsin and BSA). However, similar high adsorption of lysozyme, which has close molecular weight and p*I*, was obtained. Interestingly, the fluorescence quenching was observed in hydrogel after adsorbing only cytochrome c. The result suggested that the MIP hydrogel can be used as a fluorescence sensor for bioanalysis applications.

1. Introduction

Molecular imprinting technology is a powerful artificial molecular recognition strategy that has been continuously studied since the first introduction by Wulff and co-workers in 1972.[1,2] In general, the molecular imprinting process involves a copolymerization of the template molecules with several types of functional monomers, crosslinkers, and initiators. Functional monomers can interact with template molecules via chemical interaction during the mixing process. The polymerization with template/functional monomers/crosslinker and subsequent removal of templates can provide a cavity with complementary size, shape, and chemical moieties to the template.[1] Resulting molecularly imprinting polymer (MIP) provides a specific cavity that allows the rebinding of the template molecule with high affinity and recognizable adsorption. Thus, MIPs can be used in various applications, such as adsorbent and separation materials,[3,4] chemical reactions catalysts,[5] drug delivery materials,[6] and chemical/biosensors. [1,7]

The early works of the molecular imprinting field aimed to separate small molecules. The success cases of small molecule imprinting motivated researchers for more complicated templates.[8] Nowadays, the MIP has become an essential tool in the field of protein recognition to mimic the natural interaction of antibodies. Compared with natural antibodies, protein MIPs offer higher chemical/physical stability with a lower cost of production. However, to get high-performance protein MIPs, some obstacles related to protein properties need to be overcome. Proteins are considered large biomolecules with high molecular weight, so that it is difficult to transport proteins in the rigid and densely crosslinked network. Additionally, proteins are easily transformed their 3D structure and decomposed in organic solvents, which are typically used for the MIP preparation.[8] Consequently, we must consider enough space to facilitate the removal and rebinding of proteins, and incompatible organic porogen should be avoided for water-soluble proteins to provide conditions close to their natural environment.

To overcome the limitation of traditional MIP for proteins, novel polymerization processes have been developed, such as surface imprinting,[9] epitope-mediated imprinting,[10] and nanoparticle imprinting.[10] Protein imprinting hydrogel is one of the successful preparation strategies that have been reported by many

researchers.[11–14] Hydrogels are "soft and wet" materials composed of a three-dimensional crosslinked network that contains a large amount of aqueous solution.[15] The biocompatibility, permeability, elasticity, and stimulus responsiveness of hydrogels allow an excellent material for biomolecule with various applications, such as drug-delivery systems[16–19] and tissue engineering.[20,21]

Biochemical sensors are sensing devices that provide signals through optical, electrical, or mechanical transitions, which can subsequently be translated to specific quantitative or semi-quantitative analytical information. Biochemical sensors are in great demand for medical diagnostic,[22,23] food analysis and quality control,[24] environmental analysis,[25] and chemical warfare agents.[26] To develop biochemical sensors, both the molecular recognition ability and the signal transducer are the crucial components. By preparing MIPs with transducer molecules, the obtained MIPs can provide capturing target molecules and interaction with transducers, thus many MIP biosensors have been successfully developed.[26–31]

According to these requirements in MIP studies, we carry out a fundamental study of MIP hydrogel as the fluorescence sensor for protein detection. Cytochrome c was employed as a model template with the interaction of a fluorescein derivative to provide a fluorescence signal. The preparation conditions to obtain high cytochrome c affinity were investigated by varying types of crosslinkers, sulfonate monomers, fluorescence and sulfonate monomer concentrations, and gel washing methods. The resulting MIP hydrogels provided a satisfying imprinting efficiency compared with their non-imprinted polymer (NIP). Furthermore, the fluorescence quenching toward cytochrome c was significantly lower than other proteins, showing a promise in using MIP hydrogel as the fluorescence sensor for cytochrome c detection.

2. Experimental

2.1 Chemicals and reagents

Poly(ethylene glycol) (PEG) dimethacrylate (9G, 14G, and 23G, where the number represents repeat units) and PEG diacrylate (14G') were kindly donated from Shin-Nakamura Chemical

(Wakayama, Japan) and utilized as received. Lysozyme chloride from egg white, bovine serum albumin (BSA), sodium *p*-styrenesulfonate (SS), fluorescein, and 2,2′-azobis[2-(2-imidazolin-2-yl)propane] (AIYP) were from Wako Pure Chemical Industries (Osaka, Japan). Fluorescein 5-isothiocyanate (FITC), allylamine (AA), 2-acrylamido-2-methylpropane sulfonic acid (AMPS), and sodium allylsulfonate (AS), were from Tokyo Chemical Industry (Tokyo, Japan). Cytochrome c from the equine heart and trypsin from the bovine pancreas were from Sigma-Aldrich Japan (Tokyo, Japan), and other reagents were from Nacalai Tesque (Kyoto, Japan). All solvents were analytical or HPLC grade.

2.2 Instruments

The synthesized monomer was characterized by JNM-ECA500 (JEOL, Japan) as an NMR spectrometer and Nicolet iS5 ATR (Thermo Fisher Scientific, USA) as an FT-IR spectrometer. The absorbance of chemicals was measured using UV-2450 (Shimadzu, Japan) as a UV-Vis spectrophotometer. The fluorescence was measured using RF-5300PC (Shimadzu) as a fluorescence spectrometer. The absorbance and fluorescence were also measured using a SpectraMax iD3 plate reader (Molecular Devices, Tokyo, Japan). Photo of hydrogel under UV light can be obtained BZ-X810 fluorescence microscope (Keyence, Japan).

2.3 Preparation of MIP hydrogels

The hydrogels were prepared using the compositions shown in Tables 1 to 5. Firstly, the hydrogels were prepared by mixing the polymerization composition except for TEMED. Then, the mixing solution was purged with Ar gas for 30 min to remove oxygen. After purging Ar gas, TEMED was added into the mixture and quickly transferred to 1-mL syringes (inner diameter of 4 mm). The polymerization solution was allowed to polymerize overnight. After polymerization, the hydrogels were peeled off from the

polymerization containers, cut into small pieces, and transferred to a 50 mL microtube for washing the unreacted components. For reference, NIP hydrogels were also prepared with the same procedure without cytochrome c.

Table 1. Compositions of MIP hydrogel used in washing process experiment.

Gel#	Template	Fluorescence monomer	Monomer	Cross-linker	Initiator	Solvent
1	Cytochrome c 0.9 μmol	FITC-AA 0.9 μmol	AMPS 21.2 μmol	14G 215 μL	10.6 μL 30% APS 2 μL TEMED	1.0 mM Tris–HCl buffer (pH 7.4) 2.7 mL, DMSO 0.3 mL

Table 2. Compositions of MIP hydrogels with different AMPS: SS ratios.

Gel#	Template	Fluorescence monomer	Monomer	Cross-linker	Initiator	Solvent
2	Cytochrome c 0.45 μmol	FITC-AA 0.45 μmol	AMPS 10.6 μmol	14G' 215 μL	10.6 μL 30% APS 2 μL TEMED	1.0 mM Tris–HCl buffer (pH 7.4) 2.7 mL, DMSO 0.3 mL
3			AMPS 7.95 μmol SS 2.65 μmol			
4			AMPS 5.3 μmol SS 5.3 μmol			
5			AMPS 2.65 μmol SS 7.95 μmol			
6			SS 10.6 μmol			

Table 3. Compositions of MIP hydrogels with different cross-linker concentrations and types of cross-linkers.

Gel#	Template	Fluorescence monomer	Monomer	Cross-linker	Initiator	Solvent
7	Cytochrome c 0.45 μmol	FITC-AA 0.45 μmol	SS 10.6 μmol	14G' 215 μL (110.8 mM)	10.6 μL30% APS 2 μL TEMED	1.0 mM Tris–HCl buffer (pH 7.4) 2.7 mL, DMSO 0.3 mL
8				14G' 268.8 μL (138.45 mM)		
9				14G' 322.5 μL (166.2 mM)		
10				14G' 430 μL (221.6 mM)		
11				9G' 193.5 μL (138.45 mM)		
12				23G' 422 μL (138.45 mM)		

Table 4. Compositions of MIP hydrogels with different cytochrome c and FITC-AA concentrations.

Gel#	Template	Fluorescence monomer	Monomer	Cross-linker	Initiator	Solvent
13	Cytochrome c 0.45 μmol	FITC-AA 0.45 μmol	SS 10.6 μmol	14G' 430 μL	10.6 μL 30% APS 2 μL TEMED	1.0 mM Tris–HCl buffer (pH 7.4) 2.7 mL, DMSO 0.3 mL
14	Cytochrome c 0.225 μmol	FITC-AA 0.225 μmol				
15	Cytochrome c 0.15 μmol	FITC-AA 0.15 μmol				
16	Cytochrome c 0.113 μmol	FITC-AA 0.113 μmol				
17	Cytochrome c 0.45 μmol	FITC-AA 0.113 μmol				

* Composition of hydrogel #13 is the same as hydrogel #12 in Table 3

Table 5. Compositions of MIP hydrogels with different SS concentrations.

Gel #	Template	Fluorescence monomer	Monomer	Cross-linker	Initiator	Solvent
18	Cytochrome c 0.15 μmol	FITC-AA 0.15 μmol	SS 21.2 μmol	14G' 430 μL	10.6 μL 30% APS 2 μL TEMED	1.0 mM Tris–HCl buffer (pH 7.4) 2.7 mL, DMSO 0.3 mL
19			SS 10.6 μmol			
20			SS 5.3 μmol			
21			SS 3.53 μmol			
22			SS 2.65 μmol			

* Composition of hydrogel #19 is the same as hydrogel #15 in Table 4

To remove the templates from the MIP hydrogels, the gel pieces were immersed in 50 mL of 1 M NaCl, 1× Tris-Gly buffer pH 8.6, and 1 mM Tris-HCl pH 7.4 for 4, 2, and 1 time, respectively. The washing process was performed at 40 ºC, and each washing time was performed for 24 h. As a control reference, the NIP hydrogels were washed in the same manner.

2.4 Adsorption and fluorescence measurement

The proteins, including cytochrome c, lysozyme, trypsin, and BSA, were dissolved into a buffered solution to make an adsorption solution. The buffered solution contained (0.01 – 0.06 mM) protein in 20 mM NaCl 1 mM pH 7.4 Tris-HCl. To test the protein adsorption ability, hydrogels were put into 0.5 mL of the adsorption solution and kept shaking for 24 h with a shaking apparatus. The supernatant of the adsorption solvent was examined under a UV spectrometer or microplate reader to detect the concentration of remaining proteins, which can be further calculated to adsorption amount. Each test was conducted with three replicates. For lysozyme, trypsin, and BSA detection, the UV absorbance at 280 nm was examined. For cytochrome c detection, the UV absorbance at 410 nm was examined. The adsorption amount, percent adsorption, and imprinting factor (IF) were calculated as follows:

Adsorption amount = (protein concentration before adsorption – protein concentration after adsorption) x volume of adsorption solution (1)

$$\% \text{ Adsorption} = \frac{\text{Adsorption amount of protein in hydrogel}}{\text{Initial amount of protein in solution}} \times 100 \quad (2)$$

$$\text{Imprinting factor} = \frac{\text{Adsorption amount of MIP hydrogel}}{\text{Adsorption amount of NIP hydrogel}} \quad (3)$$

Fluorescent measurement was performed by placing each hydrogel into the well of a 96-well microplate. Fluorescence intensity was measured using $\lambda_{Excitation}$ = 450 nm (or otherwise indicated), and fluorescent spectrum was obtained in the range of 500 – 650 nm.

3. Result and discussion

3.1 Template removal conditions

Template removal process is an essential issue considerably affecting imprinting performance. The remaining templates inside of the MIP cavity may block the accessing of target molecule to the affinity site or leak templates into the solution during adsorption, leading to fault information on adsorption performance. Therefore, various types of washing solutions were used in this study. Since the functional monomers used in this study have sulfonate groups and interact with cytochrome c by electrostatic interaction, the washing solution including NaCl, Na_2SO_4, NaOH, carbonate buffer pH 11, *N*-cyclohexyl-3-aminopropanesulfonic acid (CAPS) buffer pH 11, and Tris-Glycine buffer pH 8.6 were employed. In this study, we assumed that the salted solutions as the washing solution increase the ionic strength, which subsequently interferes with the interaction between cytochrome c and sulfonate groups in hydrogels, resulting in release of cytochrome c. For basic buffered solutions, we assumed that the high abundance of OH^- species should interact with sulfonate groups inside of hydrogel, and competitive interaction between OH^- and template molecules might result in releasing the template. Our previous study found that

temperature can improve the washing efficiency since dissociation reaction is an endothermic process.[32] Therefore, the template removal process was evaluated at 40 °C. The Tris-Gly buffer was used as the washing solution on days 5-6 of all experiments since it was found that washing with salted solution alone cannot remove the unreacted FITC-AA molecule, and Tris-Gly buffer can activate FITC-AA inside of the hydrogel into the fluorescence active form. Tris-HCl buffer was used as the last washing solution to adjust the hydrogel's condition to be identical to the adsorption condition.

Table 6. Washing conditions used in this study.

Day	Method 1	Method 2	Method 3	Method 4	Method 5	Method 6	Method 7
1	1 M NaCl	1 mM NaOH	1 mM Carbonate buffer pH 11	1 mM CAPS buffer pH 11	1 M NaOH	1 M Na_2SO_4	1x Tris-Gly buffer
2	1 M NaCl	1 mM NaOH	1 mM Carbonate buffer pH 11	1 mM CAPS buffer pH 11	1 M NaOH	1 M Na_2SO_4	1x Tris-Gly buffer
3	1 M NaCl	10 mM NaOH	10 mM Carbonate buffer pH 11	10 mM CAPS buffer pH 11	1 M NaCl	1 M NaCl	1x Tris-Gly buffer
4	1 M NaCl	100 mM NaOH	100 mM Carbonate buffer pH 11	27 mM CAPS buffer pH 11	1 M NaCl	1 M NaCl	1x Tris-Gly buffer
5	1x Tris-Gly buffer						
6	1x Tris-Gly buffer						
7	1 mM Tris-HCl						

During the washing process, hydrogel shrinkage and swollen phenomenon were observed, especially a washing with Na_2SO_4 showed a significant shrinkage of the hydrogels compared with other washing solutions. However, all hydrogels swelled back again after washing with Tris-Gly and Tris-HCl. After the completion of the washing process, the hydrogels from different washing processes were tested for cytochrome c adsorption. The results revealed that only MIP hydrogels washed with NaCl and Na_2SO_4 gave better cytochrome c adsorption than that of NIP hydrogels. This result indicated that the washing solution was important in the template removal process. If an inadequate washing solution was used, it

could lead to incomplete template removal and result in an imprinting factor lower than 1. In addition, the washing solutions also affected the color/fluorescence of the hydrogel. As shown in Figure 1a, the color of the MIP hydrogel washed with method 5 was significantly different from its NIP. Although the MIP hydrogel washed with Na_2SO_4 gave the highest cytochrome c adsorption, unidentified white particles were found inside both MIP and NIP hydrogels. Therefore, NaCl solution with Tris-Gly and Tris-HCl (method 1) was selected as a washing procedure during the later experiment.

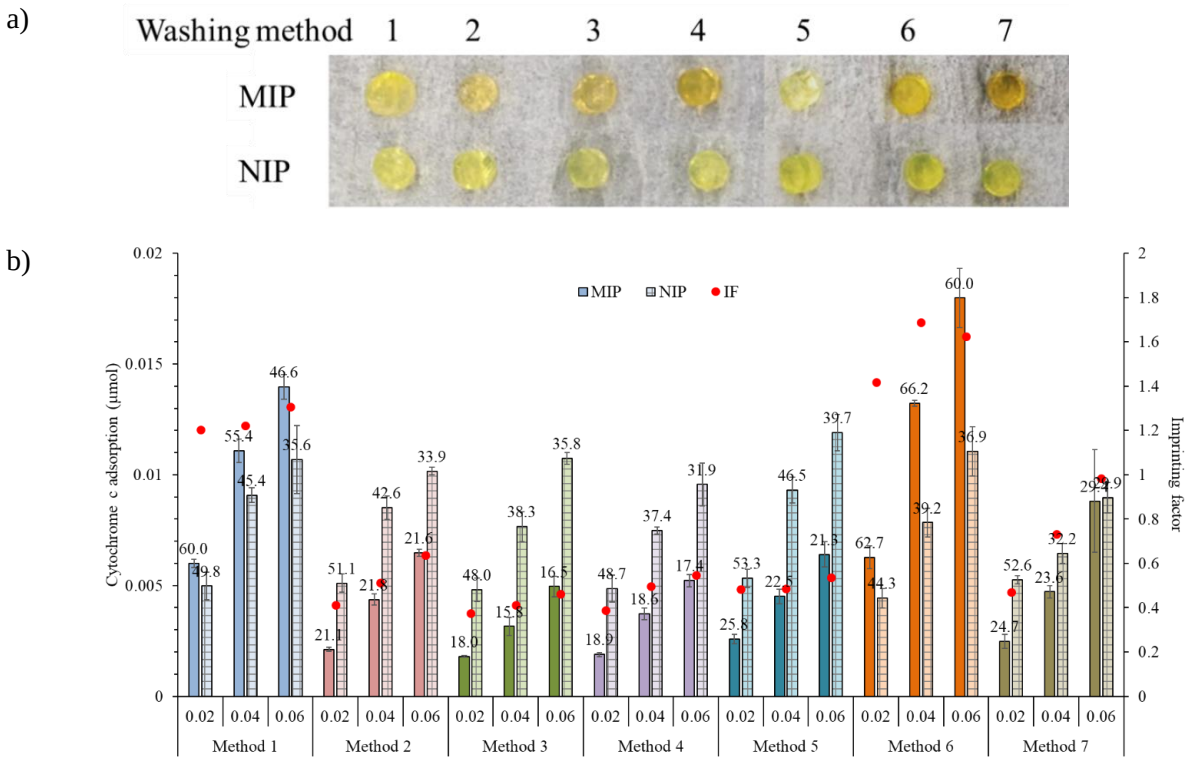

Figure 1. (a) The picture of MIP and NIP hydrogel after a 6-day washing under different conditions. (b) Cytochrome c adsorption performance of MIP and NIP hydrogels after washing with different conditions. The number above each bar indicates the adsorption percent of each hydrogel.

3.2 Effect of the ratio between AMPS and SS for cytochrome c adsorption

The main functional group that interacts with cytochrome in the prepared hydrogels is a sulfonate group. The previous study of lysozyme MIP hydrogels showed that the kinds of sulfonate monomers could affect adsorption selectivity. Therefore, the hydrogels prepared with the different types of sulfonate monomers were prepared. The result shows that AMPS gave the highest cytochrome c adsorption than that of using SS and SA, even in the NIP hydrogels (data not shown). However, it also found that the template removal from MIP hydrogels prepared with AMPS was the most difficult compared to other MIP hydrogels when the washing process was performed at room temperature. As another point, the selection of the monomers affected the alteration of color of the prepared hydrogels. Thus, the ratio between AMPS and SS was studied to obtain high adsorption performance with color/fluorescence intensity. In this experimental, the hydrogels were prepared with 14 G' instead of 14G, and the amount of fluorescence monomer was 2-times lower than above to reduce unreacted fluorescence molecule.

The result shows that all the MIP hydrogels gave higher adsorption performance than NIP hydrogels over IF of 2.5 (Figure 2a). The combination of AMPS and SS provided higher adsorption than using only one sulfonate monomer. However, when the AMPS ratio increased, the fluorescence intensity between MIP and NIP hydrogels also increased. After the adsorption, the fluorescence intensity of the hydrogel was measured. The fluorescence intensity of NIP hydrogel before adsorption was higher than MIP hydrogels in all preparation conditions. However, when comparing the fluorescence intensity in the term of the fluorescence ratio (I_0/I), it was found that all the MIP hydrogels showed I_0/I higher than that NIP hydrogels (Figure 2b), which indicated higher adsorption performance of MIP over NIP and resulted in more quenching interaction between FITC-AA and cytochrome C in MIP hydrogel.

a)

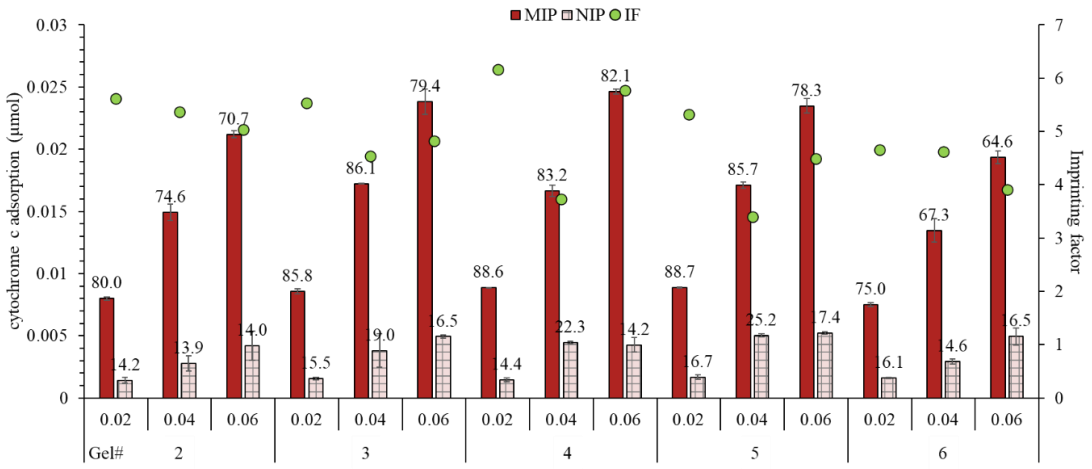

b)

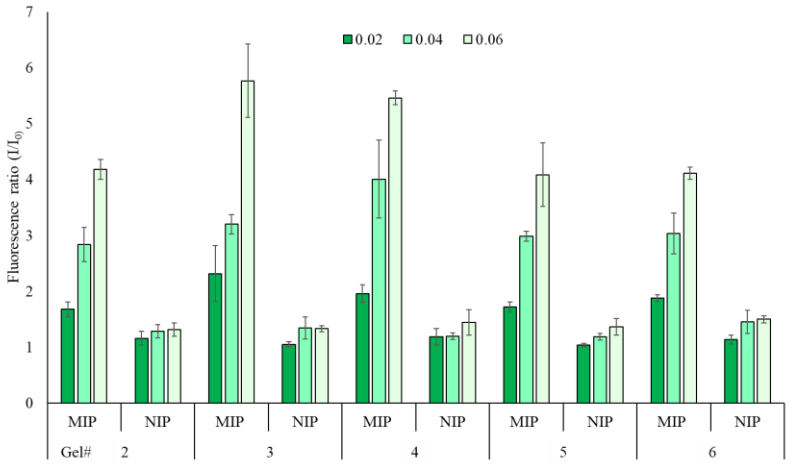

Figure 2. a) Cytochrome c adsorption at different initial concentrations using hydrogels prepared with different AMPS: SS ratios. The number above each bar indicates the adsorption percent of each hydrogel toward initial concentration of cytochrome c. b) Fluorescence ratio (I/I_0) of hydrogel after cytochrome c adsorption. Fluorescence intensity was measured at λ_{Ex} = 450 nm, λ_{Em} = 530 nm.

3.3 Effect of the types and concentration of crosslinkers

The crosslinker is an essential component of the hydrogel that can tune the flexible properties of the hydrogel. The length of crosslinkers also affects the pore size of the polymer network. At the fixed concentration, the longer chain crosslinker would give the larger pore size to facilitate the large

biomolecules uptake and elution better. On the other hand, when the amount of the crosslinker increases, it assumed that the density of the hydrogel also increases, making it difficult for large biomolecules to permeate. Thus, we employed 14G' with different concentrations and 9G'/23G' were used for hydrogel preparation.

The adsorption evaluations showed that both concentration and types of crosslinker significantly affected the recognition properties of the hydrogel. When the crosslinker concentration increases, cytochrome c adsorption also decreases due to the denser polymer network. For the crosslinker length, the MIP hydrogel prepared with 9G', which has the shortest length in this experimental, showed the highest cytochrome c adsorption (Figure 3). A shorter crosslinker provided a more rigid polymer structure; thus, the MIP sites would be more robust. Notably, NIP hydrogels also showed the same trend as MIPs, resulting in a lower imprinting factor. The high adsorption in NIP hydrogel revealed high unspecific adsorption in the hydrogel. Therefore, high cytochrome c adsorption performance with less unspecific adsorption is the key factor to be optimized.

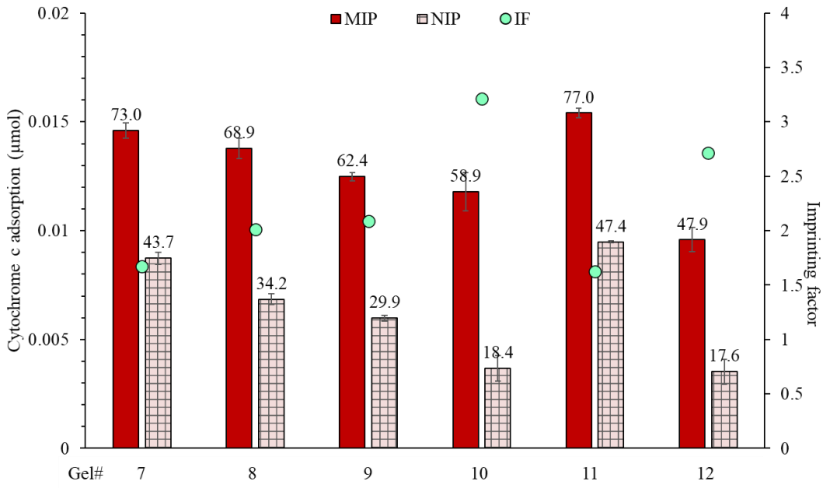

Figure 3. Cytochrome c adsorption using hydrogels prepared with different concentrations and types of crosslinkers. The number above each bar indicates the adsorption percent of each hydrogel toward initial concentration of cytochrome c. 0.04 mM cytochrome c was used in this experiment.

3.4 Effect of the concentration of FITC-AA and template

Amount of the template molecules is vital for MIP preparation. The most suitable amount of templates was investigated by preparing hydrogel at the different template and FITC-AA concentrations as shown in Table 4. The result showed that the trend in the cytochrome c adsorption could not be seen even though the amount of template and FITC-AA was decreased (Figure 4a). This result suggested that FITC-AA is not the primary functional group interacting with cytochrome c. When the amount of SS is equal in the hydrogel component, the adsorption performance is quite the same. It should be noted that when the ratio of cytochrome c: FITC-AA is 4:1, was employed, higher adsorption than at a ratio of 1:1 was observed. However, this higher ratio of cytochrome c also affects the fluorescence intensity of the obtained MIP hydrogel, which is significantly different from its NIP (Figure 4b).

a)

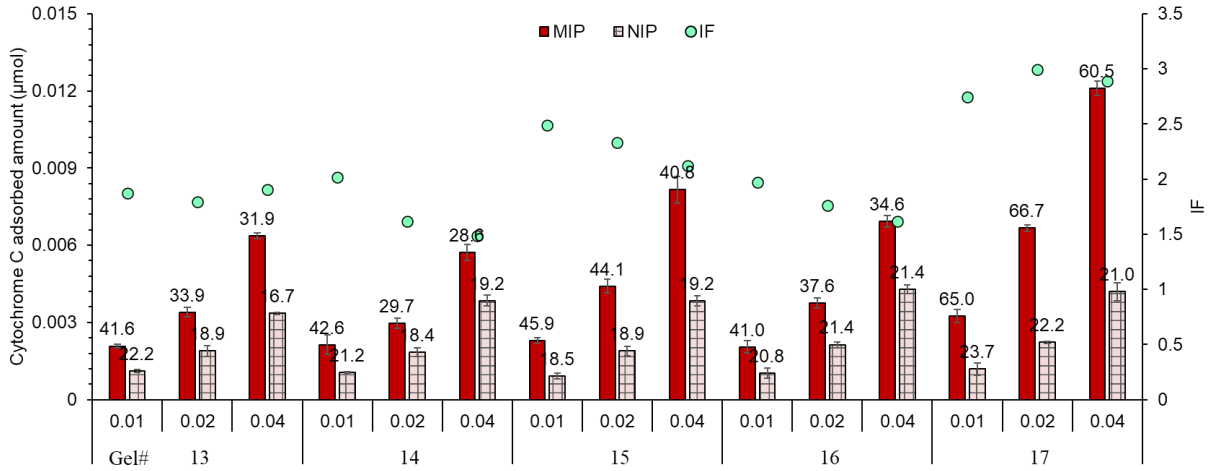

b)

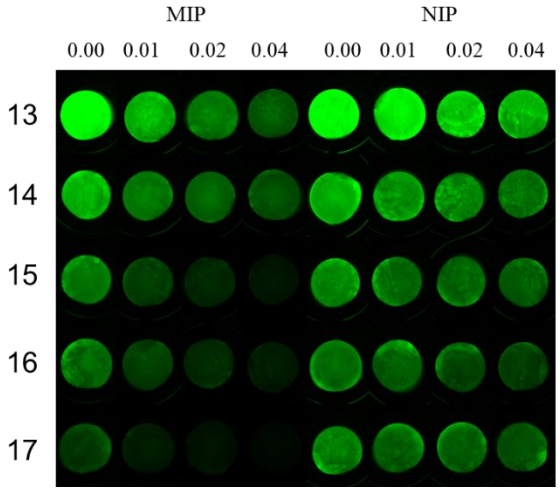

Figure 4. a) Cytochrome c adsorption at different initial concentrations using hydrogels prepared with different cytochrome c and FITC-AA concentrations. The number above each bar indicates the adsorption percent of each hydrogel toward initial concentration of cytochromec.. b) Fluorescence intensity of each hydrogel after cytochrome c adsorption.

3.5 Effect of the template ratio toward functional monomers

As discussed above, the amount of sulfonate monomer really impacted the adsorption performance of both MIP and NIP hydrogel. The amount of sulfonate monomer should be enough to interact with template molecules and create recognition sites. However, too much amount of monomers may lead to unspecific adsorption. Therefore, the ratio of SS and template was optimized in this section. Figure 5 shows the same adsorption trend as the hypothesis that the cytochrome can be adsorbed inside the MIP hydrogel better when the ratio of SS is high. However, the same trend was also observed for NIP hydrogels, meaning more unspecific adsorption occurs and lower imprinting factor. Even though MIP hydrogel prepared with lower ratio of SS provided high IF and the adsorption amount, giving the fluorescence change needs to be considered.

a)

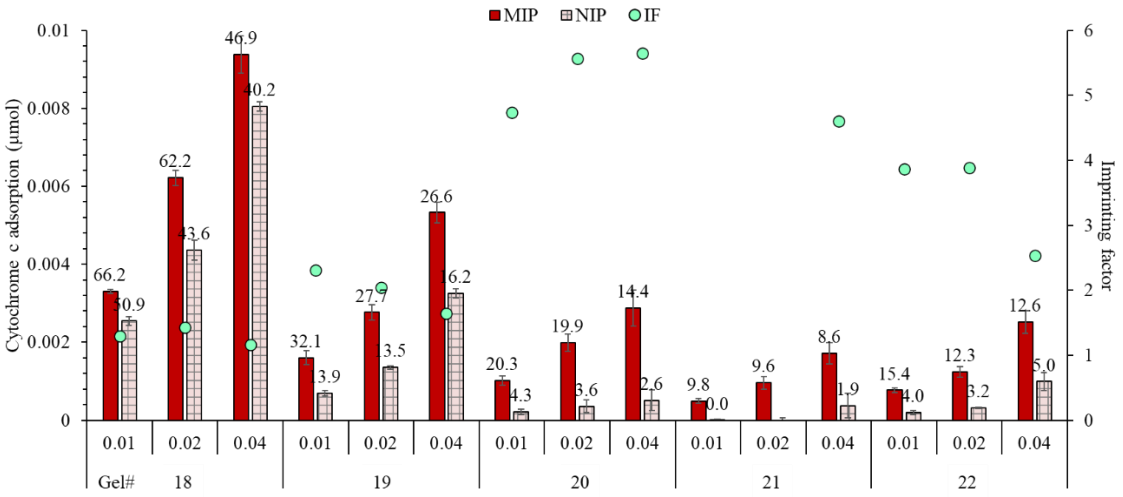

b)

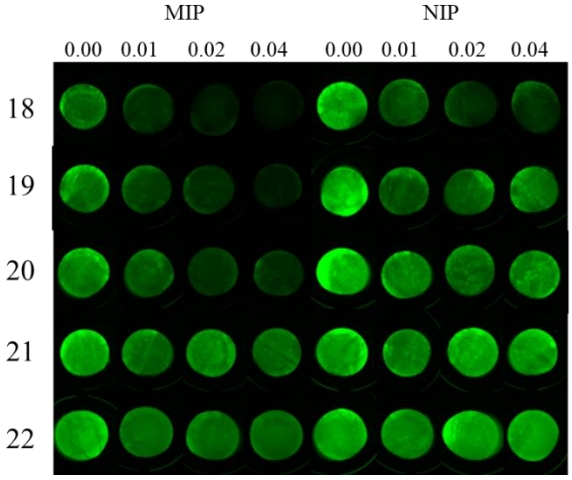

Figure 5. a) Cytochrome c adsorption at different initial concentrations using hydrogels prepared with different SS: cytochrome c ratios. The number above each bar indicates the adsorption percent of each hydrogel toward initial concentrations. b) Fluorescence intensity of each hydrogel after cytochrome c adsorption.

3.6 Adsorption selectivity and effect of ionic strength in the adsorption solvents

Another critical factor in adsorption was ionic strength of atmosphere. Then, the selectivity of hydrogels was tested at different concentrations of NaCl (0, 20, 50, 100 mM). In the adsorption without any NaCl in the adsorption solution, the selectivity between MIP and NIP cannot be observed since both hydrogels show almost 99% cytochrome c adsorption (data not shown) by strong ionic interaction. This result shows the essential of NaCl in competing with ionic interaction between proteins to functional monomers. At 20 mM NaCl, the higher cytochrome adsorption performance of MIP over its NIP was observed (Figure 6a). However, the interaction between proteins and MIP hydrogels was extensively suppressed, so less than 20% of cytochrome c was adsorbed in MIP hydrogel when NaCl concentration was over 50 mM. Therefore, 20 mM NaCl was used as the ionic strength in the adsorption performance.

The selectivity is crucial to demonstrate the specific recognition of the MIPs toward their templates. The selectivity of the cytochrome c hydrogel was tested with other non-template proteins, including lysozyme, trypsin, and BSA. Cytochrome c, lysozyme, and trypsin have similar isoelectric points (p*I*), as shown in Table 7, and carry positive charges under the experimental condition (Tris-HCl pH 7.4). These positive charged proteins might show affinity to the sulfonate monomers. On the other hand, BSA, which has a p*I* of 4.7, carries negative charges. Besides, lysozyme has a similar molecular weight to cytochrome c, whereas trypsin and BSA are around 2-fold and 5-fold larger than cytochrome c.

Table 7. Molecular weight and isoelectric point of proteins

Protein	Molecular weight (kDa)	Isoelectric point, p*I*
Cytochrome c	12.3	10.2
Lysozyme	14.4	10.8
Trypsin	23.8	10.6
BSA	66.0	4.7

For the selectivity of hydrogel, compared to cytochrome c adsorption at 20 mM NaCl, the adsorption capacity of the MIP and NIP hydrogels for BSA was significantly lower (Figure 6a). This result indicated that BSA adsorption was resisted by the ionic repulsion force. For trypsin adsorption, a larger molecule with a similar p*I*, MIP hydrogel also exhibited lower adsorption than cytochrome c. This result indicated that small cavities were formed inside this MIP gel, which could hinder the access of large molecules to specific sites. However, MIP and NIP gels showed higher lysozyme adsorption capacity. This phenomenon may be because lysozyme shares a similar molecular size and p*I* as cytochrome c, allowing it to access the imprinted cavities of cytochrome c easily. In contrast, the NIP gel demonstrated more significant adsorption to lysozyme, indicating that lysozyme had easier access to the sulfonate group than cytochrome c under the given hydrogel conditions. Although increasing NaCl concentration could suppress the lysozyme adsorption similar to cytochrome c adsorption, higher adsorption of cytochrome c was not identified in any conditions. On the other hand, interestingly, the fluorescence quenching can be observed in hydrogel after adsorbing only for cytochrome c (Figure 6b), showing that fluorescence detection is more selective toward cytochrome c than other proteins. The constructed recognition sites showed similar selectivity for cytochrome c and lysozyme, whereas fluorescent moiety was interacted only with cytochrome c. The results suggested that the fluorescent monomer was effectively functionalized for the template molecule.

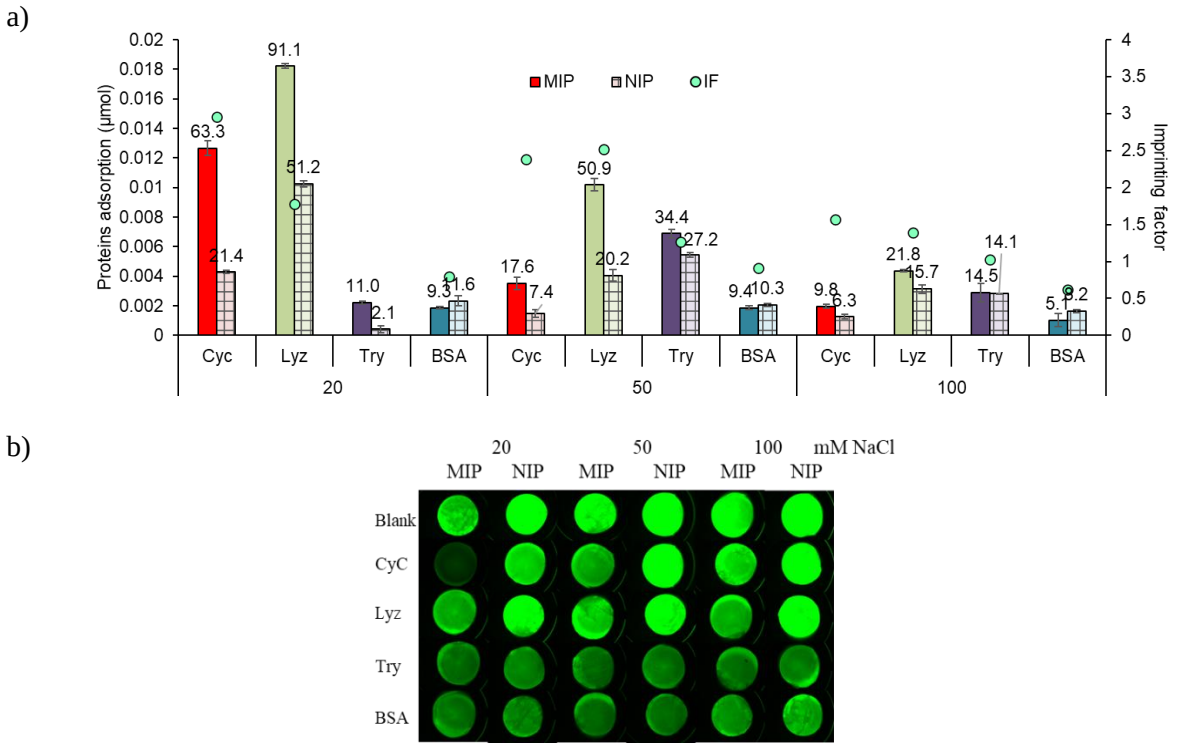

Figure 6. a) Protein adsorption of hydrogel #12 at different NaCl concentrations. b) fluorescence intensity of each hydrogel after protein adsorption. 0.04 mM of each protein was used in this experiment.

4. Conclusion

This work involves a fundamental study on preparing PEG-based MIP hydrogel as the fluorescence sensor for protein detection. Cytochrome c was employed as a model template, and FITC-AA was employed as a fluorescence probe. Various preparation and adsorption parameters, including the washing processes, ratios between AMPS and SS, concentrations of crosslinker, types of crosslinkers, template/FITC-AA/SS concentrations, and NaCl concentration in the adsorption solution, were investigated. Results showed that the combination of NaCl solution and Tris-Gly buffer provided a satisfied removal of templates. Concentrations of crosslinkers, types of crosslinkers, template/FITC-AA/SS concentrations affect both cytochrome c adsorption and fluorescence quenching on hydrogels. Most of preparation conditions provided high cytochrome c adsorption on MIP hydrogels, however, the same trend also occurred with NIP

hydrogel, indicating that the high adsorption was not due to specific recognition size. On the other hand, it was found that NaCl concentration significantly affects protein adsorption. Comparing the adsorption performance of the obtained MIP hydrogels with other proteins showed that the MIP hydrogel showed higher specificity toward cytochrome c than trypsin and BSA. Additionally, the MIP hydrogel showed similar high adsorption to lysozyme. Interestingly, the fluorescence quenching was observed in hydrogel after adsorbing only for cytochrome c. This result shows that fluorescence detection is very selective toward cytochrome c than other proteins. Consequently, the present MIP hydrogel supposed a promising use as a cytochrome c fluorescence sensor for bioanalysis applications.

References

(1) Li, R.; Feng, Y.; Pan, G.; Liu, L. Advances in Molecularly Imprinting Technology for Bioanalytical Applications. *Sensors (Switzerland)* **2019**, *19* (1).

(2) Wulff, G.; Sarhan, A. Über Die Anwendung von Enzymanalog Gebauten Polymeren Zur Racemattrennung. *Angew. Chemie* **1972**, *84* (8), 364.

(3) Hu, Y.; Pan, J.; Zhang, K.; Lian, H.; Li, G. Novel Applications of Molecularly-Imprinted Polymers in Sample Preparation. *TrAC - Trends Anal. Chem.* **2013**, *43*, 37–52.

(4) Hu, T.; Chen, R.; Wang, Q.; He, C.; Liu, S. Recent Advances and Applications of Molecularly Imprinted Polymers in Solid-Phase Extraction for Real Sample Analysis. *J. Sep. Sci.* **2021**, *44* (1), 274–309.

(5) Muratsugu, S.; Shirai, S.; Tada, M. Recent Progress in Molecularly Imprinted Approach for Catalysis. *Tetrahedron Lett.* **2020**, *61* (11), 151603.

(6) Sanadgol, N.; Wackerlig, J. Developments of Smart Drug-Delivery Systems Based on Magnetic Molecularly Imprinted Polymers for Targeted Cancer Therapy: A Short Review. *Pharmaceutics* **2020**, *12* (9), 1–31.

(7) Zhang, J.; Wang, Y.; Lu, X. Molecular Imprinting Technology for Sensing Foodborne Pathogenic Bacteria. *Anal. Bioanal. Chem.* **2021**, *413* (18), 4581–4598.

(8) Culver, H. R.; Peppas, N. A. Protein-Imprinted Polymers: The Shape of Things to Come? *Chem. Mater.* **2017**, *29* (14), 5753–5761.

(9) Dong, C.; Shi, H.; Han, Y.; Yang, Y.; Wang, R.; Men, J. Molecularly Imprinted Polymers by the Surface Imprinting Technique. *Eur. Polym. J.* **2021**, *145* (September 2020), 110231.

(10) Khumsap, T.; Corpuz, A.; Nguyen, L. T. Epitope-Imprinted Polymers: Applications in Protein Recognition and Separation. *RSC Adv.* **2021**, *11* (19), 11403–11414.

(11) Adrus, N.; Ulbricht, M. Molecularly Imprinted Stimuli-Responsive Hydrogels for Protein Recognition. *Polymer (Guildf).* **2012**, *53* (20), 4359–4366.

(12) Venkataraman, A. K.; Clegg, J. R.; Peppas, N. A. Polymer Composition Primarily Determines the Protein Recognition Characteristics of Molecularly Imprinted Hydrogels. *J. Mater. Chem. B* **2020**, *8* (34), 7685–7695.

(13) Kubo, T.; Arimura, S.; Tominaga, Y.; Naito, T.; Hosoya, K.; Otsuka, K. Molecularly Imprinted Polymers for Selective Adsorption of Lysozyme and Cytochrome c Using a PEG-Based Hydrogel: Selective Recognition for Different Conformations Due to PH Conditions. *Macromolecules* **2015**, *48* (12), 4081–4087.

(14) Cheubong, C.; Yoshida, A.; Mizukawa, Y.; Hayakawa, N.; Takai, M.; Morishita, T.; Kitayama, Y.; Sunayama, H.; Takeuchi, T. Molecularly Imprinted Nanogels Capable of Porcine Serum Albumin Detection in Raw Meat Extract for Halal Food Control. *Anal. Chem.* **2020**, *92* (9), 6401–6407.

(15) Sun, X.; Agate, S.; Salem, K. S.; Lucia, L.; Pal, L. Hydrogel-Based Sensor Networks: Compositions, Properties, and Applications - A Review. *ACS Appl. Bio Mater.* **2021**, *4* (1), 140–162.

(16) Dreiss, C. A. Hydrogel Design Strategies for Drug Delivery. *Curr. Opin. Colloid Interface Sci.* **2020**, *48*, 1–17.

(17) Mortensen, N.; Toews, P.; Bates, J. Crosslinking-Dependent Drug Kinetics in Hydrogels for Ophthalmic Delivery. *Polymers (Basel).* **2022**, *14* (2), 248.

(18) Scrivano, L.; Parisi, O. I.; Iacopetta, D.; Ruffo, M.; Ceramella, J.; Sinicropi, M. S.; Puoci, F. Molecularly Imprinted Hydrogels for Sustained Release of Sunitinib in Breast Cancer Therapy. *Polym. Adv. Technol.* **2019**, *30* (3), 743–748.

(19) He, R.; Niu, Y.; Li, Z.; Li, A.; Yang, H.; Xu, F.; Li, F. A Hydrogel Microneedle Patch for Point-of-Care Testing Based on Skin Interstitial Fluid. *Adv. Healthc. Mater.* **2020**, *9* (4), 1–11.

(20) Rahimnejad, M.; Zhong, W. Mussel-Inspired Hydrogel Tissue Adhesives for Wound Closure. *RSC Adv.* **2017**, *7* (75), 47380–47396.

(21) Choi, S. W.; Guan, W.; Chung, K. Basic Principles of Hydrogel-Based Tissue Transformation Technologies and Their Applications. *Cell* **2021**, *184* (16), 4115–4136.

(22) Vo-Dinh, T.; Cullum, B. Biosensors and Biochips: Advances in Biological and Medical Diagnostics. *Fresenius. J. Anal. Chem.* **2000**, *366* (6), 540–551.

(23) Malhotra, B. D.; Chaubey, A. Biosensors for Clinical Diagnostics Industry. *Sensors Actuators B Chem.* **2003**, *91* (1), 117–127.

(24) Mello, L. D.; Kubota, L. T. Review of the Use of Biosensors as Analytical Tools in the Food and Drink Industries. *Food Chem.* **2002**, *77* (2), 237–256.

(25) Justino, C. I. L.; Duarte, A. C.; Rocha-Santos, T. A. P. Recent Progress in Biosensors for Environmental Monitoring: A Review. *Sensors* . 2017.

(26) Pohanka, M. Current Trends in the Biosensors for Biological Warfare Agents Assay. *Materials* . 2019.

(27) Qi, J.; Tan, D.; Wang, X.; Ma, H.; Wan, Y.; Hu, A.; Li, L.; Xiao, B.; Lu, B. A Novel Acetylcholinesterase Biosensor with Dual-Recognized Strategy Based on Molecularly Imprinted Polymer. *Sensors Actuators B Chem.* **2021**, *337*, 129760.

(28) Zhang, G.; Yu, Y.; Guo, M.; Lin, B.; Zhang, L. A Sensitive Determination of Albumin in Urine by Molecularly Imprinted Electrochemical Biosensor Based on Dual-Signal Strategy. *Sensors Actuators B Chem.* **2019**, *288*, 564–570.

(29) Jesadabundit, W.; Jampasa, S.; Patarakul, K.; Siangproh, W.; Chailapakul, O. Enzyme-Free Impedimetric Biosensor-Based Molecularly Imprinted Polymer for Selective Determination of L-Hydroxyproline. *Biosens. Bioelectron.* **2021**, *191*, 113387.

(30) Lee, W.-I.; Subramanian, A.; Mueller, S.; Levon, K.; Nam, C.-Y.; Rafailovich, M. H. Potentiometric Biosensors Based on Molecular-Imprinted Self-Assembled Monolayer Films for Rapid Detection of Influenza A Virus and SARS-CoV-2 Spike Protein. *ACS Appl. Nano Mater.* **2022**, *5* (4), 5045–5055.

(31) Di Giulio, T.; Mazzotta, E.; Malitesta, C. Molecularly Imprinted Polyscopoletin for the Electrochemical Detection of the Chronic Disease Marker Lysozyme. *Biosensors* . 2021.

(32) Liu, C.; Kubo, T.; Otsuka, K. Specific Recognition of a Target Protein, Cytochrome c, Using Molecularly Imprinted Hydrogels. *J. Mater. Chem. B* **2022**.

General conclusion

The biomedical analysis is an important aspect related to human life. Many analytical techniques for separation, identification, and quantitative determination are involved in this process. The development of determination techniques, from traditional laboratory instruments to point-of-care testing devices, is essential for improving the analytical performance in biomarker determination. With these aims, this thesis reports several developments in analytical methods targeting biomolecules for separation and detection in both traditional laboratory instruments and small detection platforms. The details in each chapter are as follows:

Chapter II targets on development of an online sample preconcentration technique in CE based on transient trapping (tr-trapping) in MEKC mode for steroid determination. The steroids can be detected with UV and ESI-MS detectors. Six steroids, including androsterone, cortisone, estradiol (with α-, β-stereoisomers), hydrocortisone, progesterone, and testosterone, were successfully separated with the tr-trapping technique. Using the tr-trapping technique with ESI-MS can eliminate the interference effect of micelle with MS instruments which can be troublesome for normal MEKC mode. Moreover, tr-trapping-ESI-MS shows a 50-fold improvement in limit of detection compared with CZE-ESI-MS. The proposed technique is suitable for biomolecules that are difficult to be detected with the UV-vis and fluorescence instruments.

Chapter III focuses on the development of an equipment-free detection for protein. The possibility of using hydrogel in the distance-based measurement of protein was studied. Results show that the color/fluorescence change inside of hydrogel in the presence of trypsin was observed from the top surface to the bottom. Besides, the relationship between the distance change and trypsin concentrations was observed, which shows the possibility of using hydrogel in the distance-based measurement of large biomolecules.

Chapter IV further focuses on improving hydrogel in point of the adsorption selectivity for protein by using the MIP technique in hydrogel preparation. A variety of preparation conditions for MIP hydrogels with lysozyme as a template were examined via microfluidic dispensing devices, and the parameters affecting lysozyme adsorption were studied. Microfluidic dispensing devices show comparable performance with a commercially available micropipette with less time to distribute the solution. Furthermore, the multivariate data on the lysozyme adsorption performance was obtained, and the equations that predict adsorption performance with studied parameters were constructed. Finally, a MIP hydrogel which provides a high imprinting factor and adsorption specificity toward lysozyme was successfully obtained. These MIP hydrogels can be used for protein separation and preconcentration.

Chapter V demonstrates the development of MIP hydrogel as the fluorescence sensor. Cytochrome c was employed as a template in the MIP hydrogel preparation, and parameters affecting cytochrome c adsorption and fluorescence determination were studied. Under the optimal condition, the MIP hydrogel showing high selective adsorption and fluorescence response for cytochrome c can be obtained. Additionally, comparing with other proteins, the fluorescence quenching can be observed in hydrogel after adsorbing only for cytochrome c, showing that fluorescence detection is very selective to cytochrome c. This result shows a promise to use cytochrome c MIP hydrogel as a fluorescence sensor. Moreover, the use of the same fluorescence monomer in chapters III and V show the possibility of using the MIP technique for hydrogel preparation to improve specificity in distance-based measurement.

The author believes that these studies would contribute to the progress in analytical chemistry, especially for the biomolecules on medical, pharmaceutical, agricultural, environmental, food, and engineering fields.

List of publications

Chapter II

Manmana, Y.; Liu, C.; Koino, H.; Sueyoshi, K.; Kitagawa, F.; Kubo, T.; Otsuka, K.:

Development of transient trapping micellar electrokinetic chromatography coupled with mass spectrometry for steroids analysis,

Chirality **2022**, in press. [**DOI:** 10.1002/chir.23489]

Chapter III

Manmana, Y.; Kubo, T.; Otsuka, K.:

Protein determination by distance and color change via PEG-based hydrogels,

(to be submitted)

Chapter IV

Manmana, Y.; Hiraoka, H.; Naito, T.; Kubo, T.; Otsuka, K.:

Development of a microfluidic dispensing device for multivariate data acquisition and application in molecularly imprinting hydrogel preparation,

J. Mater. Chem. B **2022**, in press [DOI:10.1039/D2TB00685E]

Chapter V

Manmana, Y.; Kubo, T.; Otsuka, K.:

Specific adsorption and fluorescence detection of cytochrome c using molecularly imprinted PEG hydrogel,

(to be submitted)

Other publication

Review

Manmana, Y.; Kubo, T.; Otsuka, K.:

Recent developments of point-of-care (POC) testing platforms for biomolecules,

TrAC – Trends Anal. Chem. **2020**, *135*(5), 116160. [DOI:10.1016/j.trac.2020.116160]

Acknowledgments

The present thesis summarizes the author's research work from April 2019 to June 2022. These studies were conducted in Department of Material Chemistry, Graduate School of Engineering, Kyoto University, under the supervision of Professor Koji Otsuka. Here, the author would like to express his gratitude to Professor Otsuka for offering the opportunity to study Ph.D. under his supervision. His warm support and instruction help the author to make his research successful.

The author is grateful to Professor Keiji Numata (Graduate School of Engineering, Kyoto University) and Professor Makoto Ouchi (Graduate School of Engineering, Kyoto University) for their splendid comments and discussions.

The author would like to thank Associate Professor Takuya Kubo (Graduate School of Engineering, Kyoto University) for his discussion, suggestions, and instruction during this study. In addition, the author feels grateful to Dr. Toyohiro Naito (RIKEN Innovation Co., Ltd), Dr. Tetsuya Tanigawa (Chemco Scientific Co., Ltd.), and Dr. Yoshiyuki Watabe (Shimadzu General Services, Inc.) for their valuable instructions and comments on the instrument detail and experimental design in this study.

The author feels thankful to Dr. Eisuke Kanao (Graduate School of Pharmaceutical Sciences, Kyoto University), Dr. Chenchen Liu (Graduate School of Science, Kyushu University), and the other members (present and graduated) of the Otsuka Lab for many help both related to the experiment and other problems in the daily life of author in Japan.

The author would like to acknowledge the financial supports from the Ministry of Education, Culture, Sports, Science and Technology, Japan (MEXT) and the Otsuka lab. The author thanks the MEXT scholarship for granting the opportunity for the author to study in Japan. Without these financial supports, the author's Ph.D. study in Japan seems impossible.

The author would like to thank friends in Japan and other parts of the world for mentally supporting and thoughtful suggestions when the author had difficult times. Furthermore, the author would like to thank the Thai community in Kansai that making life in Japan more lively. Finally, the author would like to thank his family for supporting every decision he made from a young age to the present. Without support from his family, the author cannot be this far in his academic career.

June 2022

Manmana Yanawut